Crisis in Gaza:

Scenario-based Health Impact Projections

Methods Technical Document

Version: 19 February 2024

Table of contents

List of tables and figures

1 Data sources

1.1 General sources of data

Pre-war data from Gaza, including indicators related to levels and causes of morbidity and mortality, and coverage of contacts with health services and of health promotive, preventive, and curative interventions, were obtained primarily from United Nations reports and the Ministry of Health (Table 1). Where such data were unavailable, we used information from the occupied Palestinian territories (oPt) as a whole, the West Bank, or from the neighbouring countries of Jordan, Egypt, or Lebanon. For data related to the ongoing war, we thoroughly searched for pertinent grey literature via Reliefweb (https://reliefweb.int/), Health [1], Nutrition [2], Food Security & Livelihoods [3] and Water, Sanitation and Hygiene (WASH) cluster [4] websites, and the Ministry of Health website [5]. Information on injuries, current food truck deliveries, WASH and shelter conditions, and disruptions in health service functionality were collected from publicly available periodic reporting by WHO UNRWA, and OCHA (see Table 1 for data sources). Information on homes destroyed came from OCHA. Additional parameters relevant to the models were extracted from peer-reviewed articles identified via PubMed and Google Scholar.

Where possible, the reliability of the extracted data was assessed based on specific criteria, including (i) data accuracy (linked to method/data collection system and considerations for ascertainment bias) and (ii) data representativeness (geographic representation of the affected population and data reflecting the most recent situation). Pre-war data were generally of good quality, characterized by accuracy and representativeness. Limitations were well-characterized with, for example, reports on quality and completeness of vital registration of births and deaths. However, data quality during the ongoing war is difficult to assess and may be variable due to challenges in data collection and analysis. Systematic errors in data collection methods are likely to result in under-reporting of events (e.g. as reporting via health information systems collapses and telecommunications are disrupted), reduced representativeness as the war progresses (e.g. missing data from the North in November MoH Emergency reports) and limited up-to-date information (e.g. in the North, WASH indicators were last reported in November 2023). Data politics may also play a role as political and advocacy imperatives may mean that information is supressed or misreported [6]. Projections are based on the most recent and publicly available data; adjustments to data sources will be made in forthcoming projections as data quality improves.

Reports and datasets extracted are available in a dataset repository available on GitHub (Gaza-projections/Data_sources).

Table 1. Main sources of data, by domain of interest.

Sources	Location	Year	Demographics	Pre-war causes of morbidity and mortality	Health services	Risk factors (WASH/shelter)	Other risk factors (Nutrition)	Traumatic Injuries	Infectious diseases	Maternal and newborn	NCDs
Pre-war data											
UNFPA population projections [7]	Gaza	2023	X								
Palestinian Central Bureau of Statistics [8]	Gaza	2000-2023	X	X				X			
UN IGME [9] & UN MMEIG [10]	Palestine	1996-2021		X						X	
MoH annual report [11]	Palestine	2008-2022		X					X	X	X
MoH annual report [12]	Gaza	2016-2022		X	X				X	X	X
UNRWA Health department annual report [13]	Gaza	2010-2022							X	X	X
UNRWA electronic health system [14]	Gaza	2019					X			X	
MoH communicable disease report [15]	Gaza	2018							X		
UNICEF Multiple indicator cluster survey [16]	Gaza	1996-2020							X	X	
WHO Immunization data portal [17]	Palestine	2023							X		
UNICEF- Mapping and Assessment of Maternal, Neonatal and Young Children Health Care Services [18]	Gaza	2019			X					X	
Multi-Sectoral Needs Assessment [19]	Gaza	2022								X	
MoH non-communicable disease report	Gaza	2018									X
Identifying a package of cost-effective interventions to address non-communicable diseases][21]	Gaza	2020-2021					X				X
WHO stepwise survey [22]	Gaza	2010,2020									X
MoH five-year cancer report [23]	West Bank	2017-2021									X
Data from the ongoing war in Gaza											
OCHA situational reports [24]					X	X		X			
UNRWA situational reports [25]					X	X		X			
WHO dashboard on health service functionality [1]					X						
WHO situational report [26]						X	X			X	
WFP situational report/ assessment [27]									X		
MoH emergency report [28]					X	X		X		X	X
The Humanitarian data exchange [29]						X					
UNRWA Supply and dispatch tracking [30]								X	X		
Palestinian Red Crescent [31]									X		

United Nations Population Fund (UNFPA); United Nations Inter-Agency Group for Child Mortality Estimation (UN IGME); UN Maternal Mortality Estimation Inter-Agency Group (MMEIG); Ministry of Health (MoH); United Nations Relief and Works Agency for Palestine Refugees in the Near East (UNRWA); World Health Organization (WHO); United Nations Office for the Coordination of Humanitarian Affairs (OCHA); World Food Programme (WFP); United Nations International Children's Emergency Fund (UNICEF).

1.2 Population denominators

To obtain sex- and age-specific population denominators (Table 2) we used UNFPA May 2023 estimates for Gaza, with some modifications, explained below. The UNFPA estimates are based on the Palestine census held on 1 December 2017, and provide five-year age groups for males and females separately for the age groups of 0-4 to 75-79, and 80+ [7]. The total population matches with the Palestine Central Bureau of Statistics (PCBS) projection for 2023, although the latter does not disaggregate by sex- or age-groups [8].

To get the proportions for each single year for children under five (i.e. to disaggregate the 0-4 age group), we used the 2022 PCBS estimates, which were given in single years (for those 0-4).In other words, rather than divide the UNFPA estimate for 0-4 years by five (i.e., multiply by 20%), we multiplied by 20.7% to get those aged under 1 year (0-11 months), by 20.3% to get those aged 1 (12-23 months), 20.0% for those aged two (24 to 35 months, 19.7% to get those aged three (36 to 47 months), and 19.3% for those aged four (48-59 months) based on 2022 PCBS proportions. To get numbers of those under one year who under one month, we divided the numbers in the first year by 12. Those aged 1-11 months were the remaining difference.

To calculate live births, we added 373 infant deaths that might have been expected to occur at the time of the estimate to the population of surviving infants (those aged under one) estimated for the mid-year (May 2023) population (n=69,721). Infant deaths were based on the United Nations Inter-Agency Group for Child Mortality Estimation (IGME) reports for 2021 (12.77 infant deaths per 1000 livebirths) multiplied by 5/12ths to estimate infant deaths for the five months from January until May (5.32 deaths per 1000 live births). This gives us 70,094 live births in a year, 5,841 live births in a month and 192 live births in a day. Since the still birth rate for Palestine in 2021 was 9.4/1000 live and stillbirths [32], we can expect births (live + still) to be roughly 9.5% higher than live births so a total of 70,688 births (live + still).

Table 2. Gaza population, UNFPA 2023 projection [7].

Age†	Population		
	male	female	total
<1mo	2,959	2,851	5,810
1-11mo	32,545	31,366	63,911
12-59mo	136,078	131,258	267,336
5-9yo	145,276	139,182	284,458
10-14yo	141,660	135,532	277,192
15-19yo	120,553	115,384	235,937
20-29yo	195,265	188,511	383,776
30-39yo	151,718	150,342	302,060
40-49yo	90,426	91,191	181,617
50-59yo	60,013	58,011	118,024
60-69yo	33,911	33,943	67,854
70-79yo	14,216	15,890	30,106
80-100yo	3,293	5,170	8,463
Total	1,127,913	1,098,631	2,226,544

† (mo) month old (yo) year old.

2 Traumatic injuries

2.1 Estimation of total injury deaths

2.1.1 Projecting injury deaths in the status quo and escalation scenarios

During the course of the war to date, the MoH in Gaza, as well as other groups, have reported numbers of people killed, as well as somewhat less precise number of people who may not have been accounted for in in these reports due to being missing, suspected to have died under rubble, or other reasons. We can therefore write

$$D_t = p_c D_t + (1 - p_c) D_t$$

where D_t is traumatic injury deaths during time unit t (one day) and p_c is the fraction of all injury deaths that are actually counted. Thus, $p_c D_t$ is the number eventually reported by the MoH ($D_{c,t,\mathrm{MoH}}$): we show the distribution and trend of this quantity over the war period to date in Figure 1, Panels A-B. We referred to this observed trend in order to project reported deaths in the status quo and escalation scenarios. Specifically:

- For the status quo scenario, we considered the daily time series of MoH-reported deaths during the period 15 October 2023 to 15 January 2024;

- For the escalation scenario, we considered the consecutive 30-day period with the highest reported death toll (11 October to 10 November 2023).

We fit null negative binomial models, offset by the log of total population, to the above time series, and sampled from these to project daily reported death counts under either scenario.

Separately, we also projected the number of reported injuries using the same time windows as above and based on negative binomial models of MoH-reported injury caseloads. We call this quantity $I_{c,t}$. We made a simplifying assumption that the reporting fraction p_c is the same for deaths and injuries. We work out this fraction below.

2.1.2 Projecting injury deaths in the ceasefire scenario

For the ceasefire scenario, we assumed no more traumatic injuries due to active warfare, but we recognised and summed together two residual sources of injuries and injury mortality:

- Deaths due to wounds sustained during the period to date: these are considered below; and

- Deaths and injuries due to unexploded ordnance and mines. To project these quantities, we compared the total reported deaths and injuries during the previous (2014) war in Gaza (2251 [33] and 10,895 [34], respectively) with the corresponding totals as estimated by us for the 2023-2024 war period to date: these ratios were considered a proxy of relative war intensity and thus relative exposure to unexploded ordnance and mines in the post-war period. For the 2014 war we also had data on the number of deaths and injuries during the 12 months following the war's end (converted to daily amounts). We used these numbers (13 and 56 respectively [35]) and the 2023-2024 to 2014 ratios above to estimate the daily rate of ordnance-related injury and deaths during the projection period:

$$D_{t,\text{ordnance}} = \frac{D_{t,\text{2023-2024}}}{D_{t,\text{2014}}} D_{t,\text{ordnance,2014}} \text{ and } I_{t,\text{ordnance}} = \frac{I_{t,\text{2023-2024}}}{I_{t,\text{2014}}} I_{t,\text{ordnance,2014}}$$
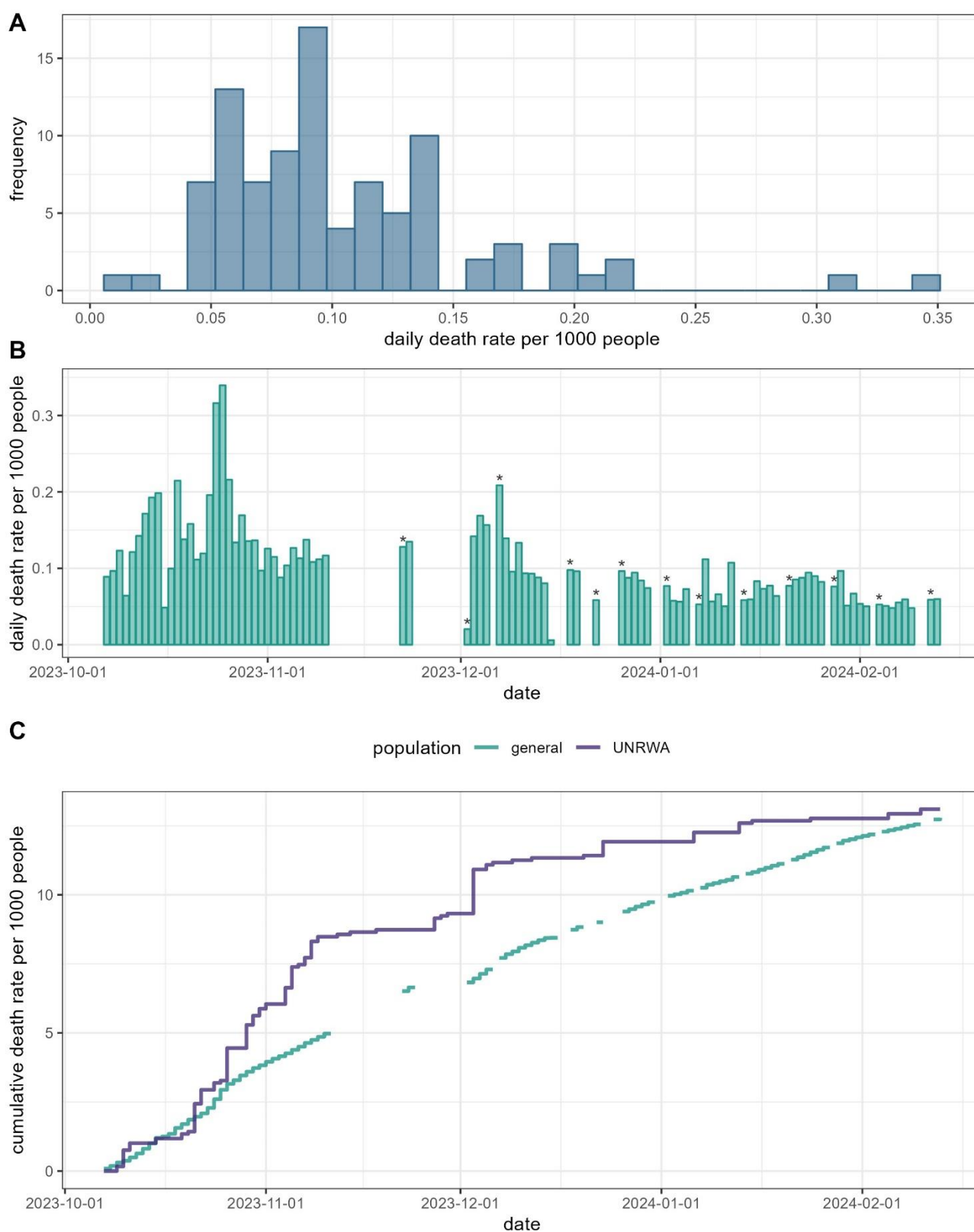
Figure 1. Panel A: Distribution of daily death rates according to the MoH report, during the period to date. Panel B: Evolution of the daily death rate according to the MoH report, by date. Asterisks above certain bars indicate that the value is a linearly interpolated mean since the last date of reporting. Panel C: Comparison of the death rate among UNRWA staff and the general population (based on MoH reports), over time.

2.1.3 Estimating the reporting fraction

In the ceasefire scenario we assumed that $p_c = 100\%$, reflecting improved security, MoH operationality and access to trauma care. For the other scenarios we estimated p_c by comparing the death rate among UNRWA staff (based on their officially reported starting staff size of 11,908) with that among the general population, again based on MoH reports. As previously published [36, 37], we assume that UNRWA's reporting fraction is 100%, and thus that the difference between the two death rates is a reasonable proxy of underreporting.

Accordingly, we fit a beta-distributed general additive model (GAM) to the daily ratio $\frac{d_{c,t,\text{MoH}}}{d_{c,t,\text{UNRWA}}} \approx p_c$ using the R `mgcv` package [38], excluding values before 20 October 2023, when we assumed from the similarity of the two sources that MoH information systems were fully operational (the beta distribution is suited to model quantities bounded by 0 and 1). We included two predictors in the model: (i) the MoH death rate itself (we reasoned that the reporting fraction would be lower, the higher the number of casualties to count) and (ii) the proportion of people living in government or UNRWA shelters, sourced from OCHA (we assumed that, as people moved out of apartment blocks into shelters, the general population death rate would decrease somewhat and/or reporting would become easier). The model had reasonable fit to the data (Figure 2), with an R^2 of 85% and highly significant associations for both predictors (p < 0.001). For the projections, we used the negative binomial prediction of death rate (see above) and the proportion living in shelters at the end of the period to date as predictor values for the GAM model, and drew from the model's resulting prediction and its standard error to get the projected value of p_c, lastly dividing projected reported deaths by p_c to get the overall D_t.
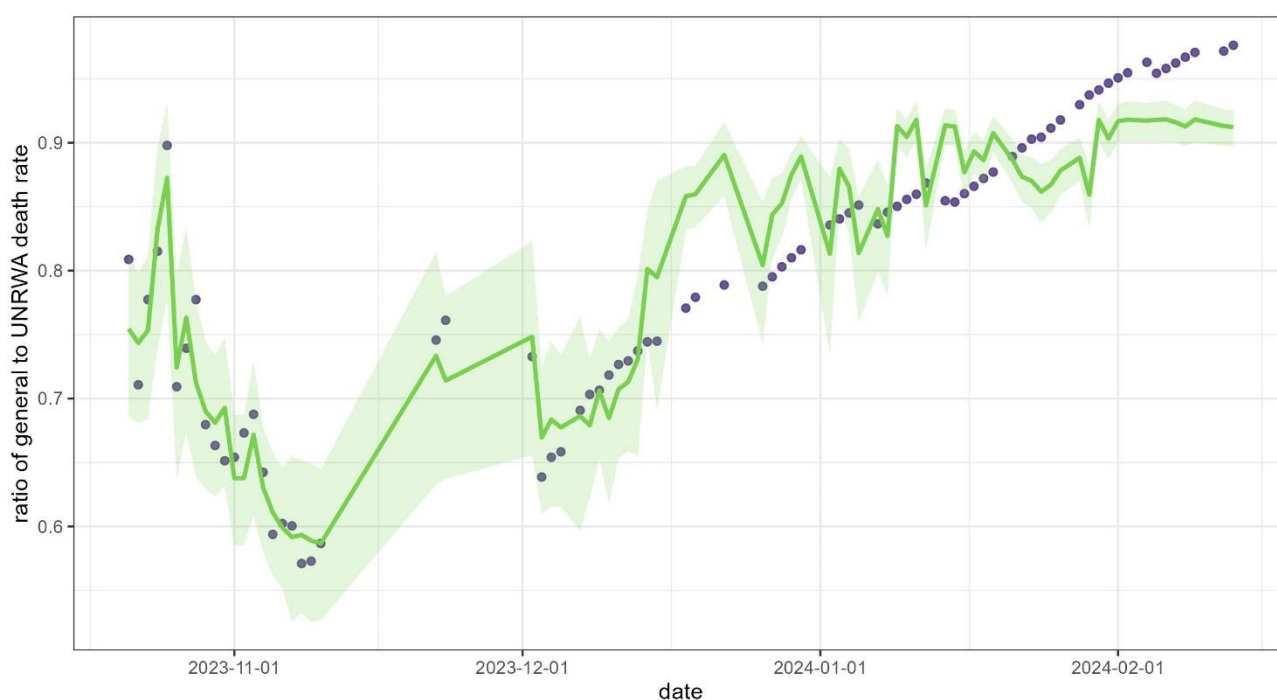
Figure 2. Fit of a general additive, beta-distributed regression model (green line, with shaded area indicating the 95% confidence interval of fitted values) to the observed ratio of general population to UNRWA death rate (purple dots).

2.1.4 Age and gender distribution

The MoH has twice published line lists of individuals who have died since the war's start (once on 26 October 2023 and once on 7 January 2024) [39]. We removed duplicates (based on the decedent's registration ID) and missing or unclear ages and gender values from this dataset. The resulting dataset comprised of 13,140 observations. We assumed that the age-sex distribution in this dataset would apply to traumatic injury deaths in our projections.

2.1.5 Adjustment for non-specific injury death reporting

We assumed that the MoH reports, which do not explicitly state cause of death, may include some people who died of reasons other than traumatic injury. We used the total age-specific number of daily deaths from non-injury causes, projected as part of the other modules in this project (see subsequent chapters of this document), to adjust for this bias. Specifically, for each age group we multiplied this non-injury level by a uniform distribution between 0 and 0.5 (namely the proportion of non-injury deaths that are included in MoH reporting) and subtracted the result from the injury deaths projected for that same age group. We did not apply this adjustment to the ceasefire scenario, as we assumed that in this scenario mortality reporting would regain its pre-war specificity of causal attribution.

2.1.6 Working out injury-caused maternal and neonatal deaths and stillbirths

Based on the total population N and the pre-war crude birth rate b, we expected 70,688 births B per year, which, assuming a gestation period of 9 months and a post-partum period of 1.5 months over which maternal deaths are usually counted, correspond to 61,852 prevalent pregnant or post-partum women at any given time ($B\frac{9+1.5}{12}$, or 11.3% of the reproductive age female population N_r, i.e. those aged 15 to 49yo). Similarly, the proportion who are in the stage of their pregnancy (28 weeks or beyond) during which stillbirth is typically counted would have been 2.9% ($B\frac{9-28/40}{12N_r}$). We therefore multiplied the number of projected injury deaths among females of reproductive age by 11.3% and 2.9% to obtain the number of maternal deaths and stillbirths due to traumatic injury, respectively. We assumed that non-fatal injuries would not increase the risk of stillbirth. Lastly, neonatal injury deaths were simply babies aged 0mo among all projected to die of injury.

2.2 Distinguishing between immediate and delayed deaths

2.2.1 Working out the proportion of immediate injury deaths

We next wished to quantify the number of traumatic injury deaths that result from wounds, i.e. among those who initially survive their injury (and may or may not be able to access care). To do this, we had to estimate the proportion of injuries that result in immediate death, or p_m . This can be done by considering only the subset of injuries and deaths that are reported (subscript c), as follows:

$$D_{c,t} = D_{m,t,c} + D_{s,c,t} = p_m I_{c,t} + (1 - p_m) \sum_{t-\tau_{\max}}^{t} I_{c,t-\tau}\mu_{s,\tau,c}$$

where $D_{m,t,c} = p_m I_{c,t}$ is injuries that result in immediate death and $D_{s,c,t}$, its complement, is people who die later of wounds. Because death may occur with a variable delay τ from the time of injury, deaths now are the

sum of injuries sustained at all possible times in the past, multiplied by the case-fatality ratio (CFR, $\mu_{s,\tau,c}$) among reported injuries at the corresponding time delay since injury. We work out this CFR later.

Over the entire period to date, we can thus sum reported deaths as follows:

$$D_{c,T} = p_m \underbrace{\sum_{t=1}^{T} I_{c,t}}_{\text{immediate}} + (1-p_m) \underbrace{\sum_{t=1}^{T} I_{c,t}\mu_{s,c}}_{\text{die of wounds later}} - (1-p_m) \underbrace{\sum_{t=T-\tau_{\max}}^{t=T} I_{c,t}\mu_{s,\tau,c}}_{\text{die of wounds later and after period}} \quad , \text{where} \quad \mu_{s,c} = \sum_{\tau=1}^{\tau_{\max}} \mu_{s,\tau,c}$$

The last term of the above equation is wound deaths that take place beyond the end of the period and must therefore be subtracted from the total for T. After rearrangement,

$$D_{c,T} = p_m I_{c,T} + (1-p_m) \underbrace{\left(\mu_{s,c} I_{c,T} - \sum_{t=T-\tau_{\max}}^{t=T} I_{c,t}\mu_{s,\tau,c} \right)}_{A}$$

We can lastly solve for p_m , the proportion who die immediately:

$$p_m = \frac{D_{c,T} - A}{I_{c,T} - A}$$

2.2.2   Estimating the case-fatality ratio of not immediately-fatal injuries

We defined the cumulative CFR $\mu_{s,c}$ of not immediately-fatal injuries as the weighted mean of the CFR across different injury sites w (e.g. head; thorax) and severity levels k (1= mild; 2 = moderate; 3 = severe):

$$\mu_{s,c} = \sum_{w=1}^{W} \sum_{k=1}^{K} \mu_{s,c,w,k} p_{I,c,w,k}$$

where $p_{I,c,w,k}$ is the proportion of all reported injury deaths who fall within a given w, k class. To derive these proportions, we combined data from (i) a line list of 217 traumatic injury patients who were medically evacuated from Gaza for rehabilitation care, which provided a breakdown of injury sites (Figure 3) [28] and (ii) data from the MoH on injuries to date and their severity (these data were last updated on 12 December 2023 and comprised of 50,172 cases, of whom 37.4% or 18,781 classified as mild, 31.1% or 15,597 as moderate, 16.5% or 8254 as severe and 15.0% or 7540 of unknown severity) [28]. We back-calculated the original breakdown of injury sites among evacuated patients by dividing the above proportions by the injury site-specific CFRs for the status quo period (see below), so as to approximate the true distribution of injury sites at the time of injury (Table 3).
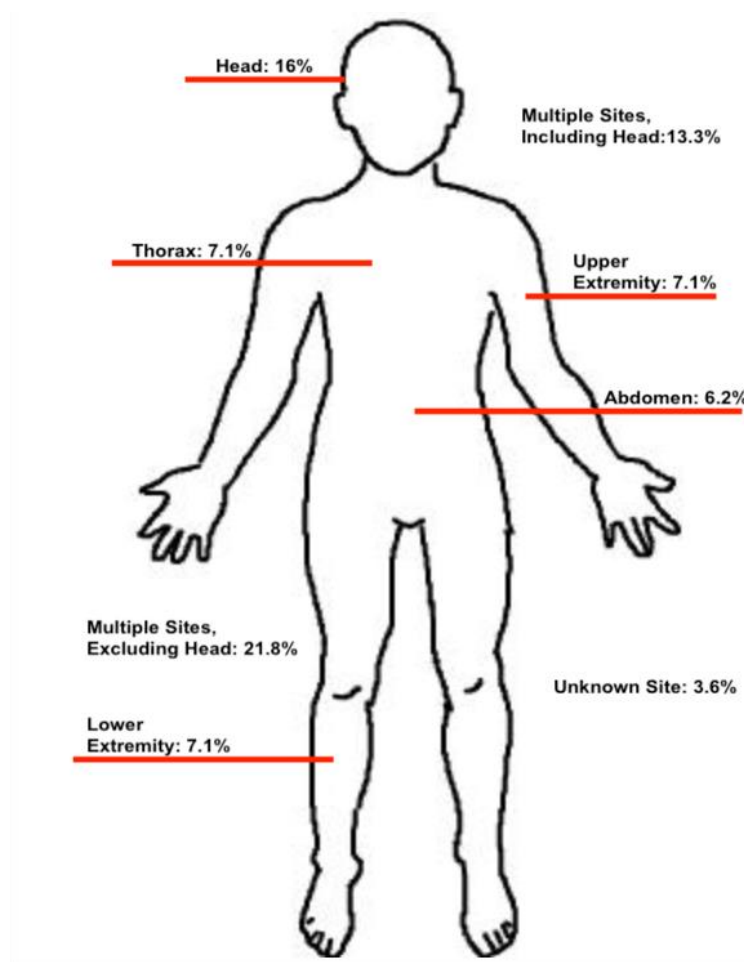
Figure 3. Percent of medically evacuated patients, by injury location.

To estimate CFRs by severity and injury site, we convened a panel of three emergency medicine physicians and surgeons, one of whom was performing medical procedures for the injured in Gaza during the current war. They were given a list of traumatic injury types using medical terminology, as shown in Table 3, and were asked to provide their estimates of CFR based on the values of trauma surgery and emergency care availability specified in each scenario (see main Report). For reference, we also provided them with CFRs expected in high-resource, non-war settings, based on the literature (Table 3). We assumed that mild injuries would be non-fatal, and weighted experts' average CFR estimates by the relative proportion of moderate and severe injuries, which we assumed to be the same across injury site.

Table 3. Back-calculated proportion of injury locations and corresponding expert-estimated CFRs by scenario, with accompanying values from the literature.

Injury site (notes)	Back-calculated proportion	Expert-provided mean estimate of CFR			Values from the literature [40–42] [43–54]
		ceasefire	status quo†	escalation	
Head, including traumatic brain injury	27%	56%	67%	73%	Mild / moderate brain injury: 4.3-7.6% Severe brain injury: 88.1%
Thorax	4%	8%	12%	22%	Spinal cord injury, paraplegia: 3%
Abdomen	5%	20%	35%	50%	Spinal cord injury, tetraplegia: 22%
Upper extremity	5%	12%	16%	19%	Thoracic trauma: 1.4-36.4%

Injury site (notes)	Back-calculated proportion	Expert-provided mean estimate of CFR			Values from the literature [40–42] [43–54]
		ceasefire	status quo†	escalation	
Lower extremity	20%	24%	32%	38%	Crush Injury leading to rhabdomyolysis: 20%
Multiple extremities (CFR for lower extremity injury applied)	3%	24%	32%	38%	Abdominopelvic trauma: 7-18% Junctional-central vascular trauma: 10-45%
Multiple locations, including head (CFR for head injury applied)	22%	56%	67%	73%	Peripheral vascular trauma: 2-6% Open fractures: 11-22% Traumatic amputation: 15% Burns: 3-55%
Multiple locations, excluding head	14%	17%	26%	37%	
All sites (weighted means)	100%	**25%**	**32%**	**36%**	

† also used as the value for the war period to date.

Lastly, we distributed $\mu_{s,c}$ over τ based on a large cohort [55] of North American injury survivors followed for up to two years post-injury, which, considering those in the cohort who eventually died of injury complications, provided a distribution of deaths per τ. Cumulatively, 53%, 58%, 65%, 70%, 77%, 88% and 100% of all deaths in this study had occurred by days 15, 30, 60, 90, 180, 365 and 730 after injury.

2.2.3 Projecting deaths from wounds

For the status quo and escalation scenarios, having projected D_t and I_t (see above), we computed $D_{s,t}$ simply as $D_t - I_t p_m$. For the ceasefire scenario:

- since a fraction of injuries during the period to date would have gone unreported (and potentially untreated), we computed deaths due to wounds using the following equation, where $\varphi_{\mu,u}$ is a relative risk (RR) of case-fatality comparing unreported and reported deaths, and which, in the absence of empirical evidence, we took to be uniformly distributed between 1.0 (i.e. the same CFR as for reported injuries) and 2.0 (twice the CFR):

$$D_{s,t} = \left((1 - p_m)p_c + (1 - p_m)(1 - p_c)\varphi_{\mu,u}\right) \sum_{t-\tau_{\max}}^{t} I_{t-\tau}\mu_{s,\tau}$$

- for ordnance injury deaths during the ceasefire scenario we applied the proportion $D_{s,T}/D_T$ during the period to date, also tracked while estimating p_m;

- we then summed deaths due to ordnance wounds to deaths from wounds sustained during the period to date.

2.3 Model implementation

We sequenced the analysis as follows:

1. Firstly we fitted models of reported injuries, deaths and the reporting fraction p_c;

2. We then plugged the p_c model into a simulation of total injuries and deaths over the war period to date, in each run simulating from the prediction and standard error of this model and subtracting a

uniformly distributed proportion of estimated non-injury deaths; we used this model to quantify all the parameters needed to estimate p_m based on the above equation;

3. We then simulated deaths, injuries and deaths due to wounds in the projection period, in each simulation drawing from model uncertainty distributions and the empirical distribution of p_m.

For each simulation we performed 10,000 runs and extracted the mean and 95% percentile distribution of the runs.

2.4   Assumptions and limitations

The main limiting assumptions in our analysis are as follows:

▪ We assumed that the reporting fraction is the same among injuries as among deaths. While this assumption could be relaxed, e.g. by estimating a system with two unknown variables, it is plausible that the reasons for non-reporting would be similar between injuries and deaths. However, a violation of this assumption could have resulted in bias;

▪ Our estimate of the CFR among people who initially survive their injuries is largely based on a limited panel of experts and may thus be subject to bias: for example, if experts had perceived a need to over-estimate CFR our estimate of the proportion dying immediately would have been under-estimated, and the number of deaths due to wounds over-estimated. The estimate is also based on the assumed distribution of injury sites, which in turn comes from a limited and possibly non-representative subset of cases who were referred abroad. Note however that any inaccuracy in CFR would not have affected our overall projections of deaths due to injury, but rather the breakdown between immediate deaths and subsequent deaths due to wounds;

▪ We also assumed that the reporting fraction and proportion of immediate injuries do not vary by age and gender, which may be untrue (one may hypothesise, for example, that elderly people are less likely to be reported on);

▪ The age and gender distribution of projected injuries is based on its distribution to date, which may be unrealistic if the types of weaponry, military tactics and civilian exposure change in the next months.

▪ In the end, the projections for the status quo and escalation scenarios rely on strong assumptions about which time windows in the period to date to consider as the basis for these: here too, reality may evolve differently, underscoring our project's inherent unsuitability for prediction, and more conservative focus on *projecting* based on explicit assumptions.

3 Malnutrition

3.1 Overview of methods

For this analysis, nutritional status is treated as a risk factor for several processes in the natural history of infections, non-communicable diseases (NCDs) and maternal and neonatal mortality and stillbirth. The specific indicators we aimed to estimate, as proxies of these risk factors, are listed in Table 4.

Table 4. Nutritional indicators to be estimated, and their application in downstream modules of the analysis.

Risk factor	Indicator (one range per scenario)	Application in the analysis
Reduced caloric intake	Mean reduction in caloric (Kcal) intake since the start of war / over the projection period, among adults aged ≥ 40 years old . Also assumed to apply to pregnant women.	Risk factor for maternal and neonatal mortality and stillbirth module (input for Lives Saved Tool (LiST model). Risk factor for NCD module (input for structured expert elicitation of increases in case-fatality ratio (CFR), specifically for individuals with cancer and diabetes.
Increasing burden of acute malnutrition	Prevalence of global and severe acute malnutrition (GAM, SAM) among children aged 6 to 59 months. GAM is defined here as a weight-for-height Z-score (WHZ) < -2 standard deviations (SD) from the mean of the World Health Organization (WHO) reference population [56]. SAM is defined as a WHZ < -3SD from the mean. Bilateral oedema is omitted from the definition: *kwashiorkor* malnutrition is assumed to be numerically negligible based on pre-war anthropometric data (see below).	Risk factor for infections module (input for structured expert elicitation of increases in transmissibility and CFR).
Disrupted infant and young child feeding (IYCF) practices	Proportion of infants below six months of age who are exclusively fed with breast milk.	Risk factor for MNH module (input for LiST). Risk factor for infections module (input for structured expert elicitation of increases in CFR).

Based on the availability of data, we implemented the following steps to project acute malnutrition prevalence:

- Estimate (for the period between the start of the war and the start of the projection period: we call this the period 'to date') and project (for the projection period, divided into two equal three-month sub-periods) the daily per-capita caloric availability from a combination of food aid being trucked into Gaza, pre-existing stocks, and agricultural output;

- Calculate the change in daily caloric intake from baseline ($\Delta I_{0,t}$) among adults aged ≥ 40yo, by gender, age group (40 to 49yo, 50 to 59yo, 60 to 69yo, 70 to 79yo, ≥ 80yo), and overall, relative to their baseline intake (I_0) key assumption here is that availability = intake, i.e. that all food is distributed and consumed, with equal quantities per person;

- Apply an existing model of adult weight loss to estimate and project adult percent weight loss over time; and

- Assume that children experience the same relative weight loss as adults (see below) and apply this weight loss over time to baseline anthropometric data from routine child growth monitoring in Gaza, and estimate / project resulting SAM and GAM prevalence.

The above steps were implemented for each of the three scenarios, with uncertainty in input parameters propagated through the analysis over 1000 simulation runs. Outputs shown below are the mean and 95th percentile interval of the simulation runs.

3.2 Change in caloric intake

Even after the war's start, a proportion of Gaza's pre-war daily caloric intake was met by a combination of existing stocks and agricultural output. However, farming, already a marginal contributor to food security in Gaza (about 12% pre-war [57]), has reportedly been severely compromised by military activity [58]. Stocks were reported to be largely depleted around early December [59]. We thus made assumptions about the evolution of these two food sources, expressed as the proportion of I_0 that each source could fulfil (Table 5).

Table 5. Assumed contributions from existing stocks and agricultural output, by period. Ranges indicate the extremes of a uniform distribution.

Month(s)	Date range	Period	Contribution from existing stocks (p_s)	Contribution from agriculture (p_g)
1	7 Oct 2023 to 6 Nov 2023	to date	0.75 to 1.00	0.10 to 0.15
2	7 Nov 2023 to 6 Dec 2023		0.75 to 1.00	0.05 to 0.10
3	7 Dec 2023 to 6 Jan 2024		0.00 to 0.25	0.05 to 0.10
4	7 Jan 2024 to 6 Feb 2024		0.00 to 0.10	0.05 to 0.10
5 to 10	7 Feb 2024 to 6 Aug 2024	projection	0.00	0.05 to 0.10

We then estimated and projected quantities of food aid arriving into Gaza. UNRWA has reported daily numbers of trucks transporting food that arrived to the Rafah and Kerem Shalom crossings since 7 October [60]. We excluded trucks that carried water only. Missing data at the end of the period to date were imputed by assuming a constant daily number of trucks equal to the median over the last two weeks of the period of data availability.

Each truck was assumed to carry a full load, with tonnage uniformly distributed between 14 (size of a 'small' truck according to WFP) and 16 metric tonnes (MT) ('large' truck); 1 MT was assumed to provide 2,100 Kcal/day to a mean of 1,660 people (we added uncertainty of ±200 Kcal/day to this quantity) [61–63]. While there are reports of aid being rejected at the border, we assumed that typical UN rations would have been allowed through. The resulting estimated per-capita caloric availability from food aid (I_f) were computed by dividing total intake by the total population N.

During the projection period, we expressed assumed levels of food aid for each scenario as a fraction of the recommended daily caloric intake (generically 2,100 Kcal/day, but adjusted to 2,213 Kcal/day based on Gaza's population structure [64]). Scenario assumptions are provided in Table 6.

Table 6. Assumed proportions of the recommended daily intake met through food aid, by sub-period and scenario.

Sub-period	Ceasefire	Status quo	Escalation
months 1 to 3	1.10 to 1.30	1.00 to 1.20	0.80 to 1.00
months 4 to 6	1.10 to 1.30	1.00 to 1.20	0.80 to 1.00

The status quo scenario roughly assumes that, in line with aid trucked in will continue to increase to some extent (note however that truck numbers plateaued in late January). The ceasefire scenario portrays a situation in which food aid deliberately exceeds the recommended intake, thereby allowing vulnerable groups in the population to recover some of their lost weight. The escalation scenario illustrates the trajectory of continued partial starvation.

The resulting mean daily caloric intake during the period to date was thus computed as:

$$I_t = \min \left(I_0 \left(p_{s,t} + p_{a,t} \right) + I_{f,t} , I_0 \right)$$

where t = 1 day. It follows that $\Delta I_{0,t} = I_t - I_0$.

Note that in the rare case that the combination of food aid and other sources exceeded I_0, we took I_0 as the maximum boundary of food intake.

A self-weighting sample survey of NCD prevalence and risk factors was conducted among adults aged ≥ 40 years old in Gaza during 2020 [65]. The survey collected individual characteristics including weight (to the nearest 0.1 Kg), height (in cm), gender, age (in years) and current average daily caloric intake (in Kcal/day). Of the 4,576 survey observations, 380 (8.3%) had missing weight, height, age, gender or caloric intake, and were thus removed, leaving 4,196 in the analysis. We assumed the surveyed quantities remained constant up to 6 January 2023, i.e. provided a robust baseline of I_0 and other parameters (see below). With agreement from survey investigators, we publish aggregate rather than individual data from the survey, namely mean food intake and anthropometric measures by 10-year age group. These aggregate data, when weighted by relative age group size, provide almost identical estimates to those obtained from individual observations, and R scripts used in the analysis thus use aggregate data only.

3.3 Weight loss among adults

We used a mechanistic model of weight loss among adults, developed by Hall et al. [66] and validated within North American populations. The model estimates the trajectory of individual weight as a function of baseline body weight and fat mass, height, age, gender and $\Delta I_{0,t}$. We retained values of other metabolic parameters used by Hall et al., including energy consumption due to the thermic effect of food and external activities (mostly sedentary conditions). Baseline fat mass is computed within the model itself based on age, gender, height and weight. In line with Hall et al., we estimated the time-dependent resting metabolic rate, another model input, using the equations of Miffllin and St Jeor [67].

3.4 Prevalence of acute malnutrition in children

Before the war, UNRWA collected electronic data from routine growth monitoring visits of children in Gaza (note that all children are targeted for monitoring, not just those presenting to health facilities for illness). We had access to the 2019 growth monitoring dataset, which we restricted to the most recent visit for each child and ages 6 to 59 months. The data made public is an aggregate of the growth monitoring data.

Of the 150,060 child growth monitoring observations, 123 (0.1%) had missing age, gender, height/length or weight, and were thus removed, leaving 149,937 in the analysis. For computational efficiency, we worked with a random sub-sample of 10,000 observations, which we checked had negligible deviations from the full dataset

in terms of SAM and GAM prevalence. We assumed this reduced dataset provided baseline anthropometry for children in Gaza.

We computed the weight-for-height/length Z-score (WHZ) for each child using the `anthro` R package, developed by WHO and consistent with the WHO Growth Standards [56]. We excluded flagged observations (Z-score <> 5SD) from computation of GAM and SAM prevalence. For each day included in the analysis, we applied the mean time-varying percent weight loss estimated among adults to this dataset of children, and recalculated WHZ and GAM / SAM prevalence. Children have a higher energy expenditure per capita than adults, so it may be assumed that their rate of weight loss would be greater than that of adults. On the other hand, it is plausible that caregivers would prioritise feeding their children over themselves. To represent these counteracting factors, we applied a uniformly distributed relative risk of 0.7 to 1.3 to the percent weight loss among adults.

3.5   Exclusive breastfeeding

We conducted a rapid literature review of changes in exclusive breastfeeding prevalence comparing the pre-crisis and crisis periods in the Middle East. We considered both peer-reviewed articles and grey literature reports. Search terms included [breastfeeding AND (crisis OR war OR (acute) forced displacement) internally displaced people / persons / IDP]. We graded evidence as summarised in the Data source chapter. Table 7 summarises studies included in the review.

Table 7. Prevalence of exclusive breastfeeding among children aged under 6mo in comparable crisis settings.

Country (type of crisis)	Pre-crisis		Crisis		Notes	Evidence grading
	Prevalence	Year	Prevalence	Year		
Iraq (war) [68]	--	--	21%	2006-2011	Each additional casualty per 1000 persons associated with a 2.7% decline in exclusive breastfeeding prevalence	+++
Iraq (war) [69]	--	--	7% less likely to be breastfed in high versus low conflict intensity districts	Children born after 2003.	Children born from 2000 to 2006	+++
Lebanon (war) [70]	44-52% (South Lebanon)	2006 (before the war)	5-13% (South Lebanon)	2006 (two months after the war started)		+
Lebanon (explosion) [71]	59.6%	n/a	7.7% (siblings)	2020	Mothers interviewed after 4 August 2020 blast (retrospective for siblings)	+
Syria (war) [72]	42.6% (national)	2009	30.9% (Aleppo) 32.6% (Idleb)	2017		++
Syrians in Lebanon (displacement due to war) [73]	42.6% (pre-displacement)	2009	25% (Syrian refugees in Lebanon)	2013	Syrian refugees living in Lebanon	+

To project the prevalence of exclusive breastfeeding in Gaza during the analysis period, we computed the median and 50% quantile of the relative prevalence ratio (crisis: non-crisis) in the above studies and applied it as multiplying factor to the pre-war exclusive breastfeeding prevalence in Gaza (41.6%) [74].

3.6 Limitations

We identified the following important limitations of our analysis of nutritional status:

- There is considerable uncertainty on the actual amount of food that is in fact being allowed into Gaza: not all food assistance is transported via the United Nations (though they are the main supplier) and the tonnage of trucks is at best an approximation of actual quantities brought in;

- Food that arrives into Gaza must then be equitably distributed to the population, ideally on a need basis. However, food truck access to the north of Gaza has been curtailed [75] and, more generally, we could not access data on actual food distributions. While it is reasonable to assume that, in a situation of scarcity, all food would have been distributed, it is unclear to what extent those most in need were prioritised or indeed reached;

- The model of weight loss among adults haves been validated in North American populations, but key inputs such as resting energy expenditure may differ according to the region of the world [76], and so may the key relationships among variables in the model, which have also been parameterised based on statistical models of largely European and North American adults;

- We make a key assumption that the percent weight loss experienced by adults is also experienced by children, though we partly relax this assumption by introducing uncertainty. We searched extensively for literature on weight loss among starving children, but did not find consistent reports with which to parameterise a child-specific model or establish the validity of extrapolating from adults. While children who receive insufficient food will lose weight, it is less clear how fast this will occur, and to what extent the context (e.g. exposure to infectious diseases) will influence this loss.

Taken together, the above limitations may introduce considerable unquantified inaccuracy in our projections, though it is not clear whether any bias would result, as each limitation carries plausible over- as well as under-estimation effects. It is likely however that, rather than the uniform picture our analysis produces, pockets of particularly dire food insecurity and nutritional status have been emerging in the Gaza Strip and will continue to, particularly among people who are cut off from relief and not in relatively accessible UNRWA shelters.

4 Infectious diseases

4.1 Analysis scope

Table 8 lists the infectious diseases included within the scope of estimation. For this analysis, stable transmission is defined as a relatively constant secular trend in terms of the number of infections per year, with or without a seasonal peak. An epidemic is defined as the occurrence of at least three chains (generations) of uninterrupted transmission of the pathogen within the general population, excluding instances of sustained transmission within specific groups such as hospitalised patients.

Table 8. Infectious diseases (pathogens) included within the scope of projections.

Included in Gaza routine vaccination schedule [77]?	Main route of transmission	Infectious diseases with epidemic potential	Infectious diseases with stable transmission, i.e. 'endemic' (W = highly seasonal)
yes	Airborne-droplet	Diphtheria (*Corynebacterium diphtheriae*) Pertussis (*Bordetella pertussis*) Measles (measles virus)	*Haemophilus influenzae* type b disease (*Haemophilus influenzae* type B) Pneumococcal disease (*Streptococcus pneumoniae*) COVID-19‡ (SARS-CoV-2 virus)
	Faecal-oral	Polio (wild-type poliovirus type 1 and 3)	Rotavirus disease (rotavirus) (W)
no	Airborne-droplet	Meningococcal meningitis (*Neisseria meningitidis* types A, C, W or Y)†	Influenza†, para-influenza (human influenza, para-influenza viruses) (W) Respiratory syncytial virus disease, RSV (respiratory syncytial virus) (W)
	Faecal-oral	Bacterial dysentery (*Shigella dysenteriae* type 1) Cholera (*Vibrio cholerae*) Hepatitis A (hepatitis A virus) Hepatitis E (hepatitis E virus) Polio (vaccine-derived poliovirus type 2) Typhoid fever (*Salmonella typhi*)	Bacterial gastroenteritis other than epidemic-prone causes (*Salmonella typhimurium, Escherichia coli, Clostridium difficile, Campylobacter jejuni, Shigella spp.*) Viral gastroenteritis other than rotavirus (adenovirus, astrovirus, norovirus) (W)

† Vaccination only recommended for vulnerable groups. ‡ Unclear status of vaccination coverage post-2022, with low uptake up to 2022.

By contrast, the following infections are excluded from the scope of estimation (the reason for this is provided in parentheses):

- Tuberculosis, HIV, sexually transmitted infections (very low prevalence at baseline for tuberculosis and HIV and low case-fatality for sexually transmitted infections);

- Hepatitis B, Hepatitis C (long time horizon of disease progression and mostly beyond the project's timeline);

- Mumps, rubella, rabies, chickenpox (low case-fatality or transmissibility);

- Tetanus (neonatal tetanus is covered in the maternal and neonatal health (MNH) module through antenatal care and safe delivery parameter inputs; tetanus secondary to infected injuries is covered in the injuries module);

- Other neonatal infections (also covered by MNH module); and

- Vector-borne infections (none are known to pose a substantive threat given entomological conditions in Gaza; the baseline burden of vector-borne infections was practically zero given MoH surveillance data).

Antimicrobial resistance (AMR) is also excluded from estimation due to (difficulty in separating deaths due to AMR from those due to infection as a primary cause, at least as specified in our model framework (see below)). Concerns about the spread of AMR due to the war in Gaza have nonetheless been expressed [78].

4.2 Susceptibility estimates

4.2.1 Infections included in the routine vaccination schedule

To correctly parameterise models for epidemic and endemic infections (below), we required robust estimates of susceptibility to infection and disease at the start of the crisis and over the projection periods. For infectious agents that are included in Gaza's routine vaccination schedule, we developed an age-structured dynamic cohort model to track the evolution of immunity over time based on past and projected vaccination coverage, natural exposure to infection, vaccine effectiveness estimates and the rate of immunity waning post vaccination. Age was stratified by month for the first 24 months and by year until 6 years old, then as follows: 6 to 9 years, 10 to14 years, 15 to19 years, 20 to 29 years, 30 to 39 years, 40 to 49 years, 50 to 59 years, 60 to 69 years, 70 to 79 years, and ≥ 80 years.

Figure 4 shows a simplified representation of the model for a few age groups and a single pathogen. Briefly, children are born into either the M (maternally immune) or S (susceptible compartment) based on susceptibility in the reproductive age group and a birth rate b. Children lose their maternal immunity at a rate m. They also receive their routine vaccinations as they age, moving to compartment V_λ (people with vaccine-induced immunity against infection) based on the product of c, vaccination coverage, and f_λ, vaccine effectiveness against infection; vaccination is non-specific, i.e. immune children are also vaccinated. Vaccination may also occur later in life, as booster doses. Further, all susceptible compartments experience infection based on a fixed force of infection λ.
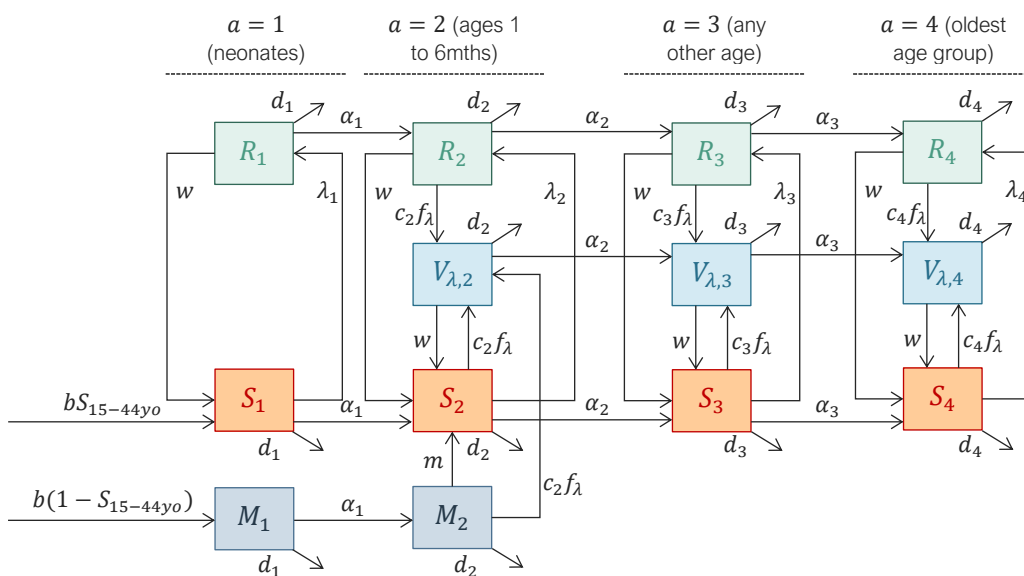
Figure 4. Diagram showing states and flows in the population immunity model, for a single pathogen. For brevity, only a few age groups are shown.

We also track compartment V_σ (people with vaccine-induced immunity against development of disease, but not infection) as the product of c and f_σ, vaccine effectiveness against severe disease. We assume that w is the same for protection against infection and protection against disease.

We make a few further simplifications:

- A single waning rate applies to natural and vaccine-acquired immunity;

- Waning time is negative-exponentially distributed with rate $w = T_{\text{waning}}^{-1}$, the inverse of the mean duration (in years) of functional protection;

- We assume the duration of maternal immunity protection to be $T_M = 6$ months, which roughly corresponds to the observed mean duration of exclusive breastfeeding in Gaza, and estimates of this parameter for different vaccines and infections. All infants lose their maternal immunity at seven months;

- Outside of waning, vaccine effectiveness is constant across age;

- Ageing in the model follows an exponential model and vaccinations occur as a proportion of those ageing into the relevant age group per the given vaccine schedules;

- All vaccines behave according to the 'all-or-nothing' model, i.e. people are either fully protected against infection or disease or not at all; and

- People acquire vaccine-derived immunity when they complete the full age-appropriate priming regimen, with subsequent booster doses returning them to the same level of protection.

Table 9 lists the set of differential equations quantifying the evolution of each model compartment over time. Vaccine effectiveness and waning estimates from the literature are summarised in Table 10.

Table 9. Differential equations governing the flow of people into and out of different immunity compartments and age groups.

Age group	Equation†
Susceptibles (S_a):	
neonates (0mo)	$\frac{dS_a}{dt} = b_t\left(\frac{S_{15-44yo}}{N_{15-44yo}}\right) + R_{a,t}w - S_{a,t}(\lambda_{a,t} + \alpha_a + d_a)$
≥ 7mo (when maternal immunity ends)	$\frac{dS_a}{dt} = (S_{a-1,t} + M_{a-1,t}) \times \alpha_{a-1}\rho_u + (R_{a,t} + V_{a,t})w - S_{a,t}(\lambda_{a,t} + \alpha_a + d_a)$
all other age groups	$\frac{dS_a}{dt} = S_{a-1,t}\alpha_{a-1}\rho_u + (R_{a,t} + V_{a,t})w - S_{a,t}(\lambda_{a,t} + \alpha_a + d_a)$
oldest age group	$\frac{dS_a}{dt} = S_{a-1,t}\alpha_{a-1}\rho_u + (R_{a,t} + V_{a,t})w - S_{a,t}(\lambda_{a,t} + d_a)$
Naturally immune (R_a):	
neonates	$\frac{dR_a}{dt} = (S_{a,t} + V_{\sigma,a,t})\lambda_{a,t} - R_{a,t}(w + \alpha_a + d_a)$
all other age groups	$\frac{dR_a}{dt} = R_{a-1,t}\alpha_{a-1}\rho_u + (S_{a,t} + V_{\sigma,a,t})\lambda_{a,t} - R_{a,t}(w + \alpha_a + d_a)$
oldest age group	$\frac{dR_a}{dt} = R_{a-1,t}\alpha_{a-1}\rho_u + (S_{a,t} + V_{\sigma,a,t})\lambda_{a,t} - R_{a,t}(w + d_a)$
Immune following vaccination ($V_{\lambda,a}$):	
1mo	$\frac{dV_{\lambda,a}}{dt} = (S_{a-1,t} + M_{a-1,t} + R_{a-1,t} + V_{\sigma,a-1,t})\rho_\lambda - V_{\lambda,a,t}(w + \alpha_a + d_a)$
2-6mo	$\frac{dV_{\lambda,a}}{dt} = V_{\lambda,a-1,t}\alpha_{a-1} + (S_{a-1,t} + M_{a-1,t} + R_{a-1,t} + V_{\sigma,a-1,t})\rho_\lambda - V_{\lambda,a,t}(w + \alpha_a + d_a)$
older ages	$\frac{dV_{\lambda,a}}{dt} = V_{\lambda,a-1,t}\alpha_{a-1} + (S_{a-1,t} + R_{a-1,t} + V_{\sigma,a-1,t})\rho_\lambda - V_{\lambda,a,t}(w + \alpha_a + d_a)$
oldest age group	$\frac{dV_{\lambda,a}}{dt} = V_{\lambda,a-1,t}\alpha_{a-1} + (S_{a-1,t} + R_{a-1,t} + V_{\sigma,a-1,t})\rho_\lambda - V_{\lambda,a,t}(w + \alpha_a)$

Immune to disease following vaccination but not infection ($V_{\sigma,a}$):	
1mo	$\frac{dV_{\sigma,a}}{dt} = (S_{a-1,t} + M_{a-1,t} + R_{a-1,t})\rho_\sigma - V_{\sigma,a,t}(w + \alpha_a + d_a)$
2-6mo	$\frac{dV_{\sigma,a}}{dt} = V_{\sigma,a-1,t}\alpha_{a-1}(\rho_u + \rho_\sigma) + (S_{a-1,t} + M_{a-1,t} + R_{a-1,t})\rho_\sigma - V_{\sigma,a,t}(w + \alpha_a + d_a)$
older ages	$\frac{dV_{\sigma,a}}{dt} = V_{\sigma,a-1,t}\alpha_{a-1}(\rho_u + \rho_\sigma) + (S_{a-1,t} + R_{a-1,t})\rho_\sigma - V_{\sigma,a,t}(w + \alpha_a + d_a)$
oldest age group	$\frac{dV_{\sigma,a}}{dt} = V_{\sigma,a-1,t}\alpha_{a-1}(\rho_u + \rho_\sigma) + (S_{a-1,t} + R_{a-1,t})\rho_\sigma - V_{\sigma,a,t}(w + d_a)$
Maternally immune (M_a):	
neonates	$\frac{dM_a}{dt} = b_t\left(1 - \frac{S_{15-44yo}}{N_{15-44yo}}\right) - M_{a,t}(\alpha_a + d_a)$
1-6mo	$\frac{dM_a}{dt} = M_{a-1,t}\alpha_{a-1}\rho_u - M_{a,t}(\alpha_a + d_a)$

† Where $\rho_\lambda = c_{t,a} \times f_\lambda$, $\rho_\sigma = c_{t,a} \times (1 - f_\lambda) \times f_\sigma'$, and $\rho_u = 1 - \rho_\lambda - \rho_\sigma$ to model vaccinations giving protection against infections, disease only, and vaccine failures combined with non-vaccination. Also, $f_\sigma' = \frac{f_\sigma - f_\lambda}{1 - f_\lambda}$ to account for protection against breakthrough infections.

Table 10. Estimates of vaccine schedule effectiveness and waning used in the immunity tracking model.

Infectious disease / vaccine	Parameter†	Central estimate	Lower bound	Upper bound	Schedule and other specifications	Sources used
Diphtheria (as part of pentavalent vaccine)	f_λ	0.600	0.510	0.680	3 infant doses at months 2, 4, and 6; booster	[79, 80]
	f_σ	0.810	0.740	0.860	around year 6.	[80]
	w	0.007	0.004	0.009	After priming doses.	[81]
Pertussis (whole-cell, as part of pentavalent vaccine)	f_λ	0.830	0.600	0.920	3 infant doses at months 2, 4, and 6. Includes effect on infectiousness to others.	[82]
	f_σ	0.940	0.880	0.970	Effectiveness in the first 5 years of life against WHO definition of severe pertussis.	[83, 84]
	w	0.043	0.034	0.059	After priming doses.	[85]
Measles (as part of MMR)	f_λ	0.850	0.250	0.970	Dose 1 at 12mths, dose 2 at 18mths.	[86]
	f_σ	0.941	0.883	0.983		[87]
	w	0.009	0.005	0.016	After priming doses. Based on antibody waning.	[88]
Polio wild-type 1 or 3 / IPV-OPV sequential	f_λ	0.817	0.387	0.940	IPV: 2 infant doses at months 1 and 2; OPV: 3 infant doses at months 2, 4, and 6 with boosters at 18mths and around year 6. Based on faecal shedding after OPV challenge.	[89, 90]
	f_σ	0.800	0.750	0.950	Paralytic poliomyelitis.	[91, 92]
	w	0.050	0.033	0.067	After priming doses. Very limited data; made assumptions based on cited studies.	[93–95]
Polio vaccine-derived cVPD2 / IPV-OPV sequential	f_λ	0.220	0.180	0.422	Shedding after mOPV2 challenge as the proxy.	[96, 97]
	f_σ	0.800	0.750	0.950	Paralytic poliomyelitis.	[91, 92]
	w	0.050	0.033	0.067	After priming doses. Very limited data; made assumptions based on cited studies.	[93–95]
Haemophilus influenzae type B (as part of pentavalent vaccine)	f_λ	0.600	0.500	0.800	3 infant doses at months 2, 4, and 6.	[98, 99]
	f_σ	0.180	-0.020	0.330	Radiologically confirmed pneumonia.	[100]
	f_σ	0.940	0.780	0.980	Meningitis.	[101, 102]
	w	0.067	0.050	0.100	After priming doses. Very limited data; made assumptions based on cited studies.	[103–105]
Pneumococcal conjugate vaccine (10-valent)	f_λ	0.560	0.410	0.720	2 infant doses at months 2, 4; dose 3 at month 12. Protection against carriage among toddlers.	[106, 107]
	f_σ	0.350	0.260	0.430	Radiologically confirmed pneumonia.	[108, 109]
	f_σ	0.920	0.580	0.990	Meningitis, other invasive disease.	[110]
	w	0.120	0.090	0.200	Based on schedule with a booster in year 2. Waning may be faster without a booster [111].	[111, 112]
Rotavirus (1-valent), ROTAVAC	f_λ	0.390	0.160	0.570	3 infant doses at months 2, 4, and 6. Based on household transmission studies.	[113]
	f_σ	0.889	0.809	0.935	Hospitalisations ('developed country' model).	[114, 115]
	w	0.285	0.000	0.494	After priming doses.	[116, 117]

† f_λ: vaccine effectiveness against infection. f_σ : vaccine effectiveness against severe disease. w: waning rate per year.

4.2.2 Other infections

Table 11 summarises starting susceptibility assumptions made for infections not included in Gaza's pre-war vaccination programme. For certain endemic infections (COVID-19, influenza and para-influenza, RSV, other bacterial gastroenteritis) we make no susceptibility assumptions in this iteration of the model (see below).

Table 11. Baseline susceptibility assumptions made for infectious diseases not included in the vaccination schedule.

Category	Infectious disease	Assumed % immune against infection and disease	Justification
Endemic	Other bacterial gastroenteritis	No assumption	We assumed that the crisis has not resulted in reductions in immunity to these pathogens.
	COVID-19		
	Influenza, para-influenza		
	Other viral gastroenteritis		
	RSV		
Epidemic	Bacterial dysentery (*Shigella dysenteriae* type 1)	0%	Likely to be circulating in Gaza based on non-zero reporting of shigellosis cases by the MoH pre-war, but at a low level.
	Cholera	0%	No known circulation in Gaza during the past decade.
	Hepatitis A	neonates (0mo): 80% 1 to 11mo: 60% 12 to 59mo: 80% 5 to 9yo: 93% older ages: 95%	Initial maternally acquired immunity followed by rapid, near-universal exposure in childhood. Values approximated from seroprevalence studies in Palestine [118] and from nearby countries [119].
	Hepatitis E	0%	No known circulation in Gaza during the past decade.
	Meningococcal meningitis	0%	While *N. meningitidis* does circulate in Gaza, it is likely based on mortality data that transmission intensity is low.
	Typhoid fever	0%	Low level of transmission in previous years (≈ 15 cases reported per year between 2016 and 2022).

4.2.3 Model implementation

We ran the model from January 2000 to the present, using historical crude birth and death rates. Death rates were distributed across age groups based on the death rates by age group in 2019 and 2022 as reported by the Ministry of Health (Gaza) [12, 120–122]. We had to make assumptions about the force of infection (FoI) that susceptible people were exposed to during the model period. The MoH reported no recorded cases of polio and diphtheria, so we assumed there was no naturally acquired immunity to these diseases. To capture naturally acquired immunity to other infections, we assumed a fixed annual FoI. Surveillance for measles and Hib disease captured small outbreaks during 2000-2023, so we used yearly incidence rates to inform force of infection (FoI). Due to lack of specific surveillance, we assumed force of infections of 500, 37 (or 50% cumulative by age 5 years), and 9 per 1000 for pertussis, pneumococcus, and rotavirus respectively, based on surveillance studies from Gaza or elsewhere [123, 124]. Due to uncertainty around these assumptions, we also performed a sensitivity analysis, finding that initial susceptibility to pertussis infection ranged from 30% under a scenario with no background infection to 10% under the assumed FoI. Rotavirus susceptibility was above 75% until FoI was increased above 0.365, where susceptibility was estimated to be around 50%.

4.3 Epidemics model

4.3.1 General framework

All epidemic-prone pathogens under consideration can be modelled using a Susceptible - Exposed - Infectious - Recovered (SEIR) framework [125], represented in Figure 5. The terms 'exposed' and 'recovered' mean infected but not yet infectious, and immune due to natural or vaccine-induced exposure, respectively. Over the short timeframe of the projection period, it is reasonable to assume zero waning of immunity back into the susceptible compartment, though this will occur for some pathogens (e.g. cholera) with time. Transitions among compartments are governed by λ, the force of infection (incidence acting on susceptibles), ρ, the rate of transition out of the pre-infectious state (where ρ^{-1} is the mean pre-infectious period) and γ, the rate of transition out of the infectious state (where γ^{-1} is the mean duration of infectiousness).

$$
\boxed{\begin{array}{c} S \\ \text{(susceptible)} \end{array}} \xrightarrow{\lambda} \boxed{\begin{array}{c} E \\ \text{(pre-infectious)} \end{array}} \xrightarrow{\rho} \boxed{\begin{array}{c} I \\ \text{(infectious)} \end{array}} \xrightarrow{\gamma} \boxed{\begin{array}{c} R \\ \text{(immune)} \end{array}}
$$
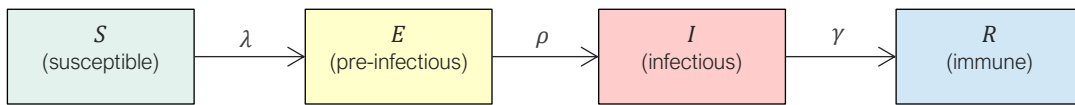
Figure 5. Schematic representation of a susceptible-exposed-infectious-recovered model.

We model deaths attributable to epidemics of each disease as realisations of a SEIR transmission dynamics process, conditional on a binomial probability of an epidemic occurring during the projection period T :

$$
\text{Bin}(p_{u,T}) \begin{cases} 1, D_{u,a,T} = \int\limits_{t=0}^{t=T} f_{\text{SEIR},t}(N_a, \mathcal{R}_{0,u,t}, \rho_u, \gamma_u, S_{\lambda,a,t=0}, \vartheta_u, \mu_{u,a,t}, S_{\vartheta,a,t=0}) \\ \\ \qquad\qquad 0, D_{u,a,T} = 0 \end{cases}
$$

where $p_{u,T}$ is the probability of an epidemic during the period; N_a is population; $\mathcal{R}_{0,u,t}$ is the basic reproduction number and is allowed to vary over time; $S_{\lambda,a,t=0}$ and $S_{\vartheta,a,t=0} = N_a - V_{\vartheta,a,t=0}$ is the number of people susceptible to infection and disease, respectively, as estimated above; ϑ_u is the proportion of infections that result in symptomatic disease; and $\mu_{u,a,t}$ is CFR, also time-varying.

Specifically, we computed deaths over each time step by multiplying incident infections by the proportion symptomatic and CFR, corrected for the time-dependent probability of being immune to severe disease, conditional on not being immune to infection:

$$
\frac{dD_a}{dt} = \frac{dE_a}{dt} \vartheta_u \mu_{a,t} \frac{S_{\vartheta,a,t}}{S_{\lambda,a,t}} \text{ , where } S_{\vartheta,a,t} = S_{\vartheta,a,t=0} - \int_0^t \frac{dE_a}{dt}
$$

The dependency of some of the above parameters on specific crisis-emergent risk factors and health service disruptions is summarised in Table 12.

Table 12. Risk factors and health service disruptions relevant to the transmissibility and case-fatality of infections (other than increased susceptibility due to reduced vaccination coverage).

Parameter	Description	Risk factor					Health service disruptions to…			
		Susceptibility (modelled)	Already circulating?	Inadequate WASH	Deteriorating nutrition	Over-crowding, poor shelter	Outpatient curative care	Inpatient antimicrobial treatment	Inpatient respiratory support	Inpatient rehydration
$p_{u,t}$	Probability of an epidemic	X	X	X	X	X	X			
$\mathcal{R}_{0,u,t}$	Basic reproduction number			X	X	X	X			
$\mu_{u,a,t}$	CFR of symptomatic cases				X		X	X	X	X

4.3.2 Model implementation

For each pathogen u, we implemented an age-structured SEIR model with the following age groups: 0 months, 1- to 11 months, 12- to 59 months, 5- to 14 months, 15- to 19 months, and thereafter ten-year age groups with the oldest age group being ≥ 80yo. We ignored births, deaths and aging due to the short model timeframe. We extracted estimates of ρ and γ from the literature (see Table 13). The force of infection λ was computed assuming transmissibility $\mathcal{R}_0/\gamma$ (where $\mathcal{R}_0$ is the basic reproduction number) and a heterogeneous age-specific contact structure, for which we used the R socialmixr [126] package to upload and prepare a contact matrix previously estimated among a population of camp-based internally displaced persons in Somaliland: to our knowledge this constitutes the only available dataset of social contact structure among displaced people [127] (Figure 6). Lastly, we initialised the $I_{a,t=0}$ compartment as 1 per million population per age group, with $E_{a,t=0} = 0$ and $R_{a,t=0} = N_a - S_{\lambda,a,t=0} - I_{a,t=0}$.

We used the R package epidemics [128] to implement multiple runs of each disease-specific SEIR model over daily time increments, and compute cumulative infections at the end of the projection period. For each simulation, we propagated uncertainty as follows:

- We sampled from an empirical distribution of p_u, the probability of an epidemic occurring during the 6-month projection period (see below for how this was estimated), and drew a random binomial realisation from the sampled p_u value to decide whether an epidemic would in fact take place during the period;

- Conditional on an epidemic taking place, we selected a random starting day for the epidemic within the projection period;

- We sampled from empirical distributions of $\mathcal{R}_0$ and μ_a (the age-specific CFR) obtained as described below, with values specific to each sub-period (months 1 to 3, months 4 to 6); and from a uniform distribution of the range of ϑ_u, the proportion of symptomatic infections, sourced from the literature (see Table 13)

We implemented 10,000 simulation runs and computed the mean and 95% percentile interval of cumulative deaths. All epidemic-attributable deaths are counted as excess mortality, due to the absence of major epidemics in Gaza over the decade prior to the war.

Table 13. Estimates of the pre-infectious and infectious period and of the proportion of symptomatic infections, by infectious pathogen.

Infectious disease	Pre-infectious period (ρ^{-1}, days)		Infectious period (γ^{-1}, days)		Proportion of symptomatic infections (ϑ)		
	value	sources	value	sources	minimum	maximum	sources
bacterial dysentery (*S. dysenteriae* type 1)	2.0	[129]	27.0	[130]	0.188	0.450	[131, 132]
cholera	1.4	[133]	5.0	[134, 135]	0.108	0.589	[136]
diphtheria	1.4	[80]	12.8	[80]	0.700	0.700	[80]
hepatitis A	16.0	[137]	21.0	[137]	0.090	0.700	[138, 139]
hepatitis E	34.0	[140]	40.0	[140]	0.300	0.540	[141]
measles	10.0	[142]	8.0	[137]	0.750	0.960	[143]
meningococcal meningitis	2.0	[144]	12.0	[144]	0.000	0.329	[145]
pertussis	9.0	[129, 137]	16.0	[129, 137]	0.700	0.950	[146]
polio - vaccine-derived	4.0	[147]	16.8	[147]	0.005	0.020	[148, 149]
polio - wildtype							
typhoid fever	10.0	[150]	28.0	[151]	0.583	0.980	[129, 152]
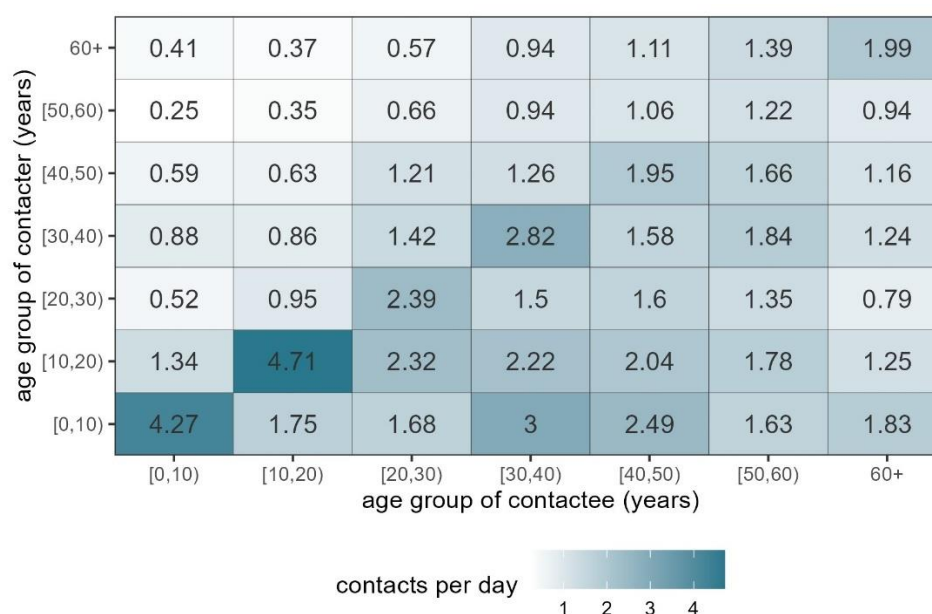
Figure 6. Number of daily contacts between age groups, based on van Zandvoort et al [127].

4.4 Endemic infections model

4.4.1 General equation

For each endemic infection u and age group a, we estimated mortality during the period to date and projection periods as a function of a counterfactual baseline drawn from pre-war data (see below), multiplied by relative risks of transmission $\varphi_{\lambda,u,t}$ and case-fatality $\varphi_{\mu,u,t}$, with adjustment for the seasonal pattern of incidence $\omega_{u,t}$, as follows:

$$D_{u,a,t} = D_{u,a,\text{base}}\omega_{u,t}\varphi_{\lambda,u,t}\varphi_{\mu,u,t}$$

Specifically, $\varphi_{\lambda,u,t}$ and $\varphi_{\mu,u,t}$ are the ratios of, respectively, $\mathcal{R}_{0,u}$ and CFR during the crisis to $\mathcal{R}_{0,u}$ and CFR under the counterfactual baseline, while $\omega_{u,t}$ is the ratio of cases expected during the calendar month that t falls within to the mean number of cases per month over a typical calendar year.

While seasonality is assumed to be crisis-independent, as for epidemics we recognise that several risk factors and health service disruptions may combine to determine $\varphi_{\lambda,u,t}$ and $\varphi_{\mu,u,t}$ (Table 12). Reduced immune protection against infection and disease would also affect $\varphi_{\lambda,u,t}$ and $\varphi_{\mu,u,t}$, respectively if the disease is targeted by the routine vaccination programme. However, for the current projections we assume that these reductions are negligible (see main Report, Annex), and that herd immunity built up over the past years of very high vaccination coverage would largely protect the most vulnerable. In future projections, we plan to relax these assumptions and explicitly introduce estimated susceptibility.

4.4.2 Counterfactual mortality

Pre-war trends in the number of deaths due to infections are shown in Figure 7. All are assumed to be due to endemic infections. We fitted a negative binomial model of this count, offset by $\ln N$ and with the proportion of deaths due to COVID-19 as the single explanatory variable. The model had reasonable fit to the data (Figure 7), and we used it to forecast a counterfactual (no war) value of infectious disease deaths in 2023 and 2024, setting the percent due to COVID-19 at 30%, consistent with COVID-19 proportional mortality in England and Wales during the first half of 2023 [153]. This provided a counterfactual level of all-age deaths.
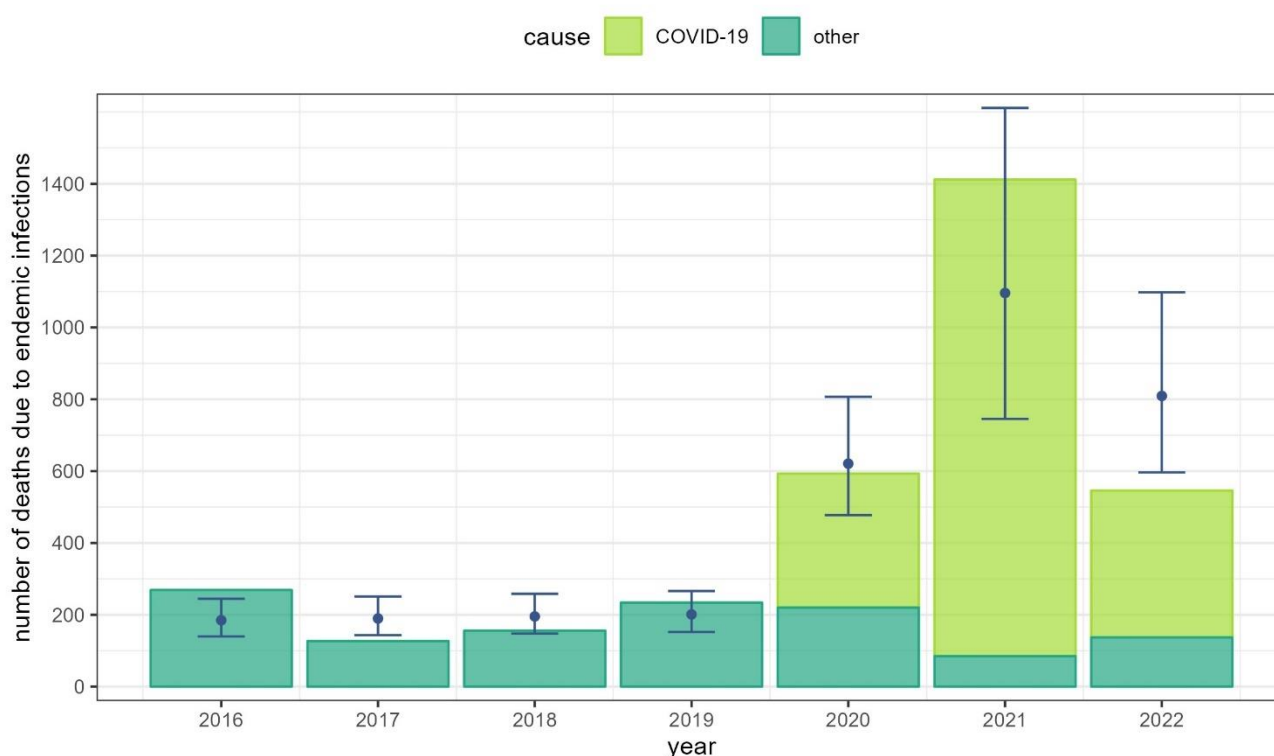
Figure 7. Number of deaths due to infectious diseases per year, by cause (COVID-19 or other). Source: Ministry of Health, Gaza. The blue dots and error bars denote, respectively, the mean and 95%CI of a negative binomial model fit to the data.

4.4.3 Age- and disease-specific distribution of mortality

We distributed deaths by specific disease and among age groups based on available pre-war data from the Gaza Strip, or, if unavailable, the West Bank. Pre-war, data from 2017 showed that infectious disease deaths were overwhelmingly due to airborne-droplet transmitted infections, with only 7 deaths cumulatively due to gastroenteritis or other mostly faecal-oral route transmitted pathogens (an alternative source, the Global Burden of Disease project, estimated that 20-25 would occur per year, still a small minority of the total). Accordingly, we assumed that on an annualised basis $D_{u,a,\text{base}}$ in the war to date and projection periods would be split into 30% due to COVID-19 (see above), with the remaining 70% divided between other airborne-droplet diseases (95% of 70% = 66%) and faecal-oral diseases (5% of 70% = 4%).

We then divided these above proportions by disease and age groups based on observational or disease burden modelling studies of Gaza, where available, the West Bank alternatively, or, as a last resort, the Middle East region: these values are shown in Table 14.

Table 14. Assumed disease-specific and age distribution of baseline endemic infectious disease mortality.

Infectious disease	Proportion of deaths	Source	Age distribution of mortality													Source
			<1 mo	1-11 mo	12-59 mo	5-9 yo	10-14 yo	15-19 yo	20-29 yo	30-39 yo	40-49 yo	50-59 yo	60-69 yo	70-79 yo	≥80 yo	
Airborne-droplet other than COVID-19 (66%)																
Hib disease	0.00	[154]	0.100	0.600	0.300	0.000	0.000	0.000	0.000	0.000	0.000	0.000	0.000	0.000	0.000	[155]
pneumococcal disease	0.50	[156]	0.002	0.023	0.096	0.024	0.015	0.010	0.022	0.035	0.051	0.088	0.151	0.189	0.295	[156]
RSV	0.13	[157]	0.011	0.124	0.520	0.152	0.008	0.008	0.000	0.024	0.000	0.016	0.023	0.040	0.073	[158]
influenza, para-influenza	0.37	all other deaths	0.000	0.003	0.014	0.030	0.015	0.019	0.061	0.131	0.138	0.249	0.069	0.110	0.160	[158]
Airborne-droplet, COVID-19 (30%																
COVID-19	0.30	see text	0.000	0.000	0.010	0.000	0.000	0.000	0.013	0.023	0.033	0.082	0.191	0.293	0.355	[159, 160]
Faecal-oral (4%)																
rotavirus	0.20	[161]	0.010	0.113	0.473	0.030	0.029	0.025	0.040	0.031	0.019	0.012	0.007	0.165	0.046	[162]
other viral gastroenteritis	0.40	[162]	0.010	0.113	0.473	0.030	0.029	0.025	0.040	0.031	0.019	0.012	0.007	0.165	0.046	[162]
bacterial gastroenteritis	0.40	[162]	0.100	0.600	0.300	0.000	0.000	0.000	0.000	0.000	0.000	0.000	0.000	0.000	0.000	[162]

4.4.4 Seasonality

We reviewed MoH data or, failing this, observational studies from Gaza, the West Bank or the Middle East to divide annual caseload (and thus mortality) into monthly fractions, as shown in Table 15.

Table 15. Assumed proportion of annual cases occurring within a given calendar month.

Infectious disease	Proportion of annual cases occurring within a given month												Source
	Jan	Feb	Mar	Apr	May	Jun	Jul	Aug	Sep	Oct	Nov	Dec	
Airborne-droplet transmitted													
Hib disease	0.083	0.083	0.083	0.083	0.083	0.083	0.083	0.083	0.083	0.083	0.083	0.083	No evidence of seasonality [154]
pneumococcal disease	0.083	0.083	0.083	0.083	0.083	0.083	0.083	0.083	0.083	0.083	0.083	0.083	No evidence of seasonality [158]

Infectious disease	Proportion of annual cases occurring within a given month												Source
	Jan	Feb	Mar	Apr	May	Jun	Jul	Aug	Sep	Oct	Nov	Dec	
RSV	0.316	0.140	0.158	0.111	0.022	0.009	0.007	0.007	0.007	0.002	0.033	0.187	[158]
COVID-19†	0.154	0.523	0.042	0.003	0.001	0.001	0.184	0.089	0.003	0.000	0.000	0.000	[159]
Influenza, para-influenza	0.338	0.163	0.137	0.054	0.022	0.004	0.001	0.001	0.003	0.005	0.031	0.240	[158]
Faecal-oral transmitted													
rotavirus	0.083	0.083	0.083	0.083	0.083	0.083	0.083	0.083	0.083	0.083	0.083	0.083	No evidence of seasonality [163]
other viral gastroenteritis	0.083	0.083	0.083	0.083	0.083	0.083	0.083	0.083	0.083	0.083	0.083	0.083	No data: assumed no seasonality
bacterial gastroenteritis	0.083	0.083	0.083	0.083	0.083	0.083	0.083	0.083	0.083	0.083	0.083	0.083	No data: assumed no seasonality

† Observed seasonal pattern may reflect transition between pandemic and endemic conditions and ongoing emergence of new variants.

4.4.5   Model implementation

We implemented 10,000 runs of the endemic infections model, each time sampling from the prediction of the negative-binomial model of baseline (counterfactual) deaths and the distributions of $\varphi_{\lambda,u,t}$ and $\varphi_{\mu,u,t}$ (see below for how these quantities were computed). In each run, we calculated excess deaths as $D_{u,a,t} - D_{u,a,\text{base}}$. We computed the mean and 95% percentile intervals of run outputs.

4.5   Sources of transmissibility and case-fatality estimates

4.5.1   Structured expert elicitation

To implement models for epidemics and endemic infections, we required estimates of several quantities not directly estimable from available data: the probability of an epidemic occurring p_u, the basic reproduction number $\mathcal{R}_{0,u}$ and the age-specific CFR $\mu_{u,a}$, which in turn are needed to construct the $\varphi_{\lambda,u,t}$ and $\varphi_{\mu,u,t}$ RRs needed for the endemic infections model.

We used structured expert elicitation (SEE) [164], combined with values from the literature, to help quantify these parameters. Seven infectious disease experts were invited via email to answer an online structured questionnaire on the ODK platform after consenting to participate in the study. The panel was provided with information related to the three scenarios (see main Report), which included information on current and estimated future values of infection-relevant risk factors (including our projections of acute malnutrition and breastfeeding prevalence: see previous chapter) and health service disruptions. After the presentation of each scenario, they were asked for their best estimates of the following: the probability of an epidemic occurring during the next six months for each epidemic-prone pathogen included in analysis; the basic reproductive number of measles and cholera, and the CFR of symptomatic measles and cholera cases. Experts were also provided with information on the occurrence and timing of epidemics in past crises (see Appendix), and on the published range of both $\mathcal{R}_{0,u}$ and CFR μ_u. Measles and cholera were selected as exemplars of two transmission routes, namely airborne-droplet and faecal-oral respectively, since these share key commonalities including risk factors and (mostly) treatment requirements (antibiotics and respiratory support for the former; antibiotics and rehydration for the latter). This was done to avoid an unmanageably long questionnaire and pre-empt repetitive or uninformative answers.

For each quantity, experts were asked to provide estimates for three probability quintiles: their lowest-reasonable estimates (10th percentile, or ' there is a <10% chance that the value is even lower'), most-likely (50th percentile) and highest-possible (90th percentile, or 'there is a <10% chance that the value is even higher'), for the two subperiods of the projection period (1-3 months and 4-6 months). Experts were also asked

to answer 10 so-called 'calibration' questions in order to assess expert reliability, using the same 10-50-90% scheme: these questions concerned key infection parameters and have a strongly evidence-based answer. The answers to the calibration questions were used to generate calibration and information scores for each expert, as shown by Cooke et al. [164] and in an online course. The two scores were multiplied together to generate a weight for each expert, and compute weighted mean probability distributions for each elicited parameter, as shown in Figure 8, Figure 9 and Figure 10.
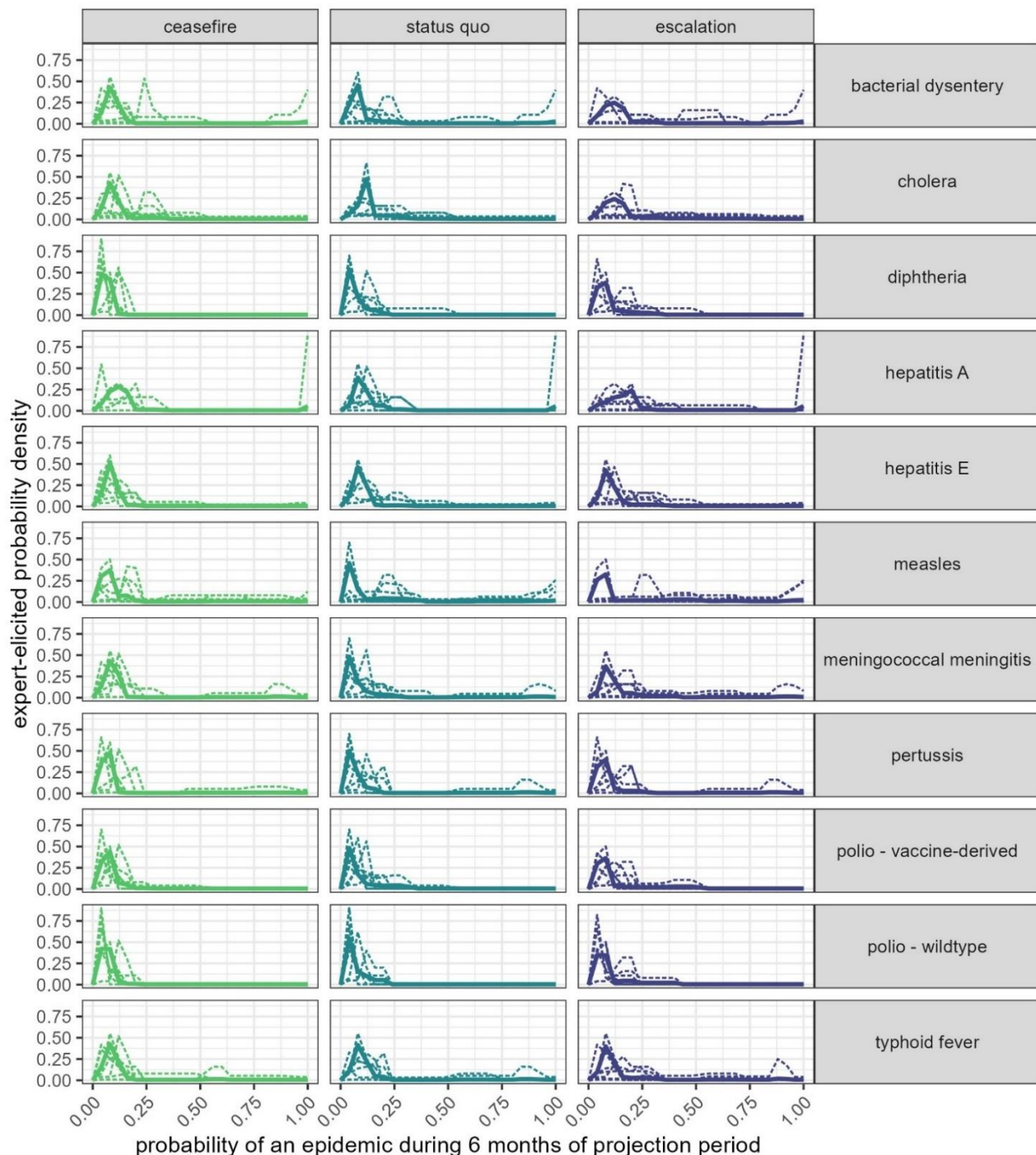
Figure 8. Probability of an epidemic in the next 6 months, according to the SEE experts under the three scenarios. The thick line represents the weighted aggregated value, used in the subsequent models.
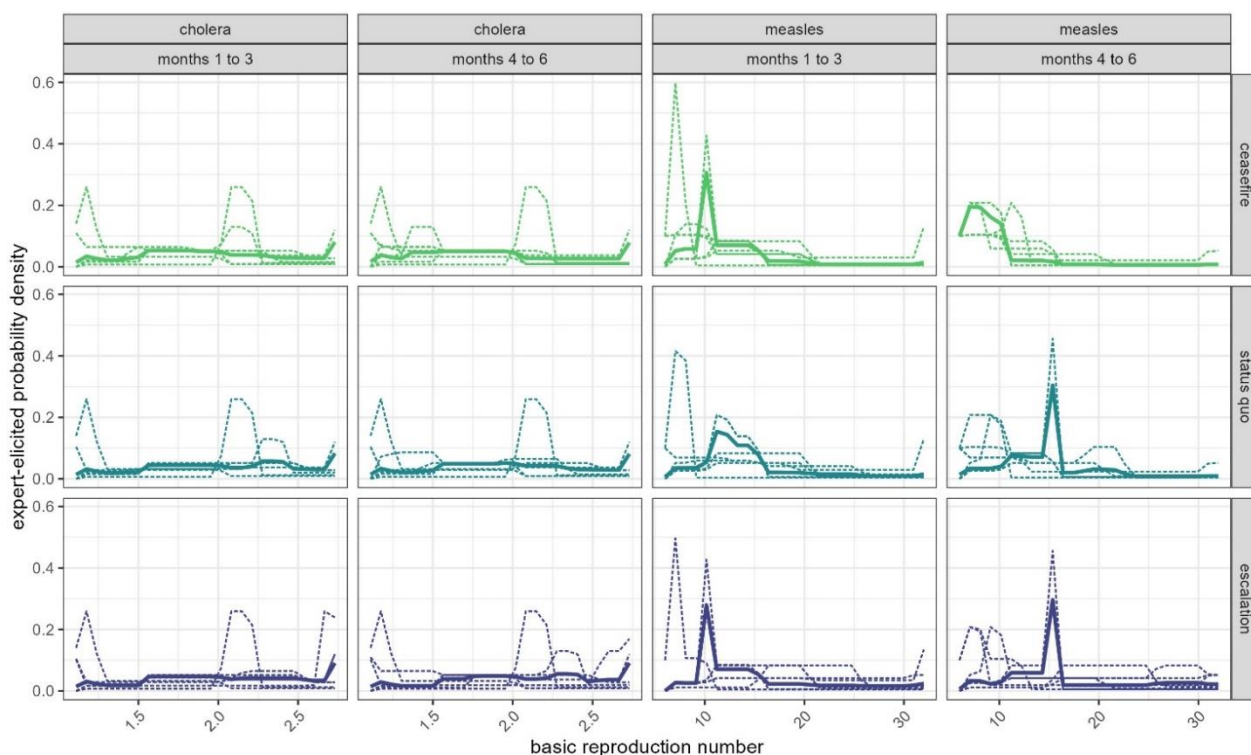
Figure 9. Basic reproductive numbers for cholera (representative disease of faecal-oral transmission diseases) and measles (representative disease for airborne droplet transmission diseases) for two sub-periods of the projections in the 3 scenarios, according to the SEE experts. The thick line represents the weighted aggregated value, used in the subsequent models.
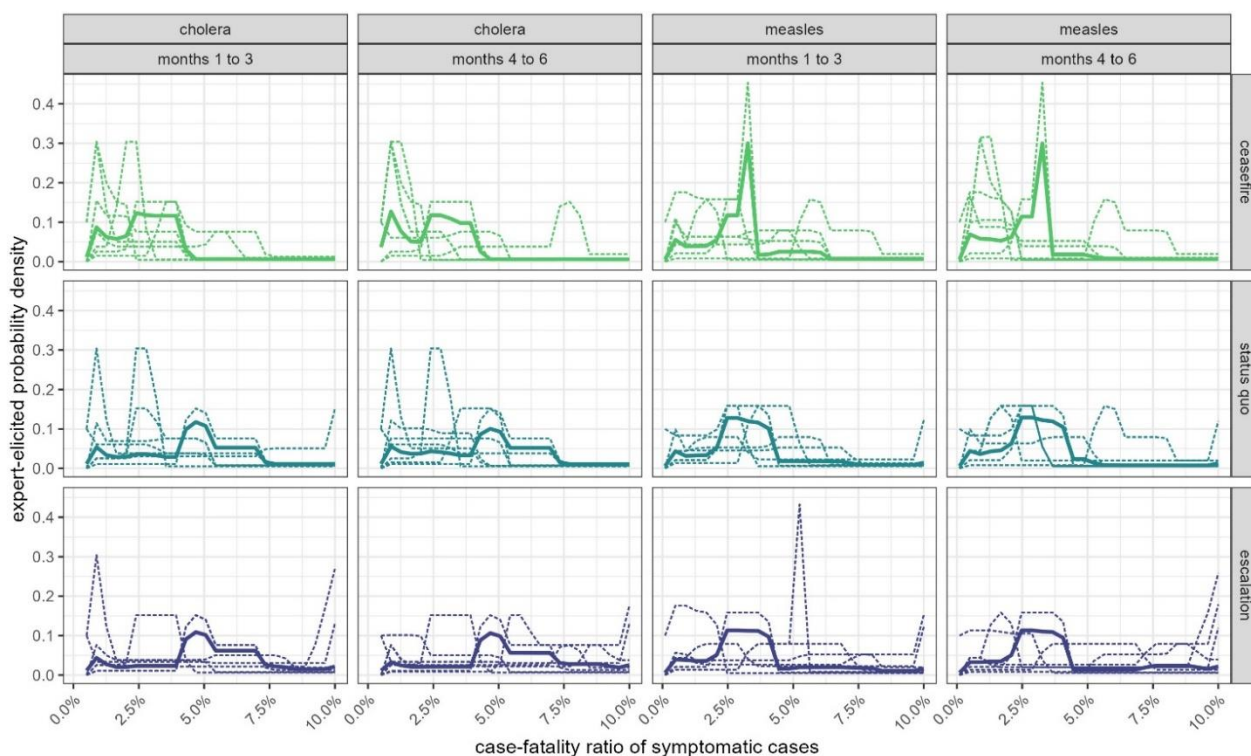
Figure 10. case-fatality ratios of symptomatic cases of cholera (representative disease of faecal-oral transmission diseases) and measles (representative disease for airborne droplet transmission diseases) for two sub-periods of the projections in the 3 scenarios, according to the SEE experts. The thick line represents the weighted aggregated value, used in the subsequent models.

For measles $\mathcal{R}_{0,u}$ specifically, we found that experts provided values that were similar or lower than plausible estimates pre-war, based on European and North American cities (12 to 18). After consultation with a separate group of infectious disease experts, we decided to override the elicitation panel and revise the distribution of $\mathcal{R}_{0,\text{measles}}$ as Runif(16,20), Runif(20,24) and Runif(24,28) for the ceasefire, status quo and escalation scenarios during months 1-3, and Runif(18,22), Runif(22,26) and Runif(26,30) respectively during months 4-6.

4.5.2 Transmissibility estimates

For measles and cholera, we directly sampled the empirical cumulative probability distributions of $\mathcal{R}_{0,u}$ as computed above during epidemic simulations (with the revised measles values). For other epidemic-prone pathogens, we quantified the projected $\mathcal{R}_{0,u}$ based on their published range, and the relative position on this range that corresponded to the relative position of their exemplar disease's $\mathcal{R}_{0,u}$. For example, for diphtheria

$$\mathcal{R}_{0,\text{diphtheria}} = \mathcal{R}_{0,\text{diphtheria,min}} + \left(\mathcal{R}_{0,\text{diphtheria,max}} - \mathcal{R}_{0,\text{diphtheria,min}}\right) \frac{\text{Rand}[\text{ECDF}(\mathcal{R}_{0,\text{measles}})]}{\left(\mathcal{R}_{0,\text{measles,max}} - \mathcal{R}_{0,\text{measles,min}}\right)}$$

where the minimum and maximum values are taken from the published literature (Table 16).

For endemic infections, we pre-defined a plausible range within which the pre-war (subscript $_\text{base}$) theoretical transmissibility of both exemplar diseases would lie. For measles, we took the published range of $\mathcal{R}_0$ in European and North American cities (i.e. $\mathcal{R}_{0,\text{measles,base}}$ = 12 to 18) [165], while for cholera we reasoned that baseline transmissibility would have been just below the minimum values estimated during actual cholera outbreaks, shown in Table 16 ($\mathcal{R}_{0,\text{cholera,base}}$ = 0.8 to 1.0); this reflects the observation that in the Middle East, cholera has only taken hold in crisis-affected settings and not where public health services were functional [166–169]. We then computed each simulation run's $\varphi_{\lambda,u,t}$ as $\frac{\text{Rand}[\text{ECDF}(\mathcal{R}_{0,\text{measles,SEE}})]}{\text{Runif}(\mathcal{R}_{0,\text{measles,base,min}}, \mathcal{R}_{0,\text{measles,base,max}})}$ for all airborne-droplet transmitted infections, and $\frac{\text{Rand}[\text{ECDF}(\mathcal{R}_{0,\text{cholera,SEE}})]}{\text{Runif}(\mathcal{R}_{0,\text{cholera,base,min}}, \mathcal{R}_{0,\text{cholera,base,max}})}$.

Table 16. Values of the basic reproduction number, for each epidemic-prone pathogen.

| Infectious disease	Minimum			Maximum		
	value	source	notes	value	source	notes
bacterial dysentery (*S. dysenteriae* type 1)	1.100	[170]	US outbreaks, but of *S. sonnei*	2.200	[170]	US outbreaks, but of *S. sonnei*
cholera	1.110	[171]	Zimbabwe	2.730	[171]	Zimbabwe
diphtheria	1.700	[80]	Synthesis of various studies	7.100	[172] [173]	Mean of two refugee camps, Bangladesh
hepatitis A	1.100	[174]	USA	2.700	[138]	children in China
hepatitis E	2.110	[175]	Uganda	8.500	[140]	Refugees in Uganda
measles	6.000	[176]	Systematic review of outbreaks	32.000	[176]	outbreaks
meningococcal meningitis	1.310	[177]	Italy	2.500	[178]	Nigeria
pertussis	5.500	[179]	Europe	17.000	[180]	Systematic review
polio - vaccine-derived	1.620	[181]	Latest polio outbreak in Israel	12.000	[182]	Afghanistan, Pakistan
polio - wildtype	1.620	[181]	Latest polio outbreak in Israel	12.000	[182]	Fully reverted vdPV seems to have similar transmissibility as wPV [183].
typhoid fever	2.800	[151]	no variability found in the literature	2.800	[151]	no variability found in the literature

4.5.3 Case-fatality parameters

We did not make any rectifications to SEE-derived CFR distributions, and sampled from these as described above, with the same scaling as for transmissibility to come up with values for the other epidemic-prone pathogens or $\varphi_{\mu,u,t}$. During SEE, we asked experts to specify the CFR while thinking of the age group 12 to 59mo, which we took as the reference. We computed the CFR for other age groups based on published estimates of their relative difference from this reference group (Table 17).

Table 17. Estimates of case fatality ratio of symptomatic cases, by age and by pathogen.

Infectious disease	Case-fatality ratio (%)				Relative risk, compared to the 12-59mo category													Source
	minimum (source)		maximum (source)		<1 mo	1-11 mo	12-59 mo	5-9 yo	10-14 yo	15-19 yo	20-29 yo	30-39 yo	40-49 yo	50-59 yo	60-69 yo	70-79 yo	≥80 yo	
bacterial dysentery	0.6	[184]	7.4	[184]	1.72	1.72	1	0.69	0.69	0.44	0.44	0.44	0.44	0.44	0.44	0.44	0.44	[185]
cholera	0.5	[186]	10.0	[186]	1.00	1.00	1	1.00	1.00	1.00	1.00	1.00	1.80	1.80	3.00	3.00	3.00	[187]
diphtheria	5.0	[80]	50.0	[80]	1.00	1.00	1	0.34	0.34	0.34	0.42	0.42	0.42	0.42	0.42	0.42	0.42	[80]
hepatitis A	0.02	[188]	1.8	[129]	1.00	1.00	1	1.00	1.00	1.00	1.35	1.35	7.89	7.89	14.88	14.88	14.88	[189]
hepatitis E	1.6	[190]	6.8	[190]	1.00	1.00	1	1.00	1.00	1.00	1.00	1.00	1.00	1.00	1.00	1.00	1.00	[191, 192]
measles	0.1	[193]	10.0	[193]	1.00	1.00	1	0.26	0.26	0.26	0.26	0.26	0.26	0.26	0.26	0.26	0.26	[193]
meningococcal meningitis	0.0	[194]	50.0	[194]	1.00	1.00	1	1.00	1.00	1.00	1.00	1.00	1.00	1.00	1.00	1.00	1.00	[194]
pertussis	0.7	[195]	15.0	[195]	3.70	3.70	1	0.10	0.10	0.10	0.10	0.10	0.10	0.10	0.10	0.10	0.10	[196]
polio - vaccine-derived	6.0	[197]	40.0	[197]	0.90	0.90	1	2.00	2.20	3.60	3.60	4.70	4.70	4.70	4.70	4.70	4.70	[198]
polio - wildtype	6.0	[197]	40.0	[197]	0.90	0.90	1	2.00	2.20	3.60	3.60	4.70	4.70	4.70	4.70	4.70	4.70	[198]
typhoid fever	0.6	[199]	8.9	[199]	1.00	1.00	1	1.00	1.00	1.00	1.00	1.00	1.00	1.00	1.00	1.00	1.00	[199]

4.6 Limitations

The following key limitations are noteworthy when interpreting findings from the infectious disease analysis:

- Both the epidemic and endemic models relied on a large number of disease-related parameters, from transmissibility to infectious periods to disease progression, that all carry some uncertainty, especially for diseases that, unlike measles, cholera or COVID-19, have been less well characterised in the literature. We did not have time and resources to conduct systematic reviews of all these parameters, though we relied on reviews where available. While it is unlikely that error in the parameters would have resulted in considerable systematic bias overall (i.e. it is implausible that we would have over- or under-estimated parameter values across all diseases), we have not fully represented this uncertainty in our estimates, especially for parameters, such as age distributions, that were held fixed;

- The immunity tracking analysis is reliant on robust assumptions about vaccine effectiveness and prior force of infection. The latter was difficult to estimate, though it is unlikely, based on sensitivity analysis, to have biassed our findings. For some older-generation vaccines, effectiveness is not particularly well-documented; moreover, we held effectiveness fixed rather than varying it to allow for uncertainty in published reports;

- The SEIR models of epidemics are relatively simplistic, and do not account for two aspects: (i) spatial heterogeneity (for example, it is plausible that there would be pockets of particularly high susceptibility or transmissibility in the worst-off communities in Gaza, among whom transmission and mortality might be a lot higher than our Gaza-scale model can capture); and (ii) interventions that may be implemented

to control epidemics, e.g. reactive vaccination against cholera (we did however incorporate availability of curative care in our scenarios);

- The critical link between malnutrition and infectious disease risk was insufficiently featured in our analysis, and relied solely on elicitation experts' incorporating the acute malnutrition and breastfeeding projections into their judgment, alongside many other risk factors: it is unclear to what extent experts were able to sufficiently weigh malnutrition in their estimates;

- Generally, SEE produced implausible estimates of transmissibility for one of the two exemplar diseases, suggesting problems with the presentation of the questions or their understanding. In future iterations of the method, experts may need to receive more explicit and clear instructions or may need more support in the form of pre-briefings to fully comprehend the information and what is being asked of them.

5   Maternal and neonatal health

5.1   Analysis scope

This module quantifies the potential effects of disruptions in maternal and neonatal health services, deteriorations in the environment, and increasing food insecurity on maternal, neonatal, and stillbirth mortality under the three scenarios (see main Report), using the Lives Saved Tool (LiST; www.livessavedtool.org) to project excess deaths [200]. Specific estimation targets are outlined in Table 18.

Table 18. Mortality outcomes (maternal, neonatal and stillbirth) and sub-causes of death included in this module and used in our models. Deaths due to war injuries and infectious diseases were estimated elsewhere.

Outcome	Definition	Sub-causes of death
Additional maternal deaths	Number of maternal deaths from any cause related to or aggravated by pregnancy or its management during pregnancy and childbirth or within 42 days of termination of pregnancy (direct or indirect maternal deaths, but excluding deaths from co-incidental causes, such as war injuries and deaths linked to any infectious disease epidemics that might occur).	Antepartum haemorrhage, postpartum haemorrhage, hypertensive diseases of pregnancy, sepsis, miscarriage, obstructed labour, ectopic pregnancy, other maternal causes of death.
Additional neonatal deaths	Number of deaths of live born babies during the first 28 completed days of life (excluding war injuries but also deaths linked to any infectious disease epidemics that might occur).	Birth asphyxia, prematurity, sepsis/pneumonia, congenital anomalies, tetanus, diarrhoea, all other causes of death.
Additional stillbirths	Number babies born without signs of life at gestation of 28 weeks or more.	Antepartum, intrapartum.

We consider the following population groups:

- Pregnant or recently delivered women of reproductive age (15-49 years old);

- Neonates (0- to 27 days); and

- Foetuses of 28+ weeks gestation (at risk of stillbirth).

5.2   General approach

Singh and colleagues' framework for understanding the drivers of maternal, neonatal and stillbirth deaths groups drivers into distal, intermediate, and proximate factors [201]. Distal factors include geographic, social, economic, and political factors (including conflict) that influence the underlying epidemiology and the intermediate and proximate risk factors for ill-health and mortality. Intermediate factors include health systems and services, as well as household circumstances, behavioural norms/decisions and individual health status and need. An important distinction from other disease modules is that maternal health status can affect the health status and needs of the foetus or newborn. The framework shows that distal and intermediate health-system factors work either by influencing underlying health status and risk factors, or by changing the coverage of specific health promotive, preventative, or curative behaviours or interventions (proximate drivers), which in turn lead to or prevent ill-health or mortality. This approach aligns with the LiST model which we used as described below [200].

The war in Gaza has impacted distal, intermediate, and proximate factors. The heavy bombardment and ground war have led to direct conflict-related fatalities, while economic collapse, environmental degradation

(e.g. poorer WASH and shelter and more over-crowding) and growing food insecurity have increased the prevalence of risk factors for ill-health and death. Contacts with health services are declining as health facilities stop functioning or become less safe to access, while shortages of health staff and commodities are eroding the coverage of effective interventions and behaviours. These factors will increase the numbers and rates of maternal and neonatal deaths and stillbirths.

5.3   The Lives Saved Tool method

5.3.1   General description

Our main approach for projecting excess deaths in this module was to use LiST to estimate the additional maternal, neonatal, and stillbirth deaths in Gaza above a pre-war baseline (before October 2023) that are likely to stem from reductions in the coverage of maternal and neonatal interventions and deteriorations in environmental conditions and food security.

As with Singh et al's framework, LiST assumes mortality rates and the structure of cause-of-death change only in response to changes in intervention coverage or in levels of risk factors. More distal variables, such as wealth, will operate through increasing coverage of interventions or reducing risk factors. LiST assumes that causes do not change dynamically, and that any differences will stem solely from changes in intervention coverage and risk factors.

LiST was initially developed in 2003 to estimate the impact of scaling-up community-based interventions on child mortality. Currently, LiST uses linear and fixed relationships between inputs and outputs (deterministic model) to estimate the effects of simultaneous changes in coverage of 77 interventions along the reproductive, maternal, newborn, and child health (RMNCH) continuum of care, including all World Health Organization (WHO) recommended interventions. The primary inputs are levels and sub-causes of mortality, and changes in the coverage of interventions. The outputs are changes in cause-specific mortality (maternal and neonatal mortality and stillbirths). The relationship between an input (e.g. a change in intervention coverage) with one or more outputs is specified in terms of the efficacy of the intervention in reducing the probability of the outcome. LiST models were built using a hierarchy of evidence on the effect of interventions on mortality. The ideal estimates of effect were taken from meta-analyses or systematic reviews of individually randomized placebo-controlled trials of the effect of interventions on cause-specific mortality. When such estimates were not available, estimates of efficacy were derived from natural experiments or expert elicitation (such as Delphi methods).

The data, methods, and assumptions of LiST have been previously published [200]. As of mid-January 2024, LiST has been referenced in over 2,360 publications. A 2017 review showed the tool had been used for evaluation, strategic planning, and advocacy [202], Most applications quantified the effect of increases in coverage of effective interventions (e.g. effect of increases in the prevalence of exclusive breastfeeding on reduced neonatal deaths) [203], but some measured the effect of decreases in coverage (e.g. projecting the effects of decreases in use of MNH services due to COVID-19 on increased deaths of mothers and neonates [204].

In this module, we focused on decreases in the coverage of preventive and curative interventions in pregnancy, childbirth, and the postnatal period caused by the war, on the main causes of maternal and neonatal mortality and stillbirth.

Table 19. shows the main interventions considered and the broad groups they affect. An interactive website shows which specific sub-cause of maternal or neonatal death or stillbirth each intervention works against (link). Annex, Figure 14 shows a static version of the same.

Intervention	Calculation	Maternal	Neonate	Stillbirth	Scenario			
					Baseline	Ceasefire	Status quo	Escalation
Antenatal care								
Antenatal care (at least 1 visit)		X	X	X	0.99	0.60	0.25	0.15
Antenatal care (at least 4 visits)			X	X	0.96	0.50	0.20	0.10
TT - Tetanus toxoid vaccination		X	X		0.99	0.99	0.99	0.99
Iron supplementation		X			1.00	0.50	0.20	0.10
Syphilis detection and treatment	ANC1		X	X	0.89	0.60	0.40	0.20
Hypertensive disorder case management	ANC4	X		X	0.85	0.70	0.60	0.50
Diabetes case management	ANC4			X	0.84	0.70	0.60	0.50
Health Facility Childbirth Care								
Health facility delivery (HFD)		X	X	X	0.99	0.90	0.80	0.50
Caesarean delivery		X	X	X	0.27	0.27	0.18	0.12
Blood transfusion	HFD	X			0.88	0.80	0.50	0.30
Assisted vaginal delivery	HFD	X	X	X	0.89	0.80	0.50	0.30
Manual removal of placenta	HFD	X			0.91	0.80	0.50	0.30
Removal of retained products of conception	HFD	X			0.90	0.80	0.50	0.30
Induction of labour for pregnancies lasting 41+ wks.	HFD			X	0.87	0.60	0.20	0.10
Antibiotics for preterm PROM	HFD	X	X		0.96	0.60	0.20	0.10
Antibiotics for maternal sepsis	HFD	X			0.96	0.60	0.20	0.10
MgSO4 for eclampsia	HFD	X			0.96	0.60	0.20	0.10
Uterotonics for postpartum haemorrhage	HFD	X			0.98	0.60	0.20	0.10
Immediate drying and additional stimulation	HFD		X		0.99	0.80	0.65	0.50
Thermal protection	HFD		X		1.00	0.80	0.65	0.50
Clean cord care	HFD		X		0.99	0.80	0.65	0.50
Clean birth environment	HFD	X	X		0.97	0.80	0.65	0.50
Neonatal resuscitation	HFD		X		0.94	0.60	0.40	0.20
Breastfeeding								
Exclusive breastfeeding <1 months			X		0.55	0.36	0.36	0.23
Predominant breastfeeding <1 months			X		0.09			
Partial breastfeeding <1 months			X		0.34			
Not breastfeeding <1 months			X		0.03	0.22	0.22	0.35
Curative neonatal care								
ORS - oral rehydration solution			X		0.25	0.15	0.08	0.02
Antibiotics for treatment of dysentery			X		0.19	0.11	0.06	0.01
Oral antibiotics for pneumonia			X		0.77	0.46	0.23	0.06
Injectable antibiotics for neonatal sepsis	HFD		X		0.96	0.60	0.20	0.10
Water and sanitation indicators (WASH)								
Basic sanitation (latrine or toilet)			X		0.99	0.10	0.01	0.01
Point-of-use filtered water			X		0.02	0.02	0.01	0.01
Piped water			X		0.03	0.03	0.01	0.01
Hand washing with soap			X		0.95	0.20	0.35	0.60
Food security as caloric restriction								
% households with food insecurity via calorie restriction			X	X	0.44	0.48	0.57	0.61

Blue shaded interventions are linked to health facility delivery (HFD) and commodities; Orange shaded: linked to HFD and ANC; Green shaded: linked to HFD and manual procedures that require staff with skills; Pink shaded: linked to HFD and other specific (paediatrician and neonatologist). Note: The interventions calculated via contact such as HFD or antenatal care (ANC) visits, the value in the row represents the level of readiness to deliver the intervention. The final coverage of these interventions was calculated as the product of contact and readiness.

LiST links with a demographic projections model (DemProj) to estimate deaths resulting from changes in cause-specific mortality rates. The equation below describes the calculation for the effects of changes in coverage of interventions on cause-specific mortality [205]:

$$R_{i,j,a,t} = \left[I_{i,j,a} \times \left(C_{i,a,t} - C_{i,a,0} \right) / \left(1 - I_{i,j,a,0} \times C_{i,a,0} \right) \right] \times AF_{i,j,a}$$

where R is the proportional change in mortality from cause of death j for population caused by intervention i at time t ($R_{i,j,a,t}$). The efficacy of each intervention is $I_{i,j,a}$. The change in the coverage of intervention is $\left(C_{i,a,t} - C_{i,a,0} \right)$ and $AF_{i,j,a}$ is the affected fraction describing the proportion of the cause-specific death that is susceptible to the intervention. There is an added term which adjusts for unrealized potential impact: $\left(1 - I_{i,j,a,0} \times C_{i,a,0} \right)$.

In our case, since coverage of more than one intervention is scaled down, the model first calculates the mortality increase for the reduction in the first intervention alone, and then the second intervention acts on the remaining mortality, the third intervention acts on yet remaining mortality etc. The total impact does not depend on the order of the intervention.

Total impact is thus the product of the impact of each intervention:

$$Ri,j,t = 1 - \left(1 - R_{1,j,a,t} \right) \times \left(1 - R_{2,j,a,t} \right) \times \left(1 - R_{3,j,a,t} \right) \times \left(1 - R_{4,j,a,t} \right)$$

LiST assumes no secular trends of mortality rates and allows that the changing coverage of one intervention may affect multiple causes-of-death. However, multiple interventions acting on the same cause are applied sequentially as described above.

The uncertainty analysis tool in LiST uses randomly sampled ranges around the model's inputs to estimate the uncertainty around the models' outputs. For the analysis, we included uncertainty for all five categories of model inputs: efficacy of interventions, mortality rates, sub-causes of death, relative risk of interventions on risk factors, and incidence of severe diseases. In general, beta distributions were used for effectiveness of interventions, correlated normal distributions for mortality rates, Dirichlet distributions for sub-causes of death, and log-normal distributions for relative risks. The plausibility bound was set at 95% (i.e. the ranges of sampled model inputs used). The iteration was set at 400 (i.e. we sampled the model's inputs 400 times). We assumed no correlations between the model inputs. We did not look at uncertainty in the coverage estimates.

5.3.2   Parameters used in the Lives Saved Tool

We estimated changes in maternal, neonatal and stillbirth deaths due to changes in the (1) coverage of single interventions; (2) prevalence of exclusive breastfeeding; (3) indicators of improved water and sanitation; and (4) an indicator of household food security. The complete list of definitions, sources and baseline indicator levels is available in the "Lives saved MNC" spreadsheet. We anticipated that levels of most of our indicators would deteriorate and decline, leading to increased numbers of deaths.

We modelled three scenarios based on varying levels of deterioration (ceasefire, status quo, escalation). We ran the analysis and projected the excess deaths per month, for 1-3 months and 3-6 months, and cumulated over the entire 6 months, starting from 7 February 2024.

Changes in coverage of interventions and exclusive breastfeeding

Pre-war (before 7 October 2023), there were good input data on contacts with key services (antenatal care (ANC) 1+, ANC4+, health facility delivery (HFD)), and on the coverage of some single interventions (e.g. caesarean section). Other interventions such as exclusive breastfeeding in the first month, could be approximated from measures of the coverage of exclusive breastfeeding in first 6 months. Yet others, such as management of hypertension during pregnancy or use of uterotonics to manage postpartum haemorrhage, were estimated based on ANC1+ and ANC4+ or HFD (and outpatient care) respectively. The proportion then getting the individual interventions was estimated by intervention. Because we were unable to find a Health Facility Assessment (HFA), Service Provision Assessment (SPA), or Service Availability and Readiness Assessment (SARA) for Gaza pre-war, we used regional defaults from LiST.

When we needed to estimate coverage for the status quo scenario (15-October to 15-January), we used data on the current functionality of healthcare facilities (ANC and HFD) published by WHO in the Health cluster [206] to roughly approximate changes in contacts with ANC and HFD services for the North and Central/South regions, assuming 20 percent of the population was distributed in the North, and the remainder in the Central/South.

To estimate changes in coverage of specific interventions among those contacting ANC, HFD and outpatient health services, we grouped the specific interventions into (a) those that were commodity-led (general commodities and those likely to be donor supported (e.g. $MgSO_4$ or iron supplementation respectively); (b) those that were primarily manual and required skilled providers (e.g., manual removal of placenta or neonatal resuscitation); (c) those related to the availability of outpatient care (e.g., treatment of neonatal sepsis); and (d) those related to women's behaviours (e.g., exclusive breastfeeding for 1 month).

The decrease in exclusive breastfeeding in the first month was estimated as described in the Malnutrition module.

Deterioration in WASH

The decrease in WASH indicators followed what was implemented in scenario section of the main report.

Increase in food insecurity

LiST includes food insecurity as a household level indicator, meaning it assumes all household members (including neonates and pregnant women) have the same level of food security. Food insecurity is a risk factor for neonatal small-for-gestational age at birth (SGA), stunting, wasting, and stillbirth. We assumed that balanced energy protein (BEP) supplementation completely removed the risk of SGA and stillbirth for food insecure pregnant women. Given that the participants recruited for BEP trials were mostly food insecure, with a marginal nutritional status or low body mass index (BMI), we considered the control group in BEP trials to be food insecure and the intervention group (who received BEP) to be food secure. We then compared the SGA and stillbirth rate between the two groups to get a relative risk of SGA/stillbirth for food insecurity.

To calculate the effect on mortality, we considered three groups: (a) food secure pregnant women, (b) food insecure pregnant women with BEP, and (c) food insecure pregnant women without BEP, as contributing to the overall stillbirth rate. With the baseline coverage of BEP, the efficacy of BEP, the relative risk of food insecurity, and the baseline overall stillbirth rate, we calculated the stillbirth rates for the three groups. The change in food insecurity over time would shift pregnant women among the three groups, resulting in a change in the overall SGA and stillbirth rate. The former would affect neonatal mortality. The increases in food insecurity were based on the percent reduction in estimated caloric intake (as a proxy) of pregnant women.

Food insecurity affects both quality and quantity, but for our model, it was the reduction in quantity that was considered to directly affect mortality.

5.4 Assumptions and limitations

General assumptions and limitations of LiST are well described by Blencowe and colleagues among others, and include the following [207]:

- LiST is a deterministic model, so the outputs are only as good as the inputs, including the baseline causes-of-death structure, the estimated effects of the interventions on mortality, and estimated coverage of the interventions. The quality of data on the sub-causes of maternal death and the antepartum/intrapartum timing of stillbirths is poor [207], and country-level causes-of-death structure for these two causes are less regularly updated. Similarly, data underpinning the efficacy/effectiveness estimates are sparse for some interventions. The ideal effectiveness values were pooled estimates from meta-analyses including several low- and middle-income countries (LMICs). The quantity and quality of studies on interventions reducing stillbirths and maternal deaths are weaker than for neonatal and child outcomes. When the evidence is sparse, effectiveness data were pulled from trials conducted in high-income countries or from expert elicitation (Delphi method). The risk factors for stillbirths and maternal deaths might be different in different countries. The estimated efficacy values from high-income countries or a limited number of LMICs might not be generalizable to other LMICs. However, in contrast to estimation in some of the other module areas in our report, LiST's estimates of effectiveness are based on several years of thorough and scientific work, and the approach is well described [207];

- The effect of an increase in food insecurity on stillbirth and neonatal death is the least tested pathway in LiST. We based the increase of food insecurity on caloric restriction;

- LiST also requires a wide range of national or regional information to set up the baseline profile, e.g. the prevalence of suboptimal birth outcomes and coverage of the interventions. In some cases, the exact data are not available, and estimations or proxies had to be used. For example, reliable population-based coverage data are not available for many interventions [207]. LiST has therefore relied on expert opinion to estimate likely levels of coverage for specific interventions using different levels of coverage reported for ANC and HFD as a proxy. For the analysis, we sought as much available data from Gaza as possible. The abundance of information needed is also the strength of the model because with more information, we were better able to capture the baseline situation of the region;

- The prevalence of specific exposures and risk factors is expected to vary, but data are not available to reliably track these trends over time [207]. LiST assumes most remain static when estimating maternal, neonatal, or stillbirth outcomes, except for certain pathogen-related illnesses (e.g. diarrhoea, pneumonia, and meningitis) which shift as certain interventions are scaled up and the etiological burden changes accordingly. LiST is not well designed to capture epidemics or external causes such as conflict-related mortality, so these are captured in other modules in this project; and

- Quantifying the numbers of lives saved or lost involves some uncertainty because of uncertainty in the ranges for the effectiveness of interventions, mortality rates, and cause-of-death distributions within maternal and neonatal deaths, and stillbirths [207]. LiST can provide upper and lower bounds for all model outcomes, and we have shown these.

Gaza-specific assumptions and limitations include:

- Gaza had good data on contacts with antenatal and childbirth services and on coverage of selected interventions pre-war. Data on provision of interventions was less robust, and there were no specific harmonized health facility assessments (HHFA) or SARA or SPAs. There were adequate data on sub-causes of neonatal death, but we had to resort to regional estimates for sub-causes of maternal deaths and stillbirths;

- Quantification of the changes in contact with services or coverage of specific interventions involved an exceedingly large degree of uncertainty. These challenges applied to reductions in contacts with services (e.g. ANC4+ coverage) and to the content of care provided once contact was made (specific interventions, whether related to commodities or to manual procedures). Moreover, different regions of Gaza were differently affected (the North more than the Central/South), but it is not clear what proportion of the population was exposed the various reductions in coverage, and for how long; and

- Because LiST works with relative risks rather than risk differences, and because in the case of Gaza we were decreasing rather that increasing coverage, we tested what would happen to mortality if we drove the coverage of interventions close to zero (0.1%), to see whether the levels we get are close to "natural" maxima seen for maternal, neonatal, and stillbirth mortality in settings with little care (i.e. 1%, 4% and 4% respectively). The scaling down of interventions to 0.1% gave 0.12%, 2.5%, and 1.3% for maternal mortality ratio, neonatal mortality rate, and stillbirth rate, respectively. This suggests mathematically that because the baseline mortality rates were all low, the estimated mortality rates when coverage is close to zero is lower than the "natural" maxima. It is possible that the model did not capture all the existing interventions in Gaza that contributed to the low pre-war mortality, for example use of rhesus testing or NICUs. The model also depends on having good measures of mortality rate and cause-specific percentages that match. Our pre-war values may be overly optimistic, particularly for MMR where even missing a few deaths makes a big difference.

6 Non-communicable diseases

6.1 Analysis scope

Table 20 lists NCDs included and excluded from the current analysis, and reasons for exclusion. We stratified estimates into the following age groups a: neonatal (<1 month), infant (1 to 11 months), 12-59 months, 5 to 9 years, 1014 years, 15-19 years, 20-29 years, 30-39 years, 40-49 years, 50-59 years, 60-69 years, 70-79 years, and ≥ 80 years.

Table 20. List of non-communicable diseases included and excluded from estimation.

Disease (ICD-10 code)	Reason / additional notes
Included	
Diabetes mellitus type 1 (DM1) (E10)	A more pragmatic distinction could be insulin-dependent versus non-insulin-dependent DM. Obesity (E65 to E68) is considered an antecedent condition.

Cardiovascular diseases (CVD), including
    Ischaemic heart disease (including myocardial infarction, I21 to I25)
    Cerebrovascular diseases including stroke (I60 to I69) (this includes both ischaemic and haemorrhagic stroke, modelled separately due to their different survival: see below)
	CVD is treated as an outcome of hypertension (and DM). As such, primary hypertensive disease (I10) is excluded from analysis.

Chronic kidney disease (CKD) (N18)	Only the most advanced stages of CKD, i.e. those requiring haemodialysis, is considered in this analysis. People requiring peritoneal dialysis are excluded.

Neoplasms (cancer), including
    Colorectal cancer (C18 to C21)
    Lung cancer (C34)
    Breast cancer (C50)
	Highest-burden forms of cancer in Gaza [208].

Excluded	
Diabetes mellitus type 2 (DM2) (E11)	Insufficient data found on survival with and without treatment.

Other forms of cardiovascular disease (CVD), including
    Rheumatic heart disease (I01-I09)
    Hypertensive diseases (I11 to I13)
    Inflammatory heart disease (I30-33, I38, I40, I42)
    Heart failure (I50)
    Diseases of arteries, arterioles and capillaries (I70 to I74)
	Baseline mortality data for Gaza did not allow for unequivocal identification of these CVD causes. Furthermore, insufficient data were found on survival with and without treatment.

Chronic lower respiratory diseases, including
    Emphysema (COPD) (J43)
    Other chronic obstructive pulmonary disease (J44)
    Asthma (J45-J46)
	Insufficient data found on survival with and without treatment.

Neoplasms (cancer), including
    Leukaemia (C91 to C95)
    Thyroid cancer (C73)
    Rarer cancers
	Though leukaemia and thyroid cancer are also among the highest-burden cancers in Gaza [208], we could not identify sufficient data on their survival with and without treatment.

6.2 Methods

6.2.1 General equations

For each NCD u, we consider that excess deaths at any given time t (where dt = 1 month) are the difference between deaths projected in the war period to date or the projection period (subscript 'crisis') and a counterfactual level of baseline mortality (subscript 'base') that would have happened in the absence of the crisis:

$$D_{u,t,\text{ excess}} = D_{u,t,\text{crisis}} - D_{u,t,\text{base}}$$

We can express both the crisis and counterfactual deaths in terms of prevalent treated and untreated cases and their respective risks of death, as follows:

$$D_{u,t,\text{ excess}} = c_{u,t,\text{crisis}} \int_{\tau=1}^{\infty} P_{u,t,\tau,\text{crisis}}\, \mu_{u,\tau,\sigma=1} + \left(1 - c_{u,t,\text{crisis}}\right) \int_{\tau=1}^{\infty} P_{u,t,\tau,\text{crisis}}\, \mu_{u,\tau,\sigma=0} -$$

$$c_{u,t,\text{base}} \int_{\tau=1}^{\infty} P_{u,t,\tau,\text{base}}\, \mu_{u,\tau,\sigma=1} + \left(1 - c_{u,t,\text{base}}\right) \int_{\tau=1}^{\infty} P_{u,t,\tau,\text{base}}\, \mu_{u,\tau,\sigma=0}$$

Here, c denotes treatment coverage, i.e. the proportion of cases who receive appropriate acute and follow-up care. Because the risk of dying for the NCDs analysed is not time-independent (see below), we track prevalent cases P at time t according to their time since onset τ. Prevalent cases experience a τ-specific hazard of death (μ), whose values vary according to whether a case is treated ($\sigma = 1$) or untreated ($\sigma = 0$). Thus, the sum of deaths is the integral of deaths over the range of τ.

6.2.2 Factors other than treatment coverage

We recognise that, in addition to receiving treatment, both the incidence (and thus prevalence) and case-fatality of NCDs may be affected by crisis-emergent risk factors, such that $P_{u,t,\text{crisis}} \sim \varphi_{u,\lambda,t} P_{u,t,\text{base}}$ and $\mu_{u,t,\text{crisis}} \sim \varphi_{u,\lambda,t} \mu_{u,t,\text{base}}$, respectively, where φ denotes a relative risk (RR). For this instance of the projections, we assume that any changes in incidence attributable to the crisis would have a modest effect on excess mortality due to the long-term progression of the NCDs being analysed, and thus set $\varphi_{u,\lambda,t} = 1$. Similarly, we make a simplifying assumption that all excess case-fatality risk is solely due to reduced coverage of acute and long-term treatment, i.e. $\varphi_{u,\mu,t} = 1$. We note for now that, depending on the NCD, both RRs can be modulated by crisis-emergent risk factors and disruptions in management of antecedent conditions, as summarised in Table 21.

Table 21. Factors that may affect the risk of NCD incidence and case-fatality (other than disrupted treatment).

Effect	Risk factor				
	Stress and worsening mental health	Changes in dietary intake and diversity	Disrupted management of antecedent conditions	Exposure to smoke and dust from explosions, debris, inappropriate cooking fuel	Exposure to cold temperatures
Increased incidence	CVD, DM2, cancer	CVD (through hypertension)	CVD (through hypertension, DM2)		
Increased disease severity and thus case-fatality	all	CVD, DM1, DM2, CKD		COPD, asthma	COPD, asthma

6.3 Treatment coverage assumptions

We assumed that pre-war essential treatment coverage was 90-100%. While this does not equate to optimal treatment [209], it reflects the widespread availability of public health services including primary and secondary care in Gaza mainly through the MoH and UNRWA [210] based on pre-war data, expert knowledge, and conversations with health actors within Gaza, it is likely that the majority of NCD cases would have had access to essential treatment [209]. In Gaza, only surgical cancer care and limited chemotherapy care were available before the war [208], and a fraction of cases were allowed to obtain radio- or chemotherapy outside Gaza, albeit with delays (see limitations) [211]. We reviewed available information to quantify ranges for the likely availability of treatment services required for management of different NCDs, both in the war period to date and over the projection period, the latter as scenario assumptions. These ranges are presented in Table 22. Specifically, we assumed that specialised services such as cancer care and haemodialysis would recover slowly during the ceasefire phase due to the destruction of key specialised care facilities and equipment and departure or death of clinical and allied health professionals needed to administer specialised NCD care. We assumed that humanitarian actors would not be able to offer cancer care even in a ceasefire scenario, and that patients would mostly not be allowed outside Gaza.

Table 22. Assumed ranges of treatment coverage for specific NCD-relevant treatment services.

Period	Month starting	Percentage of patients able to access haemodialysis			Percentage of the population with access to functional inpatient public departments that were able to administer emergency care for cardiovascular events			Percentage of patients with access to insulin			Percentage of cancer patients able to access treatment (surgery only)		
		CKD			CVD			DM1			Cancer		
Pre-war	n/a	90-100%			90-100%			90-100%			90-100%		
To-date	7 Oct 2023	70-80%			40-60%			90-100%			20-40%		
	7 Nov 2023	30-50%			10-30%			90-100%			1-5%		
	7 Dec 2023	20-40%			5-15%			90-100%			1-5%		
	7 Jan 2024	20-40%			5-15%			90-100%			1-5%		
		Scenario†											
		Cf	Sq	Es	Cf	Sq	Es	Cf	Sq	Es	Cf	Sq	Es
Projection (months 1 to 3)	7 Feb 2024	40-60%	15-20%	5-10%	20-40%	5-15%	1-5%	90-100%	70-80%	60-70%	1-5%	1-5%	1-5%
	7 Mar 2024	40-60%	15-20%	5-10%	20-40%	5-15%	1-5%	90-100%	70-80%	60-70%	1-5%	1-5%	1-5%
	7 Apr 2024	40-60%	15-20%	5-10%	20-40%	5-15%	1-5%	90-100%	70-80%	60-70%	1-5%	1-5%	1-5%
Projection (months 4 to 6)	7 May 2024	50-70%	15-20%	5-10%	30-50%	5-15%	1-5%	90-100%	70-80%	60-70%	1-5%	1-5%	1-5%
	7 Jun 2024	50-70%	15-20%	5-10%	30-50%	5-15%	1-5%	90-100%	70-80%	60-70%	1-5%	1-5%	1-5%
	7 Jun 2024	50-70%	15-20%	5-10%	30-50%	5-15%	1-5%	90-100%	70-80%	60-70%	1-5%	1-5%	1-5%

† C = ceasefire; S = status quo; E = escalation.

6.4 Mortality hazard functions

6.4.1 Acute versus long-term survival

For CVD, we considered that there is an immediate risk of death μ_{acute} following the first acute presentation of the condition (e.g. stroke or heart attack). This is conditional on surviving the acute event $(1 - \mu_{\text{acute}})$ case-fatality during any time step τ since initial case onset is modelled as a time-dependent mortality hazard function $\mu_{u,\tau}$ (see below). While we recognise that patients often experience further acute events (e.g. repeat strokes), given the varying timing of such events, we considered that population-level cohort studies of survival capture the average risk of dying since onset. For other NCDs, we omitted the acute presentation of disease, again considering that population-level cohort studies capture how mortality changes as a function of τ.

6.4.2 Sources of data

To parameterise the hazard of dying with and without treatment, we reviewed published cohort studies describing both acute (for CVD only) and long-term survival (with at least three years of follow-up), identified through a non-systematic literature search and through contact with subject experts. We extracted from each study the proportion of patients surviving up to study-reported time points, out of the total at the start of follow-up. For cancer specifically, the West Bank's MoH cancer registry provides informative data on survival with and without treatment based on follow up with cancer patients in the West Bank during 2017 to 2021 for four main cancer types (breast cancer, colorectal cancer, lung cancer and lymphoma) [212]. Treated cohorts included patients who received surgical care only, and those who received chemotherapy and/or radiotherapy instead or in addition. We computed survival functions comparing patients who received surgical care only versus no care (see Limitations).

6.4.3 Survival function fitting

We then fitted candidate survival distributions to these observations including negative-exponential, Weibull, log-normal and log-logistic, selecting the best-fitting based on maximum likelihood and conditional on acute event survival for CVD. Where alternative studies were available, we fitted functions to either, to provide an upper and lower bound.

The following decay distributions were retained, depending on the NCD:

- Log-normal: $\mu_\tau = \dfrac{f_{\mathcal{N}}\left(\frac{\ln \tau - \mu}{\sigma}\right)}{1 - F_{\mathcal{N}}\left(\frac{\ln \tau - \mu}{\sigma}\right)}$, where $f_{\mathcal{N}}$ is the probability density function of the standard normal distribution and $F_{\mathcal{N}}$ is the cumulative distribution function of the standard normal distribution;

- Log-logistic: $\mu_\tau = \dfrac{\beta\left(\frac{\tau}{\alpha}\right)^{\beta-1}}{\alpha\left(1 + \left(\frac{\tau}{\alpha}\right)^{\beta}\right)}$;

- Exponential: $\mu_\tau = \lambda$.

Parameters of each fitted survival function are provided in Table 23.

Table 23. Parameters of fitted survival functions, by disease and treatment status.

Disease	Treatment status (σ)	Bound	Probability of acute phase survival ($1 - \mu_{acute}$)	Distribution parameters	
Log-normal distributed				μ	σ
Chronic kidney disease	1	single estimate	n/a	4.00	1.68
	0	lower	n/a	3.14	1.58
		upper		3.26	1.58
Myocardial infarction	1	lower	0.94	8.10	5.19
		upper	0.97	8.10	5.19
	0	single estimate	0.60	2.90	4.50
Log-logistic distributed				α	β
Haemorrhagic stroke	1	lower	0.68	0.70	0.12
		upper	0.68	20.7	0.32
	0	single estimate	0.60	0.24	0.178
Ischemic stroke	1	single estimate	0.93	63.17	0.58
	0	single estimate	0.88	18.56	0.58
Breast cancer	1	single estimate		221.35	1.06
	0	single estimate		146.60	1.06
Colorectal cancer	1	single estimate		84.41	0.73
	0	single estimate		64.49	0.65
Lung cancer	1	single estimate		23.64	0.66
	0	single estimate		7.15	0.66
Negative exponential distributed				λ	
Diabetes mellitus type 1	1	single estimate		0.001†	
	0	lower		0.06 [213]	
		upper		0.03	

† Inverse of Gaza population life expectancy [214].

Survival function fits are shown in Figure 11, Figure 12 and Figure 13.

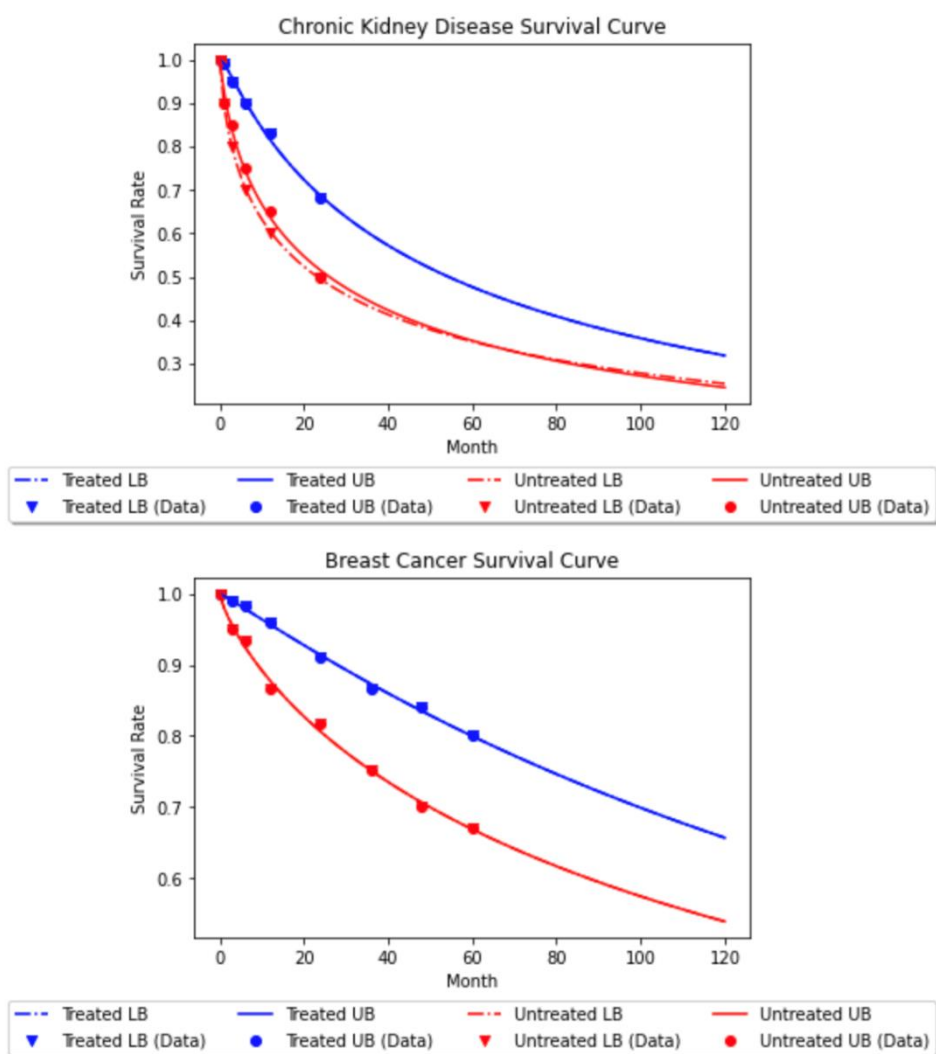Figure 11. Survival fits for chronic kidney disease [215–220] and breast cancer [23] . LB = lower bound; UB = upper bound.
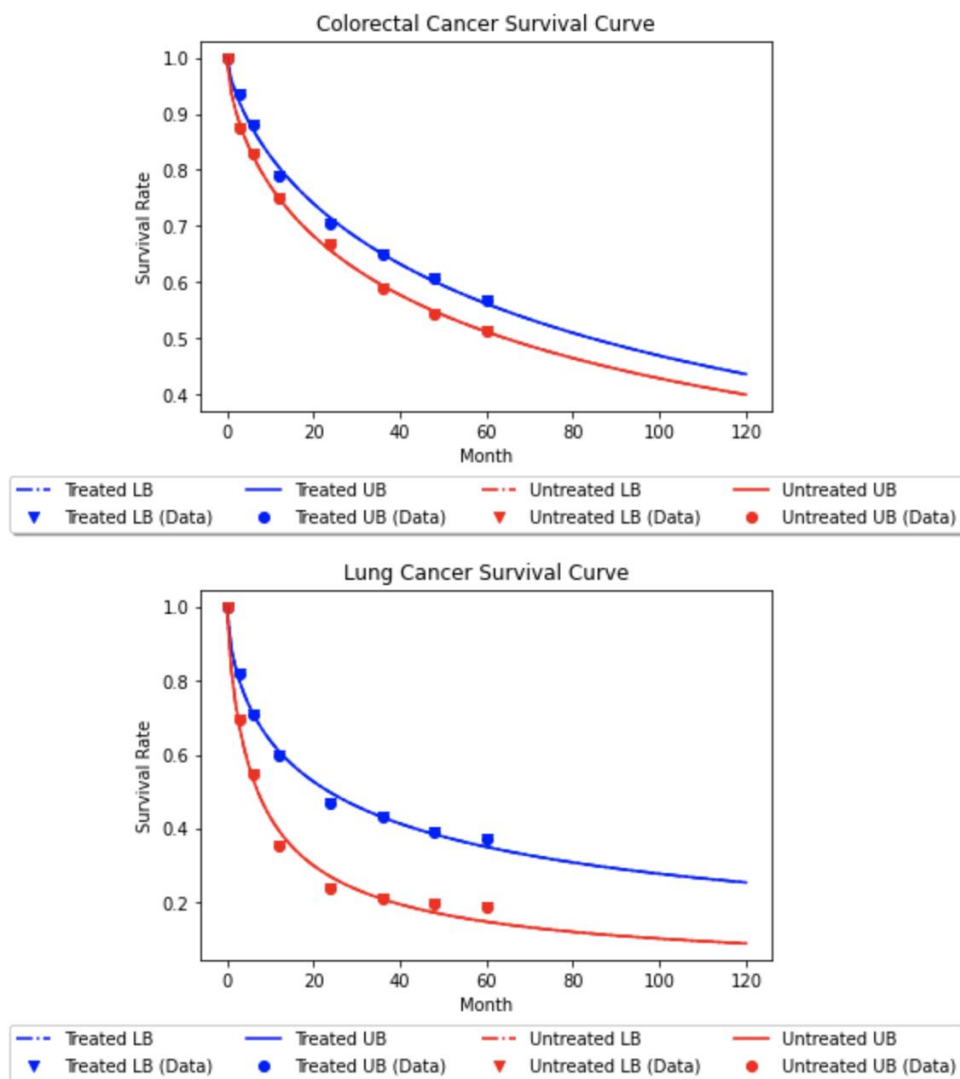
Figure 12. Survival fits for colorectal cancer and lung cancer [221]. LB = lower bound; UB = upper bound.
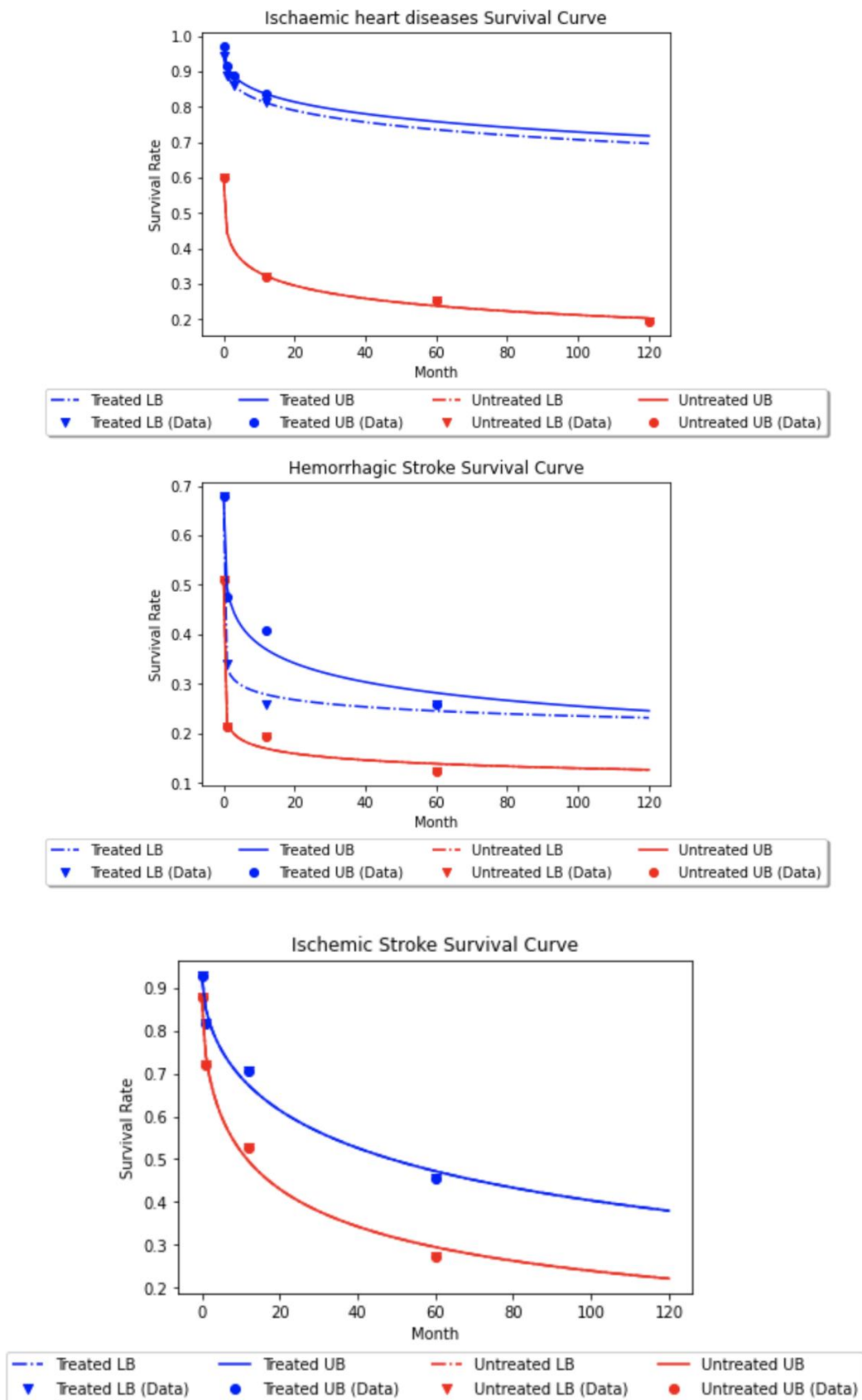
Figure 13. Survival fits for myocardial infarction [222–225], haemorrhagic stroke [226, 227] and ischaemic stroke [226, 228, 229]. LB = lower bound; UB = upper bound.

6.5 Pre-war mortality baseline

To quantify pre-war age-specific CKD, ischaemic heart disease, and cerebrovascular disease mortality, we extracted MoH data from the West Bank, since the latter applied a consistent ICD-10 classification [11], and scaled these to Gaza based on the ratio of West Bank to Gaza population size. We assumed that strokes were 50% ischaemic and 50% haemorrhagic [228, 230]. We also assumed that DM1 mortality was negligible, plausibly due to the universal coverage of insulin treatment among recognised cases. For cancer, we combined data from the International Agency for Research on Cancer and the MoH [11, 231]. Generally, the resulting figures are similar in relative mortality terms to estimates for Lebanon and do not exceed European levels [232]. We also computed the mean age-specific proportion of deaths from disease u ($p_{a,u,\text{base}}$) from the same sources.

We used a generalised least-squares regression to estimate the trend in annual deaths due to each NCD occurring pre-war, based on years of data availability. We used this model to forecast the counterfactual (no-crisis) number of deaths during 2023 and 2024, discretised to monthly increments, i.e. $D_{u,t,\text{base}}$.

6.6 Excess mortality projections

6.6.1 Model implementation

For each NCD, we simulated monthly incident cohorts of cases from January 2000 to the end of the projection period. We assumed a constant mean monthly incidence $I_{u,t,base}$, calibrated to fit $D_{u,t,\text{base}}$ as follows: for each of 1000 simulation runs, we sampled a random number of incident cases from a Poisson distribution centred at the above mean and computed the mean of simulated baseline deaths $D'_{u,t,\text{base}}$ over the course of the convergence phase. A multiplier constant, k_D, was then used to scale $I_{u,t,base}$ so that $D'_{u,t,\text{base}} = D_{u,t,\text{base}}$.

We propagated uncertainty in treatment coverage and survival by sampling from uniform distributions of these parameters during each run (for survival, only where lower and upper bounds were available: see Table 23). Lastly, during each run we tracked both the 'crisis-exposed' cohorts (i.e. featuring the war period and scenario-projected treatment coverage) and replicate cohorts experiencing counterfactual conditions (i.e. the pre-war treatment coverage): the difference in total deaths between these cohorts is $D_{u,t,\text{ excess}}$. After simulating 1000 runs, we computed the mean and 95th percentile interval of outcomes.

We assumed that the age distribution of deaths would not be affected by the crisis, i.e. $p_{a,u,\text{base}} = p_{a,u,\text{crisis}}$, and distributed deaths accordingly. This assumption is not strictly correct: as treatment coverage decreases and survival accordingly shortens, the age distribution of excess deaths would shift towards younger populations. However, we verified that any resulting bias is negligible within the war period to date and projection periods (data not shown).

6.6.2 Modification for diabetes mellitus type 1

For DM1, baseline deaths were negligible (see above). Robust data on the number of prevalent cases at the start of the war were also available from UNRWA and the MoH in Gaza report [233, 234]. Therefore, we applied case-fatality hazards to this prevalent pool over the war period to date and the projection period based on assumed treatment coverage. We ignored incident DM1 cases since the war's start as these would have been numerically small (≈3% out of a mean 17 DM1 plus DM2 incident cases per month, or about 6 DM1 cases annually).

6.7 Model assumptions and limitations

Our analysis of NCD mortality features a number of important limitations:

- Key high-burden NCDs, including DM2 and COPD, are omitted from the analysis. While DM2 mostly leads to death via CVD cases, and thus may largely be captured by CVD MoH mortality figures, some DM2 deaths occur due to other complications including diabetic ketoacidosis and hyper-osmolar hyperglycaemic state. Altogether, the NCD conditions included in our analysis accounted for about 70-80% of all NCD deaths pre-war according to MoH data;

- We assumed that treatment coverage and survival are age-independent, but in reality this may not hold true. If these parameters are negatively correlated with age-specific incidence (i.e. the age groups with highest incidence are also those with lowest coverage and survival), our analysis would under-estimate mortality, and vice versa;

- Likewise, we did not model increases in NCD incidence and disease progression due to the war itself, resulting in further under-estimation of the excess. Such risks would plausibly play out over a long timeframe (e.g. disruptions in treatment of hypertension would lead to progression to more severe stages and eventually a higher risk of CVD), but, as the crisis continues, their effect is likely to compound, and should be considered in future iterations of these projections;

- We assumed that treatment coverage was binary, while patients may in fact be on a spectrum between excellent treatment access, minimal delays and high adherence and no treatment at all, with interruptions being a commonly described outcome in crisis settings [235]. This dichotomisation is difficult to avoid in a context of scarce evidence on survival (see below), but could have resulted in some bias if cases with partial treatment were relatively more similar to either extreme;

- We found generally limited evidence on NCD survival, particularly without treatment, and recognise that studies on which estimates are based may not be well representative of the profile of pre-war patients in Gaza due to differences in demographics, clinical presentation, and specific treatment regimens. For cancer specifically, we calculated survival based on surgically treated cases, omitting the better outcomes experienced by the fraction of cases who do have access to radio and chemotherapy: this may also have resulted in some under-estimation of excess mortality.

- Before the war, referrals outside Gaza were also common for conditions other than cancer. For instance, the 5,864 MoH-reported referrals for cancer treatment outside Gaza in 2022 accounted for only 27% of 22,123 total referrals [236]; and unsuccessful applications for permits to exit the Gaza Strip had a significant impact on mortality for cancer patients (hazard ratio 1.45) [212]. The sudden reduction in referrals during the war is not accounted for in our models.

Altogether, the above limitations bias our estimates towards considerable under-estimation of true excess mortality, and should thus be considered when interpreting our projections.

7 Aggregate all-cause analysis

7.1 General method

Having completed analysis for the traumatic injury, infectious diseases, MCH and NCD modules, we aggregated cause-specific projections into overall estimates of excess death tolls and rates. As people simultaneously face competing risks of mortality from different causes, a crude sum of all cause-specific estimates seemed inappropriate. We therefore used a common adjustment used in infection transmission modelling, whereby someone's overall risk of dying is treated as the complement of the probability of surviving all possible cause-specific risks. Accordingly, for K possible causes of death and A age groups,

$$d_a = 1 - \prod_{k=1}^{K}\left(1 - d_{a,k}\right)$$

Where d is the per-capita death rate (equivalent to a risk for small time units). We did this adjustment by age group to avoid potential age confounding due to certain causes of death being distributed mainly in specific age groups. We treated k at the lowest possible stratification included in our analysis (i.e. each individual infectious disease and NCD was treated separately). We did the above adjustment separately for counterfactual (no crisis) and scenario-specific projections.

Lastly, we computed adjustment factors for each age group, as the ratios of adjusted to crude age-specific death rates, which we applied to each cause-specific module to downward-revise estimates. We then aggregated estimates and uncertainty intervals across age, cause of death or other stratification variables. Of note, age-specific adjustment factors were > 0.95 for all age groups save for persons aged ≥ 80yo (> 0.90), i.e. made little difference to results.

7.2 Limitations

While the above approach improves on crude summation of cause-specific mortality, it does feature a few limitations, probably of low import:

- In reality, it is likely that competing causes of death exist in a hierarchical relationship to each other. For example, someone who is bedridden due to a stroke may have a different risk of exposure to traumatic injury, compared to someone who is able to go out; featuring such hierarchies may alter the adjustment;

- There may be additional confounding other than due to age: in particular, we did not stratify the adjustment by gender;

- While summing the mean estimates across age, cause of death or other stratification variables seems appropriate, summing the uncertainty intervals is not strictly correct from a statistical point of view, as it assumed that all error distributions have the same shape. This is unlikely to be the case, as our cause-specific projections are the product of several error distributions, some non-parametric. A better approach, which we will attempt in future instances of the project, could be to collect the empirical distributions for each age-, cause- and period-specific projection, and use bootstrapping (i.e. repeatedly sample from these distributions) to construct uncertainty intervals with better coverage.

8 References

1. World Health Organization. Health Cluster - occupied Palestinian territory. https://healthcluster.who.int/countries-and-regions/occupied-palestinian-territory. Accessed 5 Feb 2024.

2. Nutrition Cluster: Occupied Palestinian Territory. https://response.reliefweb.int/palestine/nutrition. Accessed 15 Feb 2024.

3. Food Security Cluster: Palestine. https://fscluster.org/state-of-palestine. Accessed 15 Feb 2024.

4. Water, Sanitation and Hygiene Cluster: Occupied Palestinian Territory. https://response.reliefweb.int/palestine/water-sanitation-and-hygiene. Accessed 15 Feb 2024.

5. MOH Palestine. https://site.moh.ps/. Accessed 15 Feb 2024.

6. Ruppert E, Isin E, Bigo D. Data politics. Big Data & Society. 2017;4:205395171771774.

7. UNFPA. State of Palestine - Subnational Population Statistics - Humanitarian Data Exchange. https://data.humdata.org/dataset/cod-ps-pse. Accessed 15 Feb 2024.

8. PCBS. https://www.pcbs.gov.ps/default.aspx. Accessed 5 Feb 2024.

9. CME Info - Child Mortality Estimates. https://childmortality.org/. Accessed 7 Feb 2024.

10. World Health Organization, World Bank, United Nations Population Fund, United Nations Children's Fund (UNICEF). Trends in maternal mortality: 1990-2015: estimates from WHO, UNICEF, UNFPA, World Bank Group and the United Nations Population Division. Geneva: World Health Organization; 2015.

11. Annual Health Reports. Ministry of Health - Palestine. https://site.moh.ps/index/Books/BookType/2/Language/ar. Accessed 5 Feb 2024.

12. MOH Gaza. Annual reports. Gaza, Palestine.

13. UNRWA. Annual Department of health report. UNRWA. 2024. https://www.unrwa.org/resources/reports. Accessed 5 Feb 2024.

14. Jamaluddine Z, Seita A, Ballout G, Al-Fudoli H, Paolucci G, Albaik S, et al. Establishment of a birth-to-education cohort of 1 million Palestinian refugees using electronic medical records and electronic education records. International Journal of Population Data Science. 2023;8.

15. Ministry of Health - Gaza Strip. Communicable Disease in the Gaza Strip. 2018.

16. UNICEF. The Palestinian Multiple Indicator Cluster Survey: 2019-2020. 2021. https://www.unicef.org/sop/reports/palestinian-multiple-indicator-cluster-survey. Accessed 5 Feb 2024.

17. WHO. Vaccination schedule for occupied Palestinian territory, including east Jerusalem. 2024. https://immunizationdata.who.int/pages/schedule-by-country/pse.html?DISEASECODE=&TARGETPOP_GENERAL=GENERAL. Accessed 5 Feb 2024.

18. Mapping and Assessment of Maternal, Neonatal and Young Children Health Care Services in Gaza Strip, | UNICEF State of Palestine. https://www.unicef.org/sop/reports/mapping-and-assessment-maternal-neonatal-and-young-children-health-care-services-gaza-strip. Accessed 5 Feb 2024.

19. oPt: Multi-Sectoral Needs Assessment (MSNA) Key Sectoral Findings - Gaza (July 2022) | OCHA. 2022. https://www.unocha.org/publications/report/occupied-palestinian-territory/opt-multi-sectoral-needs-assessment-msna-key-sectoral-findings-gaza-july-2022. Accessed 5 Feb 2024.

20. Identifying a Package of Cost-Effective Interventions to Address Non-communicable Diseases in Gaza. https://www.aub.edu.lb/fhs/center-for-research-on-population-and-health/Pages/crph_projects_cost-effective_interventions_non-communicable-diseases_Gaza.aspx. Accessed 5 Feb 2024.

21. Millet C, Ghattas H, Jawad M, Abu Hamad B, Jamaluddine Z, El Sayyed Ahmad R, et al. Identifying a package of cost-effective interventions to address non-communicable diseases in Gaza, 2020 [Survey Documentation]. 2021.

22. WHO. STEPS noncommunicable diseases risk factors survey 2010-2011: Occupied Palestinian Territory. https://www.who.int/teams/noncommunicable-diseases/surveillance/data/occupied-palestinian-territory. Accessed 15 Feb 2024.

23. Ministry of Health. Cancer in Palestine - West Bank. 2023.

24. UN Office for the Coordination of Humanitarian Affairs | ReliefWeb. 2024. https://reliefweb.int/organization/ocha. Accessed 5 Feb 2024.

25. UNRWA. Situational Reports. UNRWA. 2024. https://www.unrwa.org/resources/reports. Accessed 5 Feb 2024.

26. Palestine. Gaza Hostilities 2023 / 2024 - Emergency Situation Reports. World Health Organization - Regional Office for the Eastern Mediterranean. http://www.emro.who.int/opt/information-resources/emergency-situation-reports.html. Accessed 5 Feb 2024.

27. Gaza - Food Security Assessment - December 2023 | World Food Programme. 2023. https://www.wfp.org/publications/gaza-food-security-assessment-december-2023. Accessed 5 Feb 2024.

28. Ministry of Health - Gaza Strip. Emergency Report for Day 117 of October 2023 War on Gaza. 2024.

29. OCHA. The Humanitarian Data Exchange. https://data.humdata.org/. Accessed 18 Feb 2024.

30. UNRWA. Gaza supply and dispatch Tracking. https://app.powerbi.com/view?r=eyJrIjoiZTVkYmEwNmMtZWYxNy00ODhlLWI2ZjctNjIzMzQ5OGQxNzY5Iiwi dCI6IjI2MmY2YTQxLTlwZTktNDE0MC04ZDNlLWZkZjVlZWNiNDE1NyIsImMiOjl9&pageName=ReportSectio n3306863add46319dc574. Accessed 7 Feb 2024.

31. Palestine Red Crescent Society. https://www.palestinercs.org/. Accessed 5 Feb 2024.

32. UNICEF. UN Inter-agency Group for Child Mortality Estimation (UN IGME) - UNICEF DATA. 2024. https://data.unicef.org/resources/un-inter-agency-group-for-child-mortality-estimation-unigme/. Accessed 5 Feb 2024.

33. United Nations Human Rights Council. Report of the detailed findings of the independent commission of inquiry established pursuant to Human Rights Council resolution S-21/1. New York: United Nations; 2015.

34. Palestinian Center for Human Rights. Statistics: Victims of the Israeli Offensive on Gaza since 08 July 2014. Gaza City; 2014.

35. Casualties and Victim Assistance | Reports | Monitor. Landmine and Cluster Munition Monitor. 2016. http://the-monitor.org/en-gb/reports/2015/palestine/casualties-and-victim-assistance.aspx. Accessed 7 Feb 2024.

36. Jamaluddine Z, Checchi F, Campbell OMR. Excess mortality in Gaza: Oct 7–26, 2023. The Lancet. 2023;402:2189–90.

37. Huynh BQ, Chin ET, Spiegel PB. No evidence of inflated mortality reporting from the Gaza Ministry of Health. The Lancet. 2024;403:23–4.

38. Wood SN, N., Pya, S"afken B. Smoothing parameter and model selection for general smooth models (with discussion). Journal of the American Statistical Association. 2016;111:1548–75.

39. Ayoub HH, Chemaitelly H, Abu-Raddad LJ. Mortality impact of the Israel-Gaza conflicts (2008-2023): A comparative analysis of civilians versus combatants. 2024. https://doi.org/10.31235/osf.io/53w4t.

40. Tampe U, Widmer LW, Weiss RJ, Jansson K-Å. Mortality, risk factors and causes of death in Swedish patients with open tibial fractures - a nationwide study of 3, 777 patients. Scand J Trauma Resusc Emerg Med. 2018;26:62.

41. Tseng I-C, Chen I-J, Chou Y-C, Hsu Y-H, Yu Y-H. Predictors of Acute Mortality After Open Pelvic Fracture: Experience From 37 Patients From A Level I Trauma Center. World J Surg. 2020;44:3737–42.

42. Mena JH, Sanchez AI, Rubiano AM, Peitzman AB, Sperry JL, Gutierrez MI, et al. Effect of the Modified Glasgow Coma Scale Score Criteria for Mild Traumatic Brain Injury on Mortality Prediction: Comparing Classic and Modified Glasgow Coma Scale Score Model Scores of 13. J Trauma. 2011;71:1185–93.

43. El-Matbouly M, Jabbour G, El-Menyar A, Peralta R, Abdelrahman H, Zarour A, et al. Blunt splenic trauma: Assessment, management and outcomes. The Surgeon. 2016;14:52–8.

44. Taghavi S, Askari R. Liver Trauma. In: StatPearls. Treasure Island (FL): StatPearls Publishing; 2024.

45. Grotz MRW, Allami MK, Harwood P, Pape HC, Krettek C, Giannoudis PV. Open pelvic fractures: epidemiology, current concepts of management and outcome. Injury. 2005;36:1–13.

46. Peek J, Beks R, Hietbrink F, Jong M, Heng M, Beeres F, et al. Epidemiology and outcome of rib fractures: a nationwide study in the Netherlands. European Journal of Trauma and Emergency Surgery. 2022;48.

47. Kyriazidis I, Jakob D, Hernández Vargas J, Franco O, Degiannis E, Dorn P, et al. Accuracy of Diagnostic Tests in Cardiac Injury after Blunt Chest Trauma. A Systematic Review and Meta-Analysis. World Journal of Emergency Surgery. 2023;18.

48. Choudhary S, Pasrija D, Mendez MD. Pulmonary Contusion. In: StatPearls. Treasure Island (FL): StatPearls Publishing; 2024.

49. Perkins ZB, De'Ath HD, Aylwin C, Brohi K, Walsh M, Tai NRM. Epidemiology and Outcome of Vascular Trauma at a British Major Trauma Centre. European Journal of Vascular and Endovascular Surgery. 2012;44:203–9.

50. Haines LN, Doucet JJ. Severe crush injury in adults. In: UpToDate. Wolters Kluwer; 2023.

51. Gauglitz GG, Williams F. Overview of the management of the severely burned patient. In: UpToDate. Wolters Kluwer; 2023.

52. Chhabra HS, Sharawat R, Vishwakarma G. In-hospital mortality in people with complete acute traumatic spinal cord injury at a tertiary care center in India—a retrospective analysis. Spinal Cord. 2022;60:210–5.

53. Ramirez C, Menaker J. Traumatic Amputations. Relias Media. 2017. https://www.reliasmedia.com/articles/140552-traumatic-amputations. Accessed 2 Feb 2024.

54. Simon B, Ebert J, Bokhari F, Capella J, Emhoff T, Hayward TI, et al. Management of pulmonary contusion and flail chest: An Eastern Association for the Surgery of Trauma practice management guideline. Journal of Trauma and Acute Care Surgery. 2012;73:S351.

55. Shafi S, Renfro LA, Barnes S, Rayan N, Gentilello LM, Fleming N, et al. Chronic consequences of acute injuries: Worse survival after discharge. Journal of Trauma and Acute Care Surgery. 2012;73:699–703.

56. WHO Anthro Survey Analyser and other tools. https://www.who.int/tools/child-growth-standards/software. Accessed 3 Feb 2024.

57. Oxfam, FEG consulting, Humanitarian Aid and Civil Protection. HEA Livelihood Baseline Report, Occupied Palestinian Territory: Gaza Strip. 2013.

58. Satellite Analysis Reveals An Alarming 18% Agricultural Decline in Gaza Strip Amid Ongoing Conflict. UNITAR. https://unitar.org/about/news-stories/press/satellite-analysis-reveals-alarming-18-agricultural-decline-gaza-strip-amid-ongoing-conflict. Accessed 3 Feb 2024.

59. 2023/24 - WFP Palestine - Monthly Market Dashboard | World Food Programme. 2024. https://www.wfp.org/publications/202324-wfp-palestine-monthly-market-dashboard. Accessed 3 Feb 2024.

60. UNRWA. UNRWA- Gaza Supplies and Dispatch Tracking. https://app.powerbi.com/view?r=eyJrIjoiZTVkYmEwNmMtZWYxNy00ODhlLWI2ZjctNjIzMzQ5OGQxNzY5Iiwi dCI6IjI2MmY2YTQxLTIwZTktNDE0MC04ZDNlLWZkZjVlZWNiNDE1NyIsImMiOjl9&pageName=ReportSectio n3306863add46319dc574. Accessed 3 Feb 2024.

61. WFP at a Glance | World Food Programme. 2024. https://www.wfp.org/stories/wfp-glance. Accessed 11 Feb 2024.

62. M.I. WFP Palestine Emergency Response - IPC analysis concludes that Gaza already surpassed the acute food insecurity threshold of famine - Situation Report 12. Question of Palestine. https://www.un.org/unispal/document/wfp-palestine-emergency-response-situation-report-12-jan4-2024/. Accessed 11 Feb 2024.

63. WFP delivers first aid convoy from Jordan to Gaza. | World Food Programme. 2023. https://www.wfp.org/news/wfp-delivers-first-aid-convoy-jordan-gaza. Accessed 11 Feb 2024.

64. Mehrabi Z. Israel has now fully deployed its most deadly weapon. Medium. 2023. https://ziamehrabi.medium.com/israel-has-now-fully-deployed-its-most-deadly-weapon-5bce7d539795. Accessed 3 Feb 2024.

65. Abu Hamad BA, Jamaluddine Z, Safadi G, Ragi M-E, Ahmad RES, Vamos EP, et al. The hypertension cascade of care in the midst of conflict: the case of the Gaza Strip. Journal of Human Hypertension. 2023;37:957–68.

66. Hall KD, Sacks G, Chandramohan D, Chow CC, Wang YC, Gortmaker SL, et al. Quantification of the effect of energy imbalance on bodyweight. The Lancet. 2011;378:826–37.

67. Mifflin MD, St Jeor ST, Hill LA, Scott BJ, Daugherty SA, Koh YO. A new predictive equation for resting energy expenditure in healthy individuals. The American journal of clinical nutrition. 1990;51:241–7.

68. Diwakar V, Malcolm M, Naufal G. Violent conflict and breastfeeding: the case of Iraq. Conflict and health. 2019;13:1–20.

69. Guerrero Serdan G. The effects of the war in Iraq on nutrition and health: an analysis using anthropometric outcomes of children. Available at SSRN 1359161. 2009.

70. Save the Children UK. Infant Feeding in Emergencies – Lebanon. 2007.

71. Lebanon Nutrition Taskforce. Call for action on Infant and Young Child Feeding and Nutrition in the response to the Beirut port explosion. 2020.

72. Akik C, Semaan A, Shaker-Berbari L, Jamaluddine Z, Saad GE, Lopes K, et al. Responding to health needs of women, children and adolescents within Syria during conflict: intervention coverage, challenges and adaptations. Conflict and health. 2020;14:1–19.

73. UNICEF. Joint Nutrition Assessment Syrian Refugees in Lebanon. 2013.

74. The Palestinian Multiple Indicator Cluster Survey | UNICEF State of Palestine. 2021. https://www.unicef.org/sop/reports/palestinian-multiple-indicator-cluster-survey. Accessed 5 Feb 2024.

75. Humanitarian Access North of Wadi Gaza (1-14 January 2024) - occupied Palestinian territory | ReliefWeb. 2024. https://reliefweb.int/report/occupied-palestinian-territory/humanitarian-access-north-wadi-gaza-1-14-january-2024. Accessed 3 Feb 2024.

76. Almajwal AM, Abulmeaty MMA. New Predictive Equations for Resting Energy Expenditure in Normal to Overweight and Obese Population. International Journal of Endocrinology. 2019;2019:e5727496.

77. Vaccination schedule for occupied Palestinian territory, including east Jerusalem. https://immunizationdata.who.int/pages/schedule-by-country/pse.html?DISEASECODE=&TARGETPOP_GENERAL=GENERAL. Accessed 5 Feb 2024.

78. Moussally K, Abu-Sittah G, Gomez FG, Fayad AA, Farra A. Antimicrobial resistance in the ongoing Gaza war: a silent threat. The Lancet. 2023;402:1972–3.

79. Miller LW. Diphtheria Immunization: Effect Upon Carriers and the Control of Outbreaks. Am J Dis Child. 1972;123:197.

80. Truelove SA, Keegan LT, Moss WJ, Chaisson LH, Macher E, Azman AS, et al. Clinical and Epidemiological Aspects of Diphtheria: A Systematic Review and Pooled Analysis. Clinical Infectious Diseases. 2020;71:89–97.

81. Antia A, Ahmed H, Handel A, Carlson NE, Amanna IJ, Antia R, et al. Heterogeneity and longevity of antibody memory to viruses and vaccines. PLOS Biology. 2018;16:e2006601.

82. Preziosi M. Effects of pertussis vaccination on transmission: vaccine efficacy for infectiousness. Vaccine. 2003;21:1853–61.

83. Fulton TR, Phadke VK, Orenstein WA, Hinman AR, Johnson WD, Omer SB. Protective Effect of Contemporary Pertussis Vaccines: A Systematic Review and Meta-analysis. Clin Infect Dis. 2016;62:1100–10.

84. Pertussis vaccines: WHO position paper - September 2015. Wkly Epidemiol Rec. 2015;90:433–58.

85. Choi YH, Campbell H, Amirthalingam G, Van Hoek AJ, Miller E. Investigating the pertussis resurgence in England and Wales, and options for future control. BMC Med. 2016;14:121.

86. Di Pietrantonj C, Rivetti A, Marchione P, Debalini MG, Demicheli V. Vaccines for measles, mumps, rubella, and varicella in children. Cochrane Database of Systematic Reviews. 2021;2021.

87. Uzicanin A, Zimmerman L. Field Effectiveness of Live Attenuated Measles-Containing Vaccines: A Review of Published Literature. The Journal of Infectious Diseases. 2011;204:S133–48.

88. Schenk J, Abrams S, Theeten H, Van Damme P, Beutels P, Hens N. Immunogenicity and persistence of trivalent measles, mumps, and rubella vaccines: a systematic review and meta-analysis. Lancet Infect Dis. 2021;21:286–95.

89. Ciapponi A, Bardach A, Rey Ares L, Glujovsky D, Cafferata ML, Cesaroni S, et al. Sequential inactivated (IPV) and live oral (OPV) poliovirus vaccines for preventing poliomyelitis. Cochrane Database of Systematic Reviews. 2019;2019.

90. Macklin GR, Grassly NC, Sutter RW, Mach O, Bandyopadhyay AS, Edmunds WJ, et al. Vaccine schedules and the effect on humoral and intestinal immunity against poliovirus: a systematic review and network meta-analysis. The Lancet Infectious Diseases. 2019;19:1121–8.

91. Grassly NC. Immunogenicity and Effectiveness of Routine Immunization With 1 or 2 Doses of Inactivated Poliovirus Vaccine: Systematic Review and Meta-analysis. The Journal of Infectious Diseases. 2014;210 suppl_1:S439–46.

92. World Health Organization. Table IV: Efficacy/effectiveness of inactivated polio vaccine (IPV) against clinical poliomyelitis. Geneva: WHO.

93. Gao H, Lau EHY, Cowling BJ. Waning Immunity After Receipt of Pertussis, Diphtheria, Tetanus, and Polio-Related Vaccines: A Systematic Review and Meta-analysis. The Journal of Infectious Diseases. 2022;225:557–66.

94. Ma L, Ying Z, Cai W, Wang J, Zhou J, Yang H, et al. Immune persistence of an inactivated poliovirus vaccine derived from the Sabin strain: a 10-year follow-up of a phase 3 study. eClinicalMedicine. 2023;64:102151.

95. Swartz TA, Handsher R, Manor Y, Stoeckel P, Barkay A, Mendelson E, et al. Immune response to an intercalated enhanced inactivated polio vaccine/oral polio vaccine programme in Israel: impact on the control of poliomyelitis. Vaccine. 1998;16:2090–5.

96. Bandyopadhyay AS, Modlin JF, Wenger J, Gast C. Immunogenicity of New Primary Immunization Schedules With Inactivated Poliovirus Vaccine and Bivalent Oral Polio Vaccine for the Polio Endgame: A Review. Clinical Infectious Diseases. 2018;67 suppl_1:S35–41.

97. Brickley EB, Wieland-Alter W, Connor RI, Ackerman ME, Boesch AW, Arita M, et al. Intestinal Immunity to Poliovirus Following Sequential Trivalent Inactivated Polio Vaccine/Bivalent Oral Polio Vaccine and Trivalent Inactivated Polio Vaccine–only Immunization Schedules: Analysis of an Open-label, Randomized, Controlled Trial in Chilean Infants. Clinical Infectious Diseases. 2018;67 suppl_1:S42–50.

98. Adegbola RA, Mulholland EK, Secka O, Jaffar S, Greenwood BM. Vaccination with a *Haemophilus influenzae* Type b Conjugate Vaccine Reduces Oropharyngeal Carriage of *H. influenzae* Type b among Gambian Children. J INFECT DIS. 1998;177:1758–61.

99. Murphy TV, Pastor P, Medley F, Osterholm MT, Granoff DM. Decreased Haemophilus colonization in children vaccinated with Haemophilus influenzae type b conjugate vaccine. The Journal of Pediatrics. 1993;122:517–23.

100. Theodoratou E, Johnson S, Jhass A, Madhi SA, Clark A, Boschi-Pinto C, et al. The effect of Haemophilus influenzae type b and pneumococcal conjugate vaccines on childhood pneumonia incidence, severe morbidity and mortality. International Journal of Epidemiology. 2010;39 Supplement 1:i172–85.

101. Davis S, Feikin D, Johnson HL. The effect of Haemophilus influenzaetype B and pneumococcal conjugate vaccines on childhood meningitis mortality: a systematic review. BMC Public Health. 2013;13:S21.

102. Griffiths UK, Clark A, Gessner B, Miners A, Sanderson C, Sedyaningsih ER, et al. Dose-specific efficacy of *Haemophilus influenzae* type b conjugate vaccines: a systematic review and meta-analysis of controlled clinical trials. Epidemiol Infect. 2012;140:1343–55.

103. Silfverdal SA, Assudani D, Kuriyakose S, Van Der Meeren O. Immunological persistence in 5 y olds previously vaccinated with hexavalent DTPa-HBV-IPV/Hib at 3, 5, and 11 months of age. Human Vaccines & Immunotherapeutics. 2014;10:2795–8.

104. Hammitt LL, Crane RJ, Karani A, Mutuku A, Morpeth SC, Burbidge P, et al. Effect of Haemophilus influenzae type b vaccination without a booster dose on invasive H influenzae type b disease, nasopharyngeal carriage, and population immunity in Kilifi, Kenya: a 15-year regional surveillance study. The Lancet Global Health. 2016;4:e185–94.

105. Hallander HO, Lepp T, Ljungman M, Netterlid E, Andersson M. Do we need a booster of Hib vaccine after primary vaccination? A study on anti-Hib seroprevalence in Sweden 5 and 15 years after the introduction of universal Hib vaccination related to notifications of invasive disease. APMIS. 2010;118:878–87.

106. Flasche S, Ojal J, Le Polain De Waroux O, Otiende M, O'Brien KL, Kiti M, et al. Assessing the efficiency of catch-up campaigns for the introduction of pneumococcal conjugate vaccine: a modelling study based on data from PCV10 introduction in Kilifi, Kenya. BMC Med. 2017;15:113.

107. Fleming-Dutra KE, Conklin L, Loo JD, Knoll MD, Park DE, Kirk J, et al. Systematic Review of the Effect of Pneumococcal Conjugate Vaccine Dosing Schedules on Vaccine-type Nasopharyngeal Carriage. Pediatric Infectious Disease Journal. 2014;33 Supplement 2:S152–60.

108. Loo JD, Conklin L, Fleming-Dutra KE, Deloria Knoll M, Park DE, Kirk J, et al. Systematic Review of the Effect of Pneumococcal Conjugate Vaccine Dosing Schedules on Prevention of Pneumonia. Pediatric Infectious Disease Journal. 2014;33 Supplement 2:S140–51.

109. Reyburn R, Tsatsaronis A, Von Mollendorf C, Mulholland K, Russell FM, ARI Review group. Systematic review on the impact of the pneumococcal conjugate vaccine ten valent (PCV10) or thirteen valent (PCV13) on all-cause, radiologically confirmed and severe pneumonia hospitalisation rates and pneumonia mortality in children 0-9 years old. J Glob Health. 2023;13:05002.

110. Conklin L, Loo JD, Kirk J, Fleming-Dutra KE, Deloria Knoll M, Park DE, et al. Systematic Review of the Effect of Pneumococcal Conjugate Vaccine Dosing Schedules on Vaccine-type Invasive Pneumococcal Disease Among Young Children. Pediatric Infectious Disease Journal. 2014;33 Supplement 2:S109–18.

111. Swarthout TD, Henrion MYR, Thindwa D, Meiring JE, Mbewe M, Kalizang'Oma A, et al. Waning of antibody levels induced by a 13-valent pneumococcal conjugate vaccine, using a 3 + 0 schedule, within the first year of life among children younger than 5 years in Blantyre, Malawi: an observational, population-level, serosurveillance study. The Lancet Infectious Diseases. 2022;22:1737–47.

112. Ojal J, Flasche S, Hammitt LL, Akech D, Kiti MC, Kamau T, et al. Sustained reduction in vaccine-type invasive pneumococcal disease despite waning effects of a catch-up campaign in Kilifi, Kenya: A mathematical model based on pre-vaccination data. Vaccine. 2017;35:4561–8.

113. Bennett A, Pollock L, Bar-Zeev N, Lewnard JA, Jere KC, Lopman B, et al. Community transmission of rotavirus infection in a vaccinated population in Blantyre, Malawi: a prospective household cohort study. The Lancet Infectious Diseases. 2021;21:731–40.

114. Lamberti LM, Ashraf S, Walker CLF, Black RE. A Systematic Review of the Effect of Rotavirus Vaccination on Diarrhea Outcomes Among Children Younger Than 5 Years. Pediatric Infectious Disease Journal. 2016;35:992–8.

115. Hungerford D, Smith K, Tucker A, Iturriza-Gómara M, Vivancos R, McLeonard C, et al. Population effectiveness of the pentavalent and monovalent rotavirus vaccines: a systematic review and meta-analysis of observational studies. BMC Infect Dis. 2017;17:569.

116. Haber M, Tate JE, Lopman BA, Qi W, Ainslie KEC, Parashar UD. Comparing statistical methods for detecting and estimating waning efficacy of rotavirus vaccines in developing countries. Human Vaccines & Immunotherapeutics. 2021;17:4632–5.

117. Clark A, Van Zandvoort K, Flasche S, Sanderson C, Bines J, Tate J, et al. Efficacy of live oral rotavirus vaccines by duration of follow-up: a meta-regression of randomised controlled trials. The Lancet Infectious Diseases. 2019;19:717–27.

118. Yassin K, Awad R, Tebi A, Queder A, Laaser U. The Epidemiology of Hepatitis A Infection in Palestine: A Universal Vaccination Programme Is Not Yet Needed. Epidemiology and Infection. 2001;127:335–9.

119. Badur S, Öztürk S, AbdelGhany M, Khalaf M, Lagoubi Y, Ozudogru O, et al. Hepatitis A in the Eastern Mediterranean Region: a comprehensive review. Human Vaccines & Immunotherapeutics. 2022;18:2073146.

120. Palestinian Central Bureau of Statistics. Estimated Crude Birth Rate in the State of Palestine by Region and Sex, 2017-2021. https://www.pcbs.gov.ps/Portals/_Rainbow/Documents/Birth_Rate_2017-2021_E.html. Accessed 18 Feb 2024.

121. World Bank Open Data: Birth rate - West Bank and Gaza. World Bank Open Data. https://data.worldbank.org/indicator/SP.DYN.CBRT.IN?locations=PS. Accessed 18 Feb 2024.

122. IndexMundi. Gaza Strip - Birth rate - Historical Data Graphs per Year. https://www.indexmundi.com/g/g.aspx?v=25&c=gz&l=en. Accessed 18 Feb 2024.

123. Regev-Yochay G, Abullaish I, Malley R, Shainberg B, Varon M, Roytman Y, et al. Streptococcus pneumoniae Carriage in the Gaza Strip. PLOS ONE. 2012;7:e35061.

124. Lee KS, Lee Y-R, Park S-Y, Oh I-H. The economic burden of rotavirus infection in South Korea from 2009 to 2012. PLoS ONE. 2018;13:e0194120.

125. Bjørnstad ON, Shea K, Krzywinski M, Altman N. The SEIRS model for infectious disease dynamics. Nature Methods. 2020;17:557–8.

126. Funk S, Willem L, Gruson H. socialmixr: Social Mixing Matrices for Infectious Disease Modelling. 2024.

127. van Zandvoort K, Bobe MO, Hassan AI, Abdi MI, Ahmed MS, Soleman SM, et al. Social contacts and other risk factors for respiratory infections among internally displaced people in Somaliland. Epidemics. 2022;41:100625.

128. Gupte P, Eggo R, Leeuwen EV. epidemics: A Library of Compartmental Epidemic Scenario Models. 2024.

129. Heymann DL. Control of Communicable Diseases Manual: 21st Edition. APHA Press; 2022.

130. Richardson M, Elliman D, Maguire H, Simpson J, Nicoll A. Evidence base of incubation periods, periods of infectiousness and exclusion policies for the control of communicable diseases in schools and preschools. The Pediatric Infectious Disease Journal. 2001;20:380.

131. Guerrero L, Calva JJ, Morrow AL, Velazquez FR, Tuz-Dzib F, Lopez-Vidal Y, et al. Asymptomatic Shigella infections in a cohort of Mexican children younger than two years of age. The Pediatric Infectious Disease Journal. 1994;13:597.

132. George CM, Ahmed S, Talukder KA, Azmi IJ, Perin J, Sack RB, et al. Shigella Infections in Household Contacts of Pediatric Shigellosis Patients in Rural Bangladesh. Emerging Infectious Diseases. 2015;21.

133. Azman AS, Rudolph KE, Cummings DAT, Lessler J. The incubation period of cholera: A systematic review. Journal of Infection. 2013;66:432–8.

134. Weil AA, Begum Y, Chowdhury F, Khan AI, Leung DT, LaRocque RC, et al. Bacterial shedding in household contacts of cholera patients in Dhaka, Bangladesh. Am J Trop Med Hyg. 2014;91:738–42.

135. Nelson EJ, Harris JB, Glenn Morris J, Calderwood SB, Camilli A. Cholera transmission: the host, pathogen and bacteriophage dynamic. Nat Rev Microbiol. 2009;7:693–702.

136. Lewnard JA, Antillón M, Gonsalves G, Miller AM, Ko AI, Pitzer VE. Strategies to Prevent Cholera Introduction during International Personnel Deployments: A Computational Modeling Analysis Based on the 2010 Haiti Outbreak. PLoS Med. 2016;13:e1001947.

137. Czumbel I, Quinten C, Lopalco P, Semenza JC, Tozzi AE, Weil-Oliver C, et al. Management and control of communicable diseases in schools and other child care settings: systematic review on the incubation period and period of infectiousness. BMC Infectious Diseases. 2018;18:199.

138. Zhang X-S, Iacono GL. Estimating human-to-human transmissibility of hepatitis A virus in an outbreak at an elementary school in China, 2011. PLOS ONE. 2018;13:e0204201.

139. Shin E-C, Jeong S-H. Natural History, Clinical Manifestations, and Pathogenesis of Hepatitis A. Cold Spring Harb Perspect Med. 2018;8:a031708.

140. Cooper BS, White LJ, Siddiqui R. Reactive and pre-emptive vaccination strategies to control hepatitis E infection in emergency and refugee settings: A modelling study. PLOS Neglected Tropical Diseases. 2018;12:e0006807.

141. Bagulo H, Majekodunmi AO, Welburn SC. Hepatitis E in Sub Saharan Africa – A significant emerging disease. One Health. 2020;11:100186.

142. Moss WJ. Measles. The Lancet. 2017;390:2490–502.

143. Lievano FA, Helfand RF, Harpaz R, Walls L, Katz RS, Williams I, et al. Lack of Evidence of Measles Virus Shedding in People with Inapparent Measles Virus Infections. The Journal of Infectious Diseases. 2004;189 Supplement_1:S165–70.

144. Is Meningitis Contagious? How Long Does It Last? MedicineNet. https://www.medicinenet.com/is_meningitis_contagious/article.htm. Accessed 13 Feb 2024.

145. Dogu AG, Oordt-Speets AM, van Kessel-de Bruijn F, Ceyhan M, Amiche A. Systematic review of invasive meningococcal disease epidemiology in the Eastern Mediterranean and North Africa region. BMC Infectious Diseases. 2021;21:1088.

146. Craig R, Kunkel E, Crowcroft NS, Fitzpatrick MC, de Melker H, Althouse BM, et al. Asymptomatic Infection and Transmission of Pertussis in Households: A Systematic Review. Clinical Infectious Diseases. 2020;70:152–61.

147. Yaari R, Kaliner E, Grotto I, Katriel G, Moran-Gilad J, Sofer D, et al. Modeling the spread of polio in an IPV-vaccinated population: lessons learned from the 2013 silent outbreak in southern Israel. BMC Medicine. 2016;14:95.

148. Blake IM, Martin R, Goel A, Khetsuriani N, Everts J, Wolff C, et al. The role of older children and adults in wild poliovirus transmission. Proceedings of the National Academy of Sciences. 2014;111:10604–9.

149. Nathanson N, Kew OM. From Emergence to Eradication: The Epidemiology of Poliomyelitis Deconstructed. American Journal of Epidemiology. 2010;172:1213–29.

150. Awofisayo-Okuyelu A, McCarthy N, Mgbakor I, Hall I. Incubation period of typhoidal salmonellosis: a systematic review and meta-analysis of outbreaks and experimental studies occurring over the last century. BMC Infectious Diseases. 2018;18:483.

151. Pitzer VE, Bowles CC, Baker S, Kang G, Balaji V, Farrar JJ, et al. Predicting the Impact of Vaccination on the Transmission Dynamics of Typhoid in South Asia: A Mathematical Modeling Study. PLOS Neglected Tropical Diseases. 2014;8:e2642.

152. Srinivasan M, Sindhu KN, Giri S, Kumar N, Mohan VR, Grassly NC, et al. Salmonella Typhi Shedding and Household Transmission by Children With Blood Culture-Confirmed Typhoid Fever in Vellore, South India. J Infect Dis. 2021;224 Suppl 5:S593–600.

153. Monthly mortality analysis, England and Wales - Office for National Statistics. https://www.ons.gov.uk/peoplepopulationandcommunity/birthsdeathsandmarriages/deaths/bulletins/monthlymortalityanalysisenglandandwales/latest. Accessed 23 Feb 2024.

154. World Health Organization. Health profile 2015 - Palestine. 2016.

155. Watt JP, Wolfson LJ, O'Brien KL, Henkle E, Deloria-Knoll M, McCall N, et al. Burden of disease caused by Haemophilus influenzae type b in children younger than 5 years: global estimates. The Lancet. 2009;374:903–11.

156. Ashrafi-Asgarabad A, Bokaie S, Razmyar J, Akbarein H, Nejadghaderi SA, Carson-Chahhoud K, et al. The burden of lower respiratory infections and their underlying etiologies in the Middle East and North Africa region, 1990–2019: results from the Global Burden of Disease Study 2019. BMC Pulmonary Medicine. 2023;23:2.

157. Li Y, Wang X, Blau DM, Caballero MT, Feikin DR, Gill CJ, et al. Global, regional, and national disease burden estimates of acute lower respiratory infections due to respiratory syncytial virus in children younger than 5 years in 2019: a systematic analysis. The Lancet. 2022;399:2047–64.

158. Abu Seir R, Njoum W, Najajrah R, Najjar D, Ashour M, Asakra B, et al. Acute Respiratory Tract Infections among Hospitalized Palestinian Patients (2011–2016): A Retrospective Study. Canadian Journal of Infectious Diseases and Medical Microbiology. 2021;2021:5643134.

159. MOH Gaza. Annual report 2022. Gaza, Palestine. 2022.

160. MOH Palestine. Annual Health Report 2022. Ministry of Health - Palestine. 2022. https://site.moh.ps/index/Books/BookType/2/Language/ar. Accessed 5 Feb 2024.

161. Rennert W, Hindiyeh M, Allahham M, Mercer LD, Hamad KI, Ghuneim NI, et al. Introducing ROTAVAC® to the occupied Palestinian Territories: Impact on diarrhea incidence, rotavirus prevalence and genotype composition. Vaccine. 2023;41:945–54.

162. Troeger C, Blacker BF, Khalil IA, Rao PC, Cao S, Zimsen SR, et al. Estimates of the global, regional, and national morbidity, mortality, and aetiologies of diarrhoea in 195 countries: a systematic analysis for the Global Burden of Disease Study 2016. The Lancet Infectious Diseases. 2018;18:1211–28.

163. Republic of Lebanon - Ministry of Public Health. Epidemiological Surveillance Program. Laboratory-based surveillance, Lebanon, 2024. 2024.

164. Cooke RM, Goossens LLHJ. TU Delft expert judgment data base. Reliability Engineering & System Safety. 2008;93:657–74.

165. Anderson RM, May RM. Infectious diseases of humans: dynamics and control. Reprinted. Oxford: Oxford Univ. Press; 2010.

166. Bellizzi S, Abdelbaki W, Pichierri G, Cegolon L, Popescu C. 200 years from the first documented outbreak: Dying of cholera in the Near East during 2022 (recent data analysis). J Glob Health. 2023;13:03004.

167. Al-Gheethi A, Noman E, Jeremiah David B, Mohamed R, Abdullah AbdH, Nagapan S, et al. A review of potential factors contributing to epidemic cholera in Yemen. Journal of Water and Health. 2018;16:667–80.

168. Camacho A, Bouhenia M, Alyusfi R, Alkohlani A, Naji MAM, de Radiguès X, et al. Cholera epidemic in Yemen, 2016–18: an analysis of surveillance data. The Lancet Global Health. 2018;6:e680–90.

169. Hussein NR, Rasheed NA, Dhama K. Cholera in Iraq and Syria: a silent outbreak with a serious threat to the middle-east and beyond. International Journal of Surgery: Global Health. 2023;6:e108–e108.

170. Joh RI, Hoekstra RM, Barzilay EJ, Bowen A, Mintz ED, Weiss H, et al. Dynamics of Shigellosis Epidemics: Estimating Individual-Level Transmission and Reporting Rates From National Epidemiologic Data Sets. American Journal of Epidemiology. 2013;178:1319–26.

171. Mukandavire Z, Morris JG. Modeling the Epidemiology of Cholera to Prevent Disease Transmission in Developing Countries. Microbiol Spectr. 2015;3:3.3.21.

172. Finger F, Funk S, White K, Siddiqui MR, Edmunds WJ, Kucharski AJ. Real-time analysis of the diphtheria outbreak in forcibly displaced Myanmar nationals in Bangladesh. BMC Med. 2019;17:58.

173. Matsuyama R, Akhmetzhanov AR, Endo A, Lee H, Yamaguchi T, Tsuzuki S, et al. Uncertainty and sensitivity analysis of the basic reproduction number of diphtheria: a case study of a Rohingya refugee camp in Bangladesh, November–December 2017. PeerJ. 2018;6:e4583.

174. Van Effelterre TP, Zink TK, Hoet BJ, Hausdorff WP, Rosenthal P. A Mathematical Model of Hepatitis A Transmission in the United States Indicates Value of Universal Childhood Immunization. CLIN INFECT DIS. 2006;43:158–64.

175. Nannyonga B, Sumpter DJT, Mugisha JYT, Luboobi LS. The Dynamics, Causes and Possible Prevention of Hepatitis E Outbreaks. PLoS ONE. 2012;7:e41135.

176. Guerra FM, Bolotin S, Lim G, Heffernan J, Deeks SL, Li Y, et al. The basic reproduction number (R 0) of measles: a systematic review. The Lancet Infectious Diseases. 2017;17:e420–8.

177. Lo Presti A, Vacca P, Neri A, Fazio C, Ambrosio L, Rezza G, et al. Estimates of the reproductive numbers and demographic reconstruction of outbreak associated with C:P1.5–1,10–8:F3–6:ST–11(cc11) Neisseria meningitidis strains. Infection, Genetics and Evolution. 2020;84:104360.

178. Agusto FB, Leite MCA. Optimal control and cost-effective analysis of the 2017 meningitis outbreak in Nigeria. Infectious Disease Modelling. 2019;4:161–87.

179. Kretzschmar M, Teunis PFM, Pebody RG. Incidence and Reproduction Numbers of Pertussis: Estimates from Serological and Social Contact Data in Five European Countries. PLoS Med. 2010;7:e1000291.

180. Kilgore PE, Salim AM, Zervos MJ, Schmitt H-J. Pertussis: Microbiology, Disease, Treatment, and Prevention. Clin Microbiol Rev. 2016;29:449–86.

181. Brouwer AF, Eisenberg JNS, Pomeroy CD, Shulman LM, Hindiyeh M, Manor Y, et al. Epidemiology of the silent polio outbreak in Rahat, Israel, based on modeling of environmental surveillance data. Proc Natl Acad Sci USA. 2018;115.

182. Kalkowska DA, Pallansch MA, Cochi SL, Thompson KM. Updated Characterization of Poliovirus Transmission in Pakistan and Afghanistan and the Impacts of Different Outbreak Response Vaccine Options. The Journal of Infectious Diseases. 2021;224:1529–38.

183. Thompson KM, Kalkowska DA. Reflections on Modeling Poliovirus Transmission and the Polio Eradication Endgame. Risk Analysis. 2021;41:229–47.

184. Bennish ML, Wojtyniak BJ. Mortality Due to Shigellosis: Community and Hospital Data. Reviews of Infectious Diseases. 1991;13 Supplement_4:S245-251.

185. Bennish ML, Wojtyniak BJ. Mortality Due to Shigellosis: Community and Hospital Data. Reviews of Infectious Diseases. 1991;13 Supplement_4:S245-251.

186. Sauvageot D, Njanpop-Lafourcade B-M, Akilimali L, Anne J-C, Bidjada P, Bompangue D, et al. Cholera Incidence and Mortality in Sub-Saharan African Sites during Multi-country Surveillance. PLOS Neglected Tropical Diseases. 2016;10:1–16.

187. Elimian KO, Musah A, Ochu CL, Onwah SS, Oyebanji O, Yennan S, et al. Identifying and quantifying the factors associated with cholera-related death during the 2018 outbreak in Nigeria. The Pan African Medical Journal. 2020;37.

188. Shin E-C, Jeong S-H. Natural History, Clinical Manifestations, and Pathogenesis of Hepatitis A. Cold Spring Harbor Perspectives in Medicine. 2018;8:a031708.

189. Chen C-M, Chen SC-C, Yang H-Y, Yang S-T, Wang C-M. Hospitalization and mortality due to hepatitis A in Taiwan: a 15-year nationwide cohort study. Journal of Viral Hepatitis. 2016;23:940–5.

190. Bagulo H, Majekodunmi AO, Welburn SC. Hepatitis E in Sub Saharan Africa – A significant emerging disease. One Health. 2020;11:100186.

191. Boccia D, Guthmann J-P, Klovstad H, Hamid N, Tatay M, Ciglenecki I, et al. High Mortality Associated with an Outbreak of Hepatitis E among Displaced Persons in Darfur, Sudan. Clinical Infectious Diseases. 2006;42:1679–84.

192. Amanya G, Kizito S, Nabukenya I, Kalyango J, Atuheire C, Nansumba H, et al. Risk factors, person, place and time characteristics associated with Hepatitis E Virus outbreak in Napak District, Uganda. BMC Infectious Diseases. 2017;17:451.

193. Portnoy A, Jit M, Ferrari M, Hanson M, Brenzel L, Verguet S. Estimates of case-fatality ratios of measles in low-income and middle-income countries: a systematic review and modelling analysis. The Lancet Global Health. 2019;7:e472–81.

194. Dogu AG, Oordt-Speets AM, van Kessel-de Bruijn F, Ceyhan M, Amiche A. Systematic review of invasive meningococcal disease epidemiology in the Eastern Mediterranean and North Africa region. BMC Infectious Diseases. 2021;21:1088.

195. Macina D, Evans KE. Bordetella pertussis in School-Age Children, Adolescents, and Adults: A Systematic Review of Epidemiology, Burden, and Mortality in the Middle East. Infectious diseases and therapy. 2021;10:719—738.

196. Crowcroft NS, Stein C, Duclos P, Birmingham M. How best to estimate the global burden of pertussis? The Lancet Infectious Diseases. 2003;3:413–8.

197. Mach O, Tangermann RH, Wassilak SG, Singh S, Sutter RW. Outbreaks of Paralytic Poliomyelitis During 1996–2012: The Changing Epidemiology of a Disease in the Final Stages of Eradication. The Journal of Infectious Diseases. 2014;210 suppl_1:S275–82.

198. Nathanson N, Kew OM. From Emergence to Eradication: The Epidemiology of Poliomyelitis Deconstructed. American Journal of Epidemiology. 2010;172:1213–29.

199. Marchello CS, Birkhold M, Crump JA. Complications and mortality of typhoid fever: A global systematic review and meta-analysis. Journal of Infection. 2020;81:902–10.

200. Walker N, Tam Y, Friberg IK. Overview of the lives saved tool (LiST). Springer; 2013.

201. Singh NS, Blanchard AK, Blencowe H, Koon AD, Boerma T, Sharma S, et al. Zooming in and out: a holistic framework for research on maternal, late foetal and newborn survival and health. Health Policy Plan. 2022;37:565–74.

202. Stegmuller AR, Self A, Litvin K, Roberton T. How is the Lives Saved Tool (LiST) used in the global health community? Results of a mixed-methods LiST user study. BMC Public Health. 2017;17:143–50.

203. McGee S-A, Chola L, Tugendhaft A, Mubaiwa V, Moran N, McKerrow N, et al. Strategic planning for saving the lives of mothers, newborns and children and preventing stillbirths in KwaZulu-Natal province South Africa: modelling using the Lives Saved Tool (LiST). BMC Public Health. 2015;16:1–14.

204. Roberton T, Carter ED, Chou VB, Stegmuller AR, Jackson BD, Tam Y, et al. Early estimates of the indirect effects of the COVID-19 pandemic on maternal and child mortality in low-income and middle-income countries: a modelling study. The Lancet global health. 2020;8:e901–8.

205. Winfrey W, McKinnon R, Stover J. Methods used in the lives saved tool (LiST). BMC public health. 2011;11:1–11.

206. WHO. Health cluster occupied Palestinian territory. https://healthcluster.who.int/countries-and-regions/occupied-palestinian-territory. Accessed 29 Jan 2024.

207. Blencowe H, Chou VB, Lawn JE, Bhutta ZA. Modelling stillbirth mortality reduction with the Lives Saved Tool. BMC public health. 2017;17:59–74.

208. Abdalla B, Mansour M, Ghanim M, Aia B, Yassin M. The growing burden of cancer in the Gaza Strip. The Lancet Oncology. 2019;20:1054–6.

209. Mosleh M, Aljeesh Y, Dalal K, Eriksson C, Carlerby H, Viitasara E. Perceptions of Non-Communicable Disease and War Injury Management in the Palestinian Health System: A Qualitative Study of Healthcare Providers Perspectives. J Multidiscip Healthc. 2020;13:593–605.

210. UNRWA. Health in the Gaza Strip. https://www.unrwa.org/activity/health-gaza-strip. Accessed 14 Feb 2024.

211. WHO. Occupied Palestinian Territory. Monthly Report: March 2021. 2021.

212. Bouquet B, Barone-Adesi F, Lafi M, Quanstrom K, Riccardi F, Doctor H, et al. Comparative survival of cancer patients requiring Israeli permits to exit the Gaza Strip for health care: A retrospective cohort study from 2008 to 2017. PLoS One. 2021;16:e0251058.

213. Brostoff JM, Keen H, Brostoff J. A diabetic life before and after the insulin era. Diabetologia. 2007;50:1351–3.

214. World Bank Open Data: Life expectancy at birth. World Bank Open Data. https://data.worldbank.org. Accessed 14 Feb 2024.

215. Ebad M. Survival analysis of chronic dialysis patients: Thesis University of Waterloo. 2018.

216. Ferreira E de S, Moreira TR, da Silva RG, da Costa GD, da Silva LS, Cavalier SB de O, et al. Survival and analysis of predictors of mortality in patients undergoing replacement renal therapy: a 20-year cohort. BMC Nephrology. 2020;21:502.

217. Ebrahimi V, Khademian MH, Masoumi SJ, Morvaridi MR, Ezzatzadegan Jahromi S. Factors influencing survival time of hemodialysis patients; time to event analysis using parametric models: a cohort study. BMC Nephrology. 2019;20:215.

218. Nguyen B, Fukuuchi F. Survival rates and causes of death in Vietnamese chronic hemodialysis patients. Renal Replacement Therapy. 2017;3:22.

219. Saran R, Bragg-Gresham JL, Rayner HC, Goodkin DA, Keen ML, Dijk PCV, et al. Nonadherence in hemodialysis: Associations with mortality, hospitalization, and practice patterns in the DOPPS. Kidney International. 2003;64:254–62.

220. Leggat JE, Orzol SM, Hulbert-Shearon TE, Golper TA, Jones CA, Held PJ, et al. Noncompliance in hemodialysis: Predictors and survival analysis. American Journal of Kidney Diseases. 1998;32:139–45.

221. Ministry of Health. Cancer in Palestine - West Bank. 2023.

222. Rb K, Jr K, Jy H. Epidemiology of myocardial infarction in Korea: hospitalization incidence, prevalence, and mortality. Epidemiology and health. 2022;44.

223. Norum J, Hansen TM, Hovland A, Balteskard L, Haug B, Olsen F, et al. Calculating the 30-day Survival Rate in Acute Myocardial Infarction: Should we Use the Treatment Chain or the Hospital Catchment Model? Heart Int. 2017;12:heartint.5000238.

224. Christensen DM, Schjerning A-M, Smedegaard L, Charlot MG, Ravn PB, Ruwald AC, et al. Long-term mortality, cardiovascular events, and bleeding in stable patients 1 year after myocardial infarction: a Danish nationwide study. European Heart Journal. 2023;44:488–98.

225. Law MR, Watt HC, Wald NJ. The Underlying Risk of Death After Myocardial Infarction in the Absence of Treatment. Archives of Internal Medicine. 2002;162:2405–10.

226. Fekadu G, Chelkeba L, Kebede A. Burden, clinical outcomes and predictors of time to in hospital mortality among adult patients admitted to stroke unit of Jimma university medical center: a prospective cohort study. BMC Neurol. 2019;19:213.

227. Woo D, Comeau ME, Venema SU, Anderson CD, Flaherty M, Testai F, et al. Risk Factors Associated With Mortality and Neurologic Disability After Intracerebral Hemorrhage in a Racially and Ethnically Diverse Cohort. JAMA Netw Open. 2022;5:e221103.

228. Smajlović D, Kojić B, Sinanović O. FIVE-YEAR SURVIVAL AFTER FIRST-EVER STROKE. Bosn J Basic Med Sci. 2006;6:17–22.

229. Saposnik G, Hill MD, O'Donnell M, Fang J, Hachinski V, Kapral MK. Variables Associated With 7-Day, 30-Day, and 1-Year Fatality After Ischemic Stroke. Stroke. 2008;39:2318–24.

230. Ananth CV, Brandt JS, Keyes KM, Graham HL, Kostis JB, Kostis WJ. Epidemiology and trends in stroke mortality in the USA, 1975-2019. Int J Epidemiol. 2023;52:858–66.

231. WHO: International Agency for Research on Cancer. Cancer Today. https://gco.iarc.who.int/today/. Accessed 14 Feb 2024.

232. WHO. WHO Mortality Database: Noncommunicable diseases. Mortality DB. https://platform.who.int/mortality/themes/theme-details/MDB/noncommunicable-diseases. Accessed 20 Feb 2024.

233. Ministry of Health (Palestine) | GHDx. https://ghdx.healthdata.org/organizations/ministry-health-palestine. Accessed 5 Feb 2024.

234. UNRWA. Annual Reports. UNRWA. https://www.unrwa.org/resources/reports. Accessed 14 Feb 2024.

235. Mesfin B, Mersha Demise A, Shiferaw M, Gebreegziabher F, Girmaw F. The Effect of Armed Conflict on Treatment Interruption, Its Outcome and Associated Factors Among Chronic Disease Patients in North East, Amhara, Ethiopia, 2022. Patient Related Outcome Measures. 2023;14:243–51.

236. Ministry of Health, Southern Governates-Gaza strip. Annual Report 2022. 2023.

9 Appendix

Table 24. Occurrence and timing of epidemics in past crises. Shaded cells are those for which the given pathogen caused an epidemic. Numbers in these cells indicate the recognised start of the epidemic, relative to the crisis' start (in months).

Crisis typology	Crisis-affected region (date of major escalation or displacement)	Diphtheria	Measles	Pertussis	Meningo-coccal meningitis	Polio	Hepatitis A	Hepatitis E	Cholera	Typhoid fever	Bacterial dysentery
Armed conflict	Iraq (Mar 2003)		9						1		
Armed conflict	Darfur region, Sudan and Darfurian refugees to Chad (Dec 2003)		4		13	6		5	32		7
Earthquake	Kerman province, Iran (Dec 2003)										
Armed conflict	North, South Kivu provinces, DRC (Jun 2004)								6		
Flooding disaster (Indian Ocean tsunami)	Aceh province, Indonesia (Dec 2004)		1								
Earthquake	Azad Jammu and Kashmir province, Pakistan (Oct 2005)										
Armed conflict	Iraq (Feb 2006)		36						17		
Armed conflict	Northern Province, Sri Lanka (Jan 2008)					15					
Flooding disaster (Cyclone Nargis)	Ayeyarwady Region, Myanmar (Apr 2008)										
Earthquake	Haiti (Jan 2010)								9	2	
Drought	South-Central regions, Somalia and Somali refugees to Ethiopia, Kenya (Oct 2010)		6			32			5		
Armed conflict	Ivory Coast (Nov 2010)		2		14				18		
Armed conflict	Libya (Feb 2011)										
Armed conflict	Syria and Syrian refugees to neighbouring		12			31				23	

Crisis typology	Crisis-affected region (date of major escalation or displacement)	Diphtheria	Measles	Pertussis	Meningo-coccal meningitis	Polio	Hepatitis A	Hepatitis E	Cholera	Typhoid fever	Bacterial dysentery
	countries (Mar 2011)										
Armed conflict	South Kordofan, Blue Nile states, Sudan and refugees to South Sudan (Jun 2011)						24	13			
Armed conflict	Tombouctou, Gao, Kidal, Taoudenit, Menaka regions, Mali (Jan 2012)								6		
Armed conflict	Central African Republic (Dec 2012)		1						36		
Flooding disaster (Typhoon Hayan)	Eastern Visayas (Region VIII), Philippines (Nov 2013)										
Armed conflict	South Sudan (Dec 2013)		10			11		20	1		
Armed conflict	Donetsk, Luhansk oblast, Ukraine (Apr 2014)										
Armed conflict	Libya (May 2014)										
Armed conflict	Yemen (Mar 2015)	29	10						19		
Armed conflict	Borno, Adamawa, Yobe states, Nigeria (Jan 2015)				24	19		29	2		
Armed conflict	Rohingya refugees in Cox Bazar camps, Bangladesh (Aug 2017)	4	1				2		26		
Drought	South-Central regions, Somalia (Jan 2017)		2	5					11		
Armed conflict	Northwest, Southwest regions, Cameroon (Sep 2017)								8		
Armed conflict	Tigray region, Ethiopia and Tigrayan refugees to Sudan (Nov 2020)		10					7	35		
Armed conflict	Nagorno-Karabakh region, Azerbaijan (Sep 2020)										

| Crisis typology	Crisis-affected region (date of major escalation or displacement)	Diphtheria	Measles	Pertussis	Meningo-coccal meningitis	Polio	Hepatitis A	Hepatitis E	Cholera	Typhoid fever	Bacterial dysentery
	Number of epidemics during the first 36mths	2	13	1	3	5	3	5	16	2	1
	Percentage of crises with epidemics during the first 36mths	7%	46%	4%	11%	18%	11%	18%	57%	7%	4%
	Median delay (months) between crisis onset and epidemic	17	6	5	14	19	15	13	10	13	7
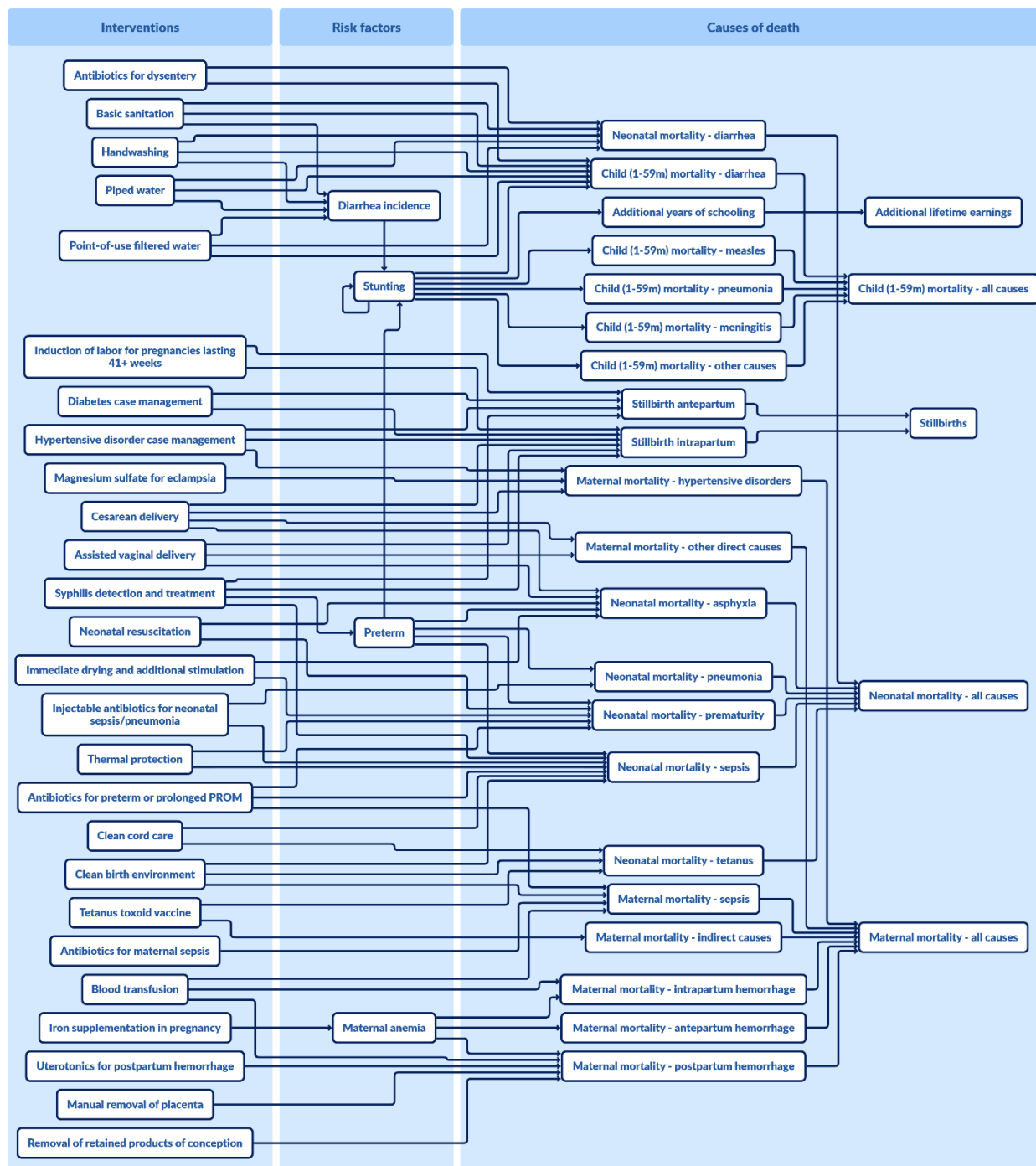
Figure 14. Pathways for interventions included in the analysis in the Lives Saved Tool (link).